The background of the cover is composed of several histological images of aneurysmal bone cysts, stained with hematoxylin and eosin (H&E). The images show characteristic features such as blood-filled spaces, fibrous septa, and the presence of multinucleated giant cells. The top-left image shows a large, irregularly shaped blood-filled space. The middle-left image shows a similar space with a more organized fibrous wall. The bottom-left image is a high-magnification view showing a multinucleated giant cell with numerous nuclei. The bottom-right image shows a cross-section of a blood-filled space with a thick, fibrous wall and some cellular debris.

JPTM

Journal of Pathology
and Translational Medicine

March 2023
Vol. 57 / No.2
jpatholm.org
pISSN: 2383-7837
eISSN: 2383-7845



Aneurysmal Bone Cyst

Aims & Scope

The *Journal of Pathology and Translational Medicine* is an open venue for the rapid publication of major achievements in various fields of pathology, cytopathology, and biomedical and translational research. The Journal aims to share new insights into the molecular and cellular mechanisms of human diseases and to report major advances in both experimental and clinical medicine, with a particular emphasis on translational research. The investigations of human cells and tissues using high-dimensional biology techniques such as genomics and proteomics will be given a high priority. Articles on stem cell biology are also welcome. The categories of manuscript include original articles, review and perspective articles, case studies, brief case reports, and letters to the editor.

Subscription Information

To subscribe to this journal, please contact the Korean Society of Pathologists/the Korean Society for Cytopathology. Full text PDF files are also available at the official website (<https://jpatholtm.org>). *Journal of Pathology and Translational Medicine* is indexed by Emerging Sources Citation Index (ESCI), PubMed, PubMed Central, Scopus, KoreaMed, KoMCI, WPRIM, Directory of Open Access Journals (DOAJ), and CrossRef. Circulation number per issue is 50.

Editors-in-Chief

Jung, Chan Kwon, MD (*The Catholic University of Korea, Korea*) <https://orcid.org/0000-0001-6843-3708>

Park, So Yeon, MD (*Seoul National University, Korea*) <https://orcid.org/0000-0002-0299-7268>

Associate Editors

Bychkov, Andrey, MD (*Kameda Medical Center, Japan; Nagasaki University Hospital, Japan*) <https://orcid.org/0000-0002-4203-5696>

Kim, Haeryoung, MD (*Seoul National University, Korea*) <https://orcid.org/0000-0002-4205-9081>

Lee, Hee Eun, MD (*Mayo Clinic, USA*) <https://orcid.org/0000-0001-6335-7312>

Shin, Eunah, MD (*Yongin Severance Hospital, Yonsei University, Korea*) <https://orcid.org/0000-0001-5961-3563>

Editorial Board

Avila-Casado, Maria del Carmen, MD (*University of Toronto, Toronto General Hospital UHN, Canada*)

Bae, Jeong Mo, MD (*Seoul National University, Korea*)

Bae, Young Kyung, MD (*Yeungnam University, Korea*)

Bongiovanni, Massimo, MD (*Lausanne University Hospital, Switzerland*)

Bova, G. Steven, MD (*University of Tampere, Finland*)

Choi, Joon Hyuk (*Yeungnam University, Korea*)

Chong, Yo Sep, MD (*The Catholic University of Korea, Korea*)

Chung, Jin-Haeng, MD (*Seoul National University, Korea*)

Fadda, Guido, MD (*Catholic University of Rome-Foundation Agostino Gemelli University Hospital, Italy*)

Fukushima, Noriyoshi, MD (*Jichi Medical University, Japan*)

Go, Heounjeong (*University of Ulsan, Korea*)

Hong, Soon Won, MD (*Yonsei University, Korea*)

Jain, Deepali, MD (*All India Institute of Medical Sciences, India*)

Kakudo, Kennichi, MD (*Izumi City General Hospital, Japan*)

Kim, Jang-Hee, MD (*Ajou University, Korea*)

Kim, Jung Ho, MD (*Seoul National University, Korea*)

Kim, Se Hoon, MD (*Yonsei University, Korea*)

Komuta, Mina, MD (*Keio University, Tokyo, Japan*)

Kwon, Ji Eun (*Ajou University, Korea*)

Lai, Chiung-Ru, MD (*Taipei Veterans General Hospital, Taiwan*)

Lee, C. Soon, MD (*University of Western Sydney, Australia*)

Lee, Hwajong, MD (*Albany Medical College, USA*)

Lee, Sung Hak, MD (*The Catholic University, Korea*)

Liu, Zhiyan, MD (*Shanghai Jiao Tong University, China*)

Lkhagvadorj, Sayamaa, MD (*Mongolian National University of Medical Sciences, Mongolia*)

Moran, Cesar, MD (*MD Anderson Cancer Center, U.S.A.*)

Paik, Jin Ho, MD (*Seoul National University, Korea*)

Park, Jeong Hwan (*Seoul National University, Korea*)

Ro, Jae Y., MD (*Cornell University, The Methodist Hospital, U.S.A.*)

Sakhuja, Puja, MD (*Govind Ballabh Pant Hospital, India*)

Shahid, Pervez, MD (*Agga Khan University, Pakistan*)

Song, Joon Seon, MD (*University of Ulsan, Korea*)

Tan, Puay Hoon, MD (*National University of Singapore, Singapore*)

Than, Nandor Gabor, MD (*Semmelweis University, Hungary*)

Tse, Gary M., MD (*The Chinese University of Hong Kong, Hong Kong*)

Yatabe, Yasushi, MD (*Aichi Cancer Center, Japan*)

Zhu, Yun, MD (*Jiangsu Institution of Nuclear Medicine, China*)

Ethic Editor

Choi, In-Hong, MD (*Yonsei University, Korea*)

Huh, Sun, MD (*Hallym University, Korea*)

Statistics Editors

Kim, Dong Wook (*National Health Insurance Service Ilsan Hospital, Korea*)

Lee, Hye Sun (*Yonsei University, Korea*)

Manuscript Editor

Chang, Soo-Hee (*InfoLumi Co., Korea*)

Layout Editor

Kim, Haeja (*iMiS Company Co., Ltd., Korea*)

Website and JATS XML File Producers

Cho, Yoonsang (*M2Community Co., Korea*)

Im, Jeonghee (*M2Community Co., Korea*)

Administrative Assistants

Kim, Da Jeong (*The Korean Society of Pathologists*)

Jeon, Anmi (*The Korean Society for Cytopathology*)

Contact the Korean Society of Pathologists/the Korean Society for Cytopathology

Publishers: Choe, Gheeyoung, MD, Lee, Seung-Sook, MD

Editors-in-Chief: Jung, Chan Kwon, MD, Park, So Yeon, MD

Published by the Korean Society of Pathologists/the Korean Society for Cytopathology

Editorial Office

Room 1209 Gwanghwamun Officia, 92 Saemunan-ro, Jongno-gu, Seoul 03186, Korea

Tel: +82-2-795-3094 Fax: +82-2-790-6635 E-mail: office@jpatholtm.org

#1508 Renaissancetower, 14 Mallijae-ro, Mapo-gu, Seoul 04195, Korea

Tel: +82-2-593-6943 Fax: +82-2-593-6944 E-mail: office@jpatholtm.org

Printed by iMiS Company Co., Ltd. (JMCI)

Jungang Bldg. 18-8 Wonhyo-ro 89-gil, Yongsan-gu, Seoul 04314, Korea

Tel: +82-2-717-5511 Fax: +82-2-717-5515 E-mail: ml@smileml.com

Manuscript Editing by InfoLumi Co.

210-202, 421 Pangyo-ro, Bundang-gu, Seongnam 13522, Korea

Tel: +82-70-8839-8800 E-mail: infolumi.chang@gmail.com

Front cover image: Histologic features of aneurysmal bone cyst (p85).

© Copyright 2023 by the Korean Society of Pathologists/the Korean Society for Cytopathology

© Journal of Pathology and Translational Medicine is an Open Access journal under the terms of the Creative Commons Attribution Non-Commercial License (<https://creativecommons.org/licenses/by-nc/4.0>).

© This paper meets the requirements of KS X ISO 9706, ISO 9706-1994 and ANSI/NISO Z.39.48-1992 (Permanence of Paper).

CONTENTS

REVIEW

- 81 Aneurysmal bone cyst: a review

Elham Nasri, John David Reith

ORIGINAL ARTICLES

- 88 Significance of tumor-associated neutrophils, lymphocytes, and neutrophil-to-lymphocyte ratio in non-invasive and invasive bladder urothelial carcinoma

Wael Abdo Hassan, Ahmed Kamal ElBanna, Noha Noufal, Mohamed El-Assmy, Hany Lotfy, Rehab Ibrahim Ali

- 95 Current state of cytopathology residency training: a Korean national survey of pathologists

Uiju Cho, Tae Jung Kim, Wan Seop Kim, Kyo Young Lee, Hye Kyoung Yoon, Hyun Joo Choi,

The Fellowship Council and Committee of Quality Improvement of the Korean Society for Cytopathology

- 102 Postmortem lung and heart examination of COVID-19 patients in a case series from Jordan

Maram AbdalJaleel, Isra Tawalbeh, Malik Sallam, Amjad Bani Hani, Imad M. Al-Abdallat, Baheth Al Omari, Sahar Al-Mustafa, Hasan Abder-Rahman, Adnan Said Abbas, Mahmoud Zureigat, Mousa A. Al-Abbadi

- 113 Clinicopathologic significance of the delta-like ligand 4, vascular endothelial growth factor, and hypoxia-inducible factor-2 α in gallbladder cancer

Sujin Park, Junsik Kim, Woncheol Jang, Kyoung-Mee Kim, Kee-Taek Jang

CASE REPORTS

- 123 Unsuspected systemic Epstein-Barr virus-positive T-cell lymphoma of childhood diagnosed at autopsy in a potential homicide case

Daniel J. Robbins, Erik A. Ranheim, Jamie E. Kallan

- 128 Solitary Peutz-Jeghers type hamartomatous polyp in duodenum with gastric foveolar epithelium: a case report

Eugene Choi, Junghwan Lee, Youngsoo Park

- 132 Unusual biclonal IgA plasma cell myeloma with aberrant expression of high-risk immunophenotypes: first report of a new diagnostic and clinical challenge

Carlos A. Monroig-Rivera, Clara N. Finch Cruz

Aneurysmal bone cyst: a review

Elham Nasri¹, John David Reith²

¹Department of Pathology, Immunology, and Laboratory Medicine, University of Florida, College of Medicine, Gainesville, FL;

²Department of Pathology, Cleveland Clinic, Cleveland, OH, USA

Aneurysmal bone cyst (ABC) is a benign locally destructive bone neoplasm composed of multi-loculated blood-filled cystic spaces. The most common sites of involvement are the meta-diaphysis of the long bones and posterior elements of the vertebrae. Secondary, ABC-like changes can complicate a variety of other benign and malignant primary bone neoplasms, including giant cell tumor, fibrous dysplasia, and osteosarcoma. About two-third of primary ABCs have a rearrangement of the *USP6* gene, which is not present in the ABC-like changes that occur secondary to other primary bone tumors (i.e., secondary ABC). Primary ABC of bone carries a variable but generally high rate of local recurrence. This paper provides an overview of the pathophysiology, clinical presentation, radiographic and pathologic findings, treatment, and prognosis of ABC.

Key Words: Bone cyst; Aneurysmal bone cyst; *USP6* gene

Received: January 25, 2023 **Revised:** February 23, 2023 **Accepted:** February 23, 2023

Corresponding Author: Elham Nasri, MD, Department of Pathology, Immunology, and Laboratory Medicine, University of Florida, College of Medicine, P.O. Box 100275, 1600 SW Archer Road, Gainesville, FL 32610-0275, USA

Tel: +1-352-627-9258, Fax: +1-352-627-9242, E-mail: elham@ufl.edu

*This invited review is a featured collaboration with PathologyOutlines.com.

Aneurysmal bone cyst (ABC) is a benign blood-filled cystic neoplasm of bone with a broad spectrum of skeletal involvement. It can present as a primary tumor, but ABC-like changes can also complicate other neoplastic diseases of bone.

ABC is a rare neoplasm with an annual prevalence of 0.32 per 100,000 young population [1], 0.14 per 100,000 general population [2], and comprising about 2.5% of all bone tumors [3]. It has an equal distribution among male and female patients [4,5], and most commonly is seen in skeletally immature patients especially in the first two decades of life [2].

Historically, it was thought that an ABC develops as the result of an underlying vascular event; increased venous blood flow; or a reaction to prior trauma [6]. However, in light of the recent molecular findings of the recurrent rearrangement involving the *USP6* gene (chr.17p13.2 locus) [7-9]. ABC is now considered a neoplasm rather than a reactive lesion.

Although ABC can affect any bone in the body, the craniofacial bones, vertebrae (particularly the posterior elements) and metaphysis of long tubular bones in the upper and lower extremities are more commonly involved [3]. Other less common sites of in-

volvement include small tubular bones of hands and feet, tarsal bones, scapula, and pelvic bones.

Patients usually present with pain and swelling of variable duration at the site of involvement. Rarely, the initial presentation is pathologic fracture specifically in the major long tubular bones of the extremities [10]. In the vertebral lesions, symptoms of compression of the spinal cord or nerve roots may be the initial presentation [11,12].

The diagnosis of ABC requires the correlation of clinical, radiographic, and histologic findings and to distinguish the primary from a secondary form of the disease.

IMAGING

The radiographic features of ABC are quite distinct and aid in diagnosing the disease. Conventional radiographs show an eccentric radiolucent lesion with expansile remodeling of bone. A thin surrounding rim of the periosteum and sub periosteal bone is usually present. The cyst wall trabeculae impart the multi-locular appearance (Fig. 1). In the vertebral column, ABC most



Fig. 1. Plain radiography of aneurysmal bone cyst. (A) X-ray demonstrates a lytic lesion in the proximal metaphysis of the tibia with slight expansile features and lucency extending through the cortex. (B) X-ray shows an expansile lucent lesion centered in the medullary cavity of the proximal humeral metaphysis with cortical thinning. (C) X-ray shows an eccentric lucent lesion of the medial side of the distal tibia. (D) X-ray shows an expansile multiloculated lucent lesion of the calcaneus.

commonly involves the posterior neural arch and can produce an eccentric “blowout” lesion [3]. In small tubular bones of hands and feet, the characteristic “finger-in-the-balloon” sign might be present.

Computed tomography shows a well-delineated lytic lesion, usually with a thin surrounding rim of reactive bone (Fig. 2A). Occasionally, fluid-fluid levels are visible. However, the best imaging modality to identify the fluid-fluid levels is magnetic resonance imaging. The cysts usually demonstrate variable signal intensity with a rim of low T1 and T2 signal. T1 post-contrast sequence may show some enhancement of septations (Fig. 2B–D) [13,14].

Isotope scan shows a peripheral uptake with central photopenia,

which imparts a “donut sign” appearance. This appearance is not specific for ABC and can also be seen in other bone lesions with ABC-like changes such as chondroblastoma and giant cell tumor of bone.

PATHOLOGY

Grossly, an ABC appears as a well-demarcated spongy hemorrhagic lesion with variably-sized multiloculations. The cystic spaces are variable in size ranging from less than one millimeter to several centimeters [3]. It has irregular, sharply demarcated borders with a thin shell of reactive bone around it. A variable amount of solid component might be present, particularly in the

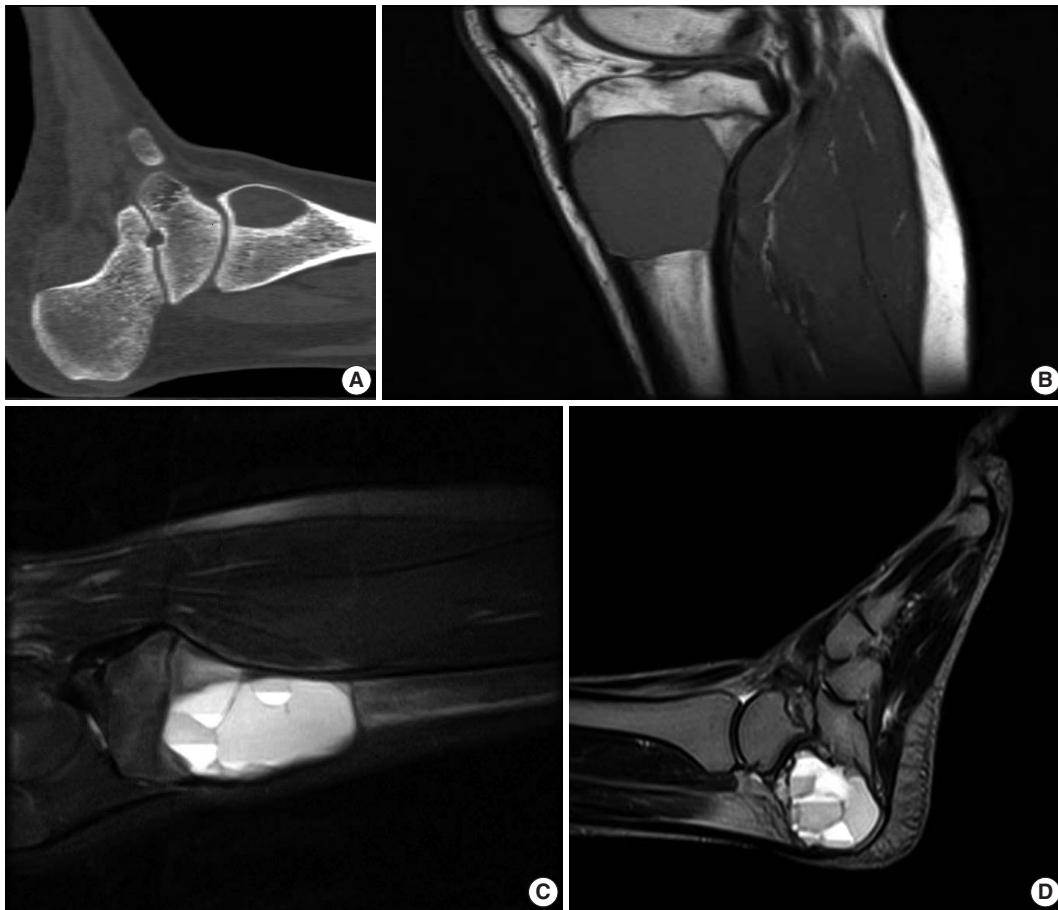


Fig. 2. Computed tomography (CT) and magnetic resonance imaging (MRI) of aneurysmal bone cyst. (A) CT scan shows a well-demarcated ovoid area of lucency within the medial aspect of the distal tibia. (B, C) MRI shows an expansile well-demarcated cystic lesion of the proximal tibia with fluid-fluid levels. (D) Sagittal view T2 MRI demonstrates multiple fluid-fluid levels of the cyst involving the calcaneus bone.

digits (Fig. 3).

When encountered in an intraoperative consultation (frozen section), ABC is characterized by small fragments of cellular septa containing fibroblast-like stromal cells, osteoclast-like giant cells, and reactive woven bone that frequently displays osteoblastic rimming. While mitoses are typically easily identified, atypical mitoses and cytologic atypia are not present, and when these features are encountered on a frozen section they warrant a detailed discussion with the surgeon (Fig. 4).

ABC is almost always received as curetted material rather than an en-bloc resection. As a rule, the curetted material must be entirely submitted for histologic evaluation. Low-power microscopic examination shows a multiloculated cystic lesion with collapsed cyst walls within the background of blood and hemorrhage. The septa show mixed inflammatory cells, reactive fibroblasts, woven bone, and some vasoformative foci; however, the cyst walls lack a true lining. Characteristic calcified basophilic material, referred

to as “blue reticulated chondroid-like material” might be present within the cyst walls [15]. The cysts are generally devoid of any lining but some flattened endothelial-like cells can be present. Osteoclast-type giant cells are found in clusters with increased numbers within the cyst wall. Mitoses can be easily identified, but atypical mitoses are not. Necrosis and cytologic atypia are not the features of ABC (Figs. 5, 6). There is no specific immunohistochemical stain for the diagnosis of ABC.

MOLECULAR AND CYTOGENETICS

Recurrent rearrangements of the short arm of chromosome 17 (p13.2) have been found in approximately 63% of cases of ABC [7]. This locus belongs to the ubiquitin-specific protease 6 (*USP6*), also known as Tre-2. Through promoter swapping, *USP6* contributes its entire coding sequence as the 3' portion, and its transcription is substantially enhanced by replaceable 5' partner genes

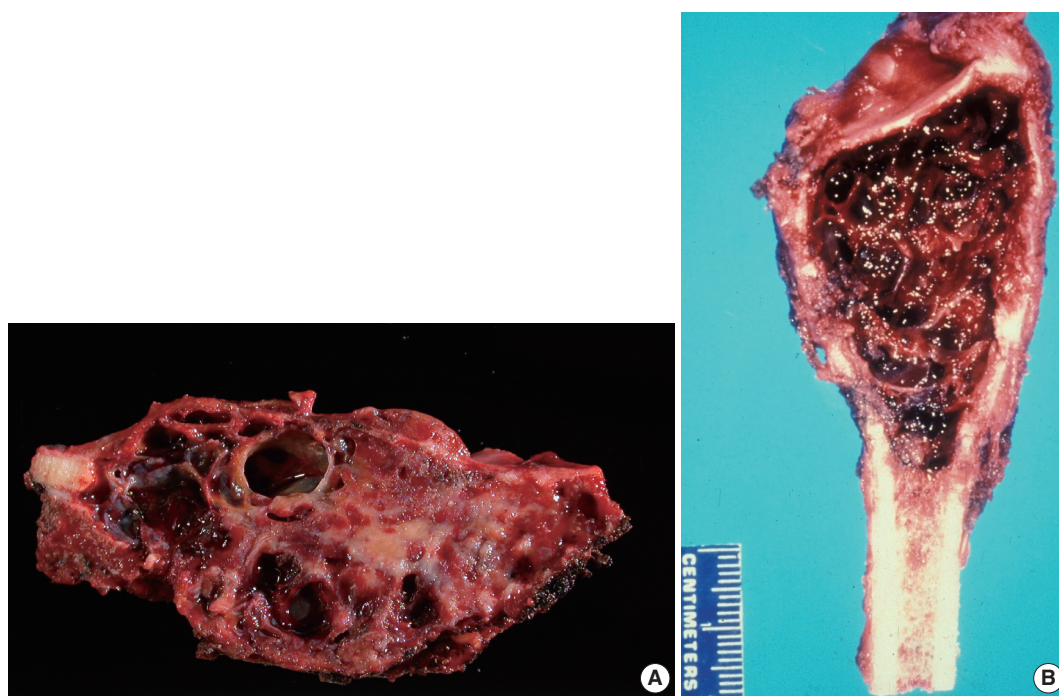


Fig. 3. Gross findings of aneurysmal bone cyst (ABC). (A) ABC involving the distal fibula, showing an expansile lesion with multiple blood-filled cystic spaces. (B) ABC involving tibia, showing an expansile lesion with multiple blood-filled cystic spaces.

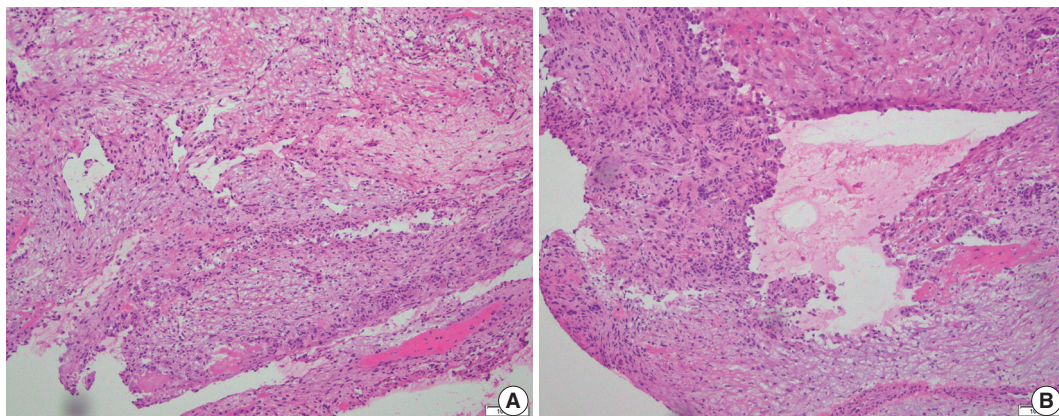


Fig. 4. Frozen section findings of aneurysmal bone cyst. (A) Frozen section of a multiloculated cystic lesion of the distal tibia. Cystic space with flat attenuated lining and increased stromal giant cells. (B) The solid area shows scattered giant cells in the background of fibrovascular stroma. Cellular atypia is not present.

juxtaposed to the untranslated regulatory element of *USP6* [16]. As a result, the gene induces the production of matrix metalloproteinase activity via nuclear factor- κ B. The most common fusion partner for the *USP6* gene is *CDH11* (about 30%); however, other genes such as *TRAP150* (*THRAP3*), *ZNF9* (*CNBP*), *OMD*, *COL1A1*, *RUNX2*, *PFAH1B1*, *CTNNB1*, *SEC31A*, *E1F1*, *FOSL2*, *STAT3*, *USP9X*, *ASAP1*, *FAT1*, *SAR1A*, *TNC*, *SPARC* have been reported [17-19]. Rare cases of an unusually aggressive ABC with soft tissue extension and *RUNX::USP6* fusion is

also reported [20]. Rearrangement of the *USP6* gene can be detected by fluorescence in-situ hybridization or fusion panel analysis such as targeted RNA sequencing.

Rearrangement of the *USP6* gene has also been found in other soft tissue neoplasms; some with a limited capacity of bone formation, mimicking sarcomas; however, with limited growth potential and non-aggressive clinical course. These entities include nodular fasciitis, cellular fibroma of tendon sheath, myositis ossificans, and fibro-osseous pseudo tumor of digit. This common

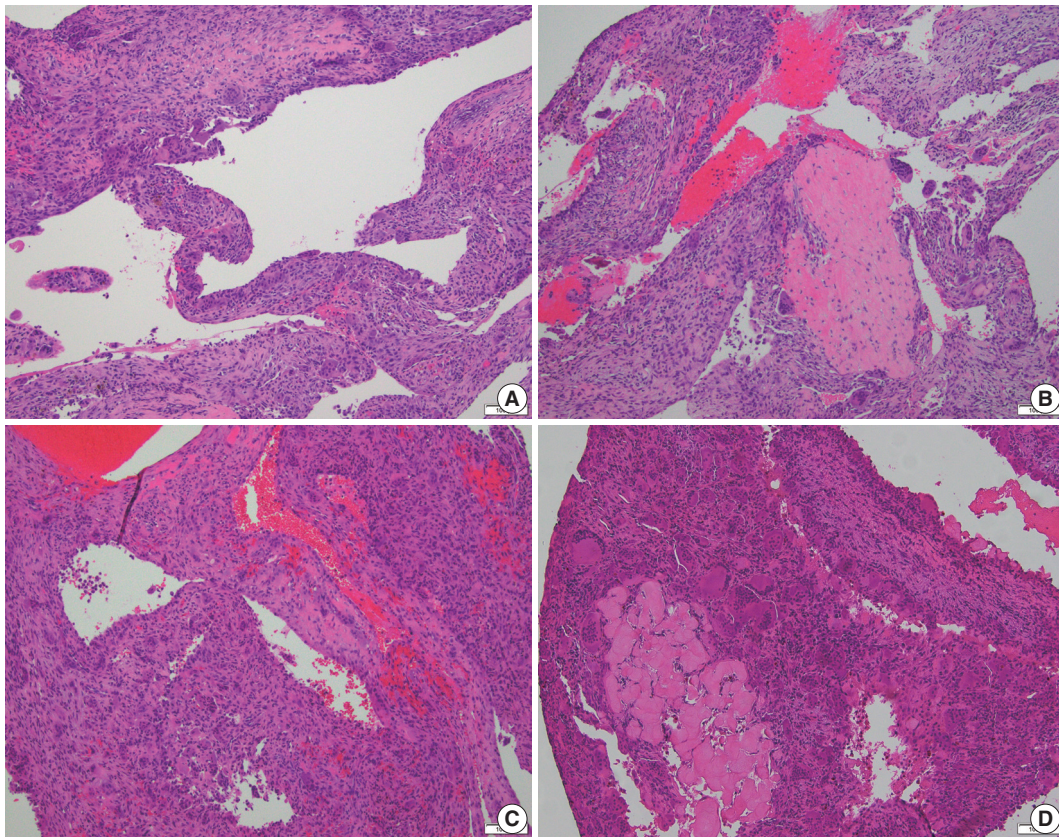


Fig. 5. Histologic features of aneurysmal bone cyst. (A) Irregular cystic spaces with multi-nucleated giant cells are present. (B) Multiple irregular cystic spaces, some filled with blood, and a variable number of giant cells in the cyst wall. (C) Blood-filled cystic spaces with cellular giant cell-rich cyst wall. (D) Cystic spaces and portion of cyst wall with scattered giant cells. No significant atypia is present.

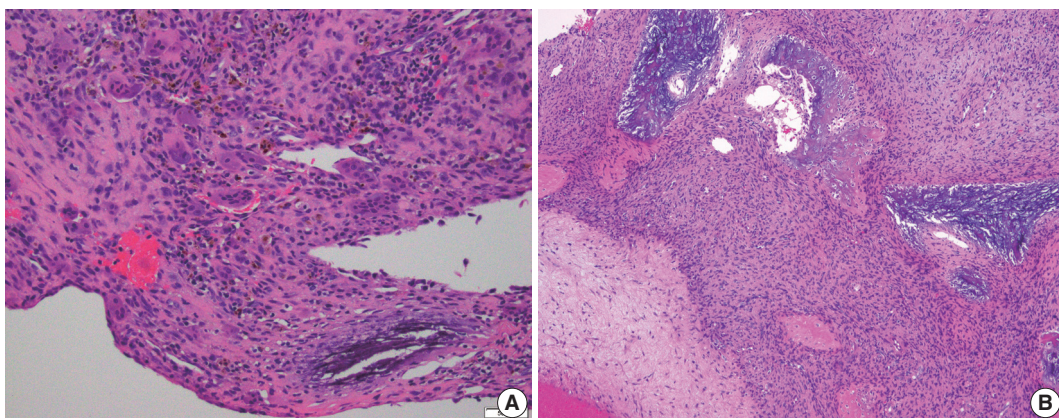


Fig. 6. Blue reticulated chondroid-like material. (A, B) Cyst wall with “blue reticulated chondroid-like material” and hemosiderin deposition.

finding suggests that these neoplasms might belong to a spectrum of disease processes that can best be referred to as USP6-associated neoplasms [16,21-24].

DIFFERENTIAL DIAGNOSIS

It is important to differentiate primary ABC from lesions with ABC-like changes. Such changes are more common in giant cell tumors of bone, fibrous dysplasia, chondroblastoma, osteoblastoma, and even osteosarcoma [4].

Radiographic findings often aid in narrowing down the differential diagnoses. As a general rule, any epiphyseal or diaphyseal-based lesion raises the possibility of ABC-like changes more than the primary ABC. For example, a diaphyseal lesion with multiple cysts and fluid-fluid levels indicates the possibility of telangiectatic osteosarcoma. The cystic epiphyseal-based lesions suggest the ABC-like changes in an underlying giant cell tumor of bone or chondroblastoma, depending on the patient's skeletal maturity.

In cases of giant cell tumor of bone with secondary ABC changes, immunohistochemical stain for H3F3A G34W (or other histone markers) can aid in diagnosis. The mononuclear cells of the giant cell tumor show nuclear immunoreactivity for the histone markers; however, the primary ABC does not demonstrate such a finding.

Distinction from telangiectatic osteosarcoma can be challenging due to some overlapping clinical and radiographic features. Unlike ABC, telangiectatic osteosarcoma shows highly atypical and anaplastic cells within the stroma, frequent atypical mitoses, and sometimes necrosis. Osteoid matrix production is minimal in these lesions. ABC shows frequent rearrangement of the *USP6* gene; however, telangiectatic osteosarcoma does not show such findings. There is no specific immunohistochemical stain that aids in the differential diagnosis of these entities.

Central giant cell granuloma involves the gnathic bones and mimics "solid ABC." It is usually solid with no or minimal cystic components. Cytologic atypia and necrosis are also not common. Unlike ABC, they lack rearrangement of the *USP6* gene [25].

TREATMENT AND PROGNOSIS

Although the overall prognosis of ABC is good, the goal of any treatment modality is to slow down the disease progression, symptom relief, and fixation or prevention of pathologic fracture. En-bloc resection, although produces the least rate of disease recurrence [26,27], is not commonly performed due to an increased rate of functional impairment and morbidity [28]. Curettage with or without bone grafting is more commonly performed especially in anatomic locations amenable to surgical intervention.

Other therapeutic modalities including percutaneous doxycycline injection [29], arterial embolization, steroid or calcitonin injection, bisphosphonates, and RANKL inhibitors have been shown to be effective in the treatment of ABC in special clinical settings [30-35].

Local recurrence is seen in up to 1/3 of the cases, especially within the few months after the initial treatment, however, it is

very rare after 2 years. Young age and open growth plates are also associated with an increased risk of local recurrence [36]. Rare cases of ABC with metastatic disease have also been reported [37].

CONCLUSION

Proper characterization of primary ABC of bone from ABC-like changes in other benign and malignant diseases requires the correlation of radiographic and pathologic findings. In challenging cases, molecular studies to identify the rearrangement of the *USP6* gene will aid in diagnosis.

Ethics Statement

Not applicable.

Availability of Data and Material

Data sharing not applicable to this article as no datasets were generated or analyzed during the study.

Code Availability

Not applicable.

ORCID

Elham Nasri <https://orcid.org/0000-0001-5894-5865>
John David Reith <https://orcid.org/0000-0002-0542-3042>

Author Contributions

Conceptualization: JDR, EN. Investigation: EN. Project administration: EN. Supervision: JDR. Visualization: EN, JDR. Writing—original draft: EN. Writing—review & editing: EN, JDR. Approval of final manuscript: EN, JDR.

Conflicts of Interest

The authors declare that they have no potential conflicts of interest.

Funding Statement

No funding to declare.

References

- Zehetgruber H, Bittner B, Gruber D, et al. Prevalence of aneurysmal and solitary bone cysts in young patients. *Clin Orthop Relat Res* 2005; 439: 136-43.
- Leithner A, Windhager R, Lang S, Haas OA, Kainberger F, Kotz R. Aneurysmal bone cyst: a population based epidemiologic study and literature review. *Clin Orthop Relat Res* 1999; (363): 176-9.
- Czerniak B. Dorfman and Czerniak's bone tumors, E-Book. 2nd ed. Philadelphia: Elsevier Health Sciences, 2015.
- Martinez V, Sissons HA. Aneurysmal bone cyst: a review of 123 cases including primary lesions and those secondary to other bone pathology. *Cancer* 1988; 61: 2291-304.
- Vergel De Dios AM, Bond JR, Shives TC, McLeod RA, Unni KK. Aneurysmal bone cyst: a clinicopathologic study of 238 cases. *Cancer* 1992; 69: 2921-31.
- Kransdorf MJ, Sweet DE. Aneurysmal bone cyst: concept, controver-

- sy, clinical presentation, and imaging. *AJR Am J Roentgenol* 1995; 164: 573-80.
7. Althof PA, Ohmori K, Zhou M, et al. Cytogenetic and molecular cytogenetic findings in 43 aneurysmal bone cysts: aberrations of 17p mapped to 17p13.2 by fluorescence in situ hybridization. *Mod Pathol* 2004; 17: 518-25.
 8. Ye Y, Pringle LM, Lau AW, et al. *TRE17/USP6* oncogene translocated in aneurysmal bone cyst induces matrix metalloproteinase production via activation of NF- κ B. *Oncogene* 2010; 29: 3619-29.
 9. Oliveira AM, Chou MM. USP6-induced neoplasms: the biologic spectrum of aneurysmal bone cyst and nodular fasciitis. *Hum Pathol* 2014; 45: 1-11.
 10. Weber MG, Fan J, Jenkins R. An Uncommon presentation of an uncommon bone tumor: a case study of a pathologic fracture of an intertrochanteric aneurysmal bone cyst. *Cureus* 2019; 11: e6461.
 11. Novais EN, Rose PS, Yaszemski MJ, Sim FH. Aneurysmal bone cyst of the cervical spine in children. *J Bone Joint Surg Am* 2011; 93: 1534-43.
 12. Papagelopoulos PJ, Currier BL, Shaughnessy WJ, et al. Aneurysmal bone cyst of the spine: management and outcome. *Spine (Phila Pa 1976)* 1998; 23: 621-8.
 13. Revel MB, Vanel D, Sigal R, et al. Aneurysmal bone cysts of the jaws: CT and MR findings. *J Comput Assist Tomogr* 1992; 16: 84-6.
 14. Mahnken AH, Nolte-Ernsting CC, Wildberger JE, et al. Aneurysmal bone cyst: value of MR imaging and conventional radiography. *Eur Radiol* 2003; 13: 1118-24.
 15. Bahk WJ, Mirra JM. Differential diagnostic value of "blue reticulated chondroid-like material" in aneurysmal bone cysts: a classic histopathologic analysis of 215 cases. *Am J Clin Pathol* 2015; 143: 823-9.
 16. Wang JC, Li WS, Kao YC, et al. Clinicopathological and molecular characterisation of USP6-rearranged soft tissue neoplasms: the evidence of genetic relatedness indicates an expanding family with variable bone-forming capacity. *Histopathology* 2021; 78: 676-89.
 17. Sekoranta D, Zupan A, Mavcic B, et al. Novel *ASAP1-USP6*, *FAT1-USP6*, *SARIA-USP6*, and *TNC-USP6* fusions in primary aneurysmal bone cyst. *Genes Chromosomes Cancer* 2020; 59: 357-65.
 18. Guseva NV, Jaber O, Tanas MR, et al. Anchored multiplex PCR for targeted next-generation sequencing reveals recurrent and novel *USP6* fusions and upregulation of *USP6* expression in aneurysmal bone cyst. *Genes Chromosomes Cancer* 2017; 56: 266-77.
 19. Blackburn PR, Davila JI, Jackson RA, et al. RNA sequencing identifies a novel *USP9X-USP6* promoter swap gene fusion in a primary aneurysmal bone cyst. *Genes Chromosomes Cancer* 2019; 58: 589-94.
 20. Warren M, Xu D, Li X. Gene fusions *PFAFH1B1-USP6* and *RUNX2-USP6* in aneurysmal bone cysts identified by next generation sequencing. *Cancer Genet* 2017; 212-213: 13-8.
 21. Mantilla JG, Gross JM, Liu YJ, Hoch BL, Ricciotti RW. Characterization of novel *USP6* gene rearrangements in a subset of so-called cellular fibroma of tendon sheath. *Mod Pathol* 2021; 34: 13-9.
 22. Svajdler M, Michal M, Martinek P, et al. Fibro-osseous pseudotumor of digits and myositis ossificans show consistent *COL1A1-USP6* rearrangement: a clinicopathological and genetic study of 27 cases. *Hum Pathol* 2019; 88: 39-47.
 23. Patel NR, Chrisinger JSA, Demicco EG, et al. USP6 activation in nodular fasciitis by promoter-swapping gene fusions. *Mod Pathol* 2017; 30: 1577-88.
 24. Nakayama S, Nishio J, Aoki M, Koga K, Nabeshima K, Yamamoto T. Ubiquitin-specific peptidase 6 (*USP6*)-associated fibroblastic/myofibroblastic tumors: evolving concepts. *Cancer Genomics Proteomics* 2021; 18: 93-101.
 25. Lee JC, Huang HY. Soft tissue special issue: giant cell-rich lesions of the head and neck region. *Head Neck Pathol* 2020; 14: 97-108.
 26. Campanacci M, Capanna R, Picci P. Unicameral and aneurysmal bone cysts. *Clin Orthop Relat Res* 1986; (204): 25-36.
 27. Mankin HJ, Hornicek FJ, Ortiz-Cruz E, Villafuerte J, Gebhardt MC. Aneurysmal bone cyst: a review of 150 patients. *J Clin Oncol* 2005; 23: 6756-62.
 28. Flont P, Kolacinska-Flont M, Niedzielski K. A comparison of cyst wall curettage and en bloc excision in the treatment of aneurysmal bone cysts. *World J Surg Oncol* 2013; 11: 109.
 29. Shiels WE 2nd, Mayerson JL. Percutaneous doxycycline treatment of aneurysmal bone cysts with low recurrence rate: a preliminary report. *Clin Orthop Relat Res* 2013; 471: 2675-83.
 30. Lange T, Stehling C, Frohlich B, et al. Denosumab: a potential new and innovative treatment option for aneurysmal bone cysts. *Eur Spine J* 2013; 22: 1417-22.
 31. Cornelis F, Truchetet ME, Amoretti N, et al. Bisphosphonate therapy for unresectable symptomatic benign bone tumors: a long-term prospective study of tolerance and efficacy. *Bone* 2014; 58: 11-6.
 32. Falappa P, Fassari FM, Fanelli A, et al. Aneurysmal bone cysts: treatment with direct percutaneous Ethibloc injection: long-term results. *Cardiovasc Intervent Radiol* 2002; 25: 282-90.
 33. Varshney MK, Rastogi S, Khan SA, Trikha V. Is sclerotherapy better than intralesional excision for treating aneurysmal bone cysts? *Clin Orthop Relat Res* 2010; 468: 1649-59.
 34. Rossi G, Rimondi E, Bartalena T, et al. Selective arterial embolization of 36 aneurysmal bone cysts of the skeleton with N-2-butyl cyanoacrylate. *Skeletal Radiol* 2010; 39: 161-7.
 35. Bush CH, Adler Z, Drane WE, Tamurian R, Scarborough MT, Gibbs CP. Percutaneous radionuclide ablation of axial aneurysmal bone cysts. *AJR Am J Roentgenol* 2010; 194: W84-90.
 36. Gibbs CP Jr, Hefele MC, Peabody TD, Montag AG, Aithal V, Simon MA. Aneurysmal bone cyst of the extremities. Factors related to local recurrence after curettage with a high-speed burr. *J Bone Joint Surg Am* 1999; 81: 1671-8.
 37. van de Luijngaarden AC, Veth RP, Slootweg PJ, et al. Metastatic potential of an aneurysmal bone cyst. *Virchows Arch* 2009; 455: 455-9.

Significance of tumor-associated neutrophils, lymphocytes, and neutrophil-to-lymphocyte ratio in non-invasive and invasive bladder urothelial carcinoma

Wael Abdo Hassan^{1,2}, Ahmed Kamal ElBanna^{2,3}, Noha Noufal^{1,4}, Mohamed El-Assmy⁵, Hany Lotfy^{2,6}, Rehab Ibrahim Ali^{1,7}

¹Department of Pathology, Faculty of Medicine, Suez Canal University, El Sheikh Zayed, Egypt;

²Department of Basic Sciences, College of Medicine, Suliman Al Rajhi University, Al Bukairiyah, Saudi Arabia;

³Department of Anatomy, Faculty of Medicine, Al-Azhar University, Cairo, Egypt;

⁴Department of Basic Medical Sciences, College of Medicine, Dar Al Uloom University, Riyadh, Saudi Arabia;

⁵Department of Clinical Sciences, Suliman Al Rajhi University, Bukayriah, Saudi Arabia;

⁶Department of Microbiology and Immunology, Faculty of Medicine, Mansoura University, Mansoura, Egypt;

⁷Department of Pathology, College of Medicine, Jouf University, Al-Jawf, Saudi Arabia

Background: Tumor-infiltrating neutrophils and lymphocytes play essential roles in promoting or combating various neoplasms. This study aimed to investigate the association between tumor-infiltrating neutrophils and lymphocytes and the neutrophil-to-lymphocyte ratio in the progression of urothelial carcinoma. **Methods:** A total of 106 patients diagnosed with urothelial carcinoma were was. Pathological examination for tumor grade and stage and for tumor-infiltrating neutrophils, both CD4 and CD8⁺ T lymphocytes, as well as the neutrophil-to-lymphocyte ratio were evaluated. **Results:** The presence of neutrophils and the neutrophil-to-lymphocyte ratio correlated with high-grade urothelial neoplasms. In both low- and high-grade tumors, the lymphocytes increased during progression from a non-invasive neoplasm to an early-invasive neoplasm. CD8⁺ T lymphocytes increased in low-grade non-muscle-invasive tumors compared to non-invasive tumors. Additionally, there was a significant decrease in CD8⁺ T lymphocytes during progression to muscle-invasive tumors. **Conclusions:** Our results suggest that tumor-infiltrating neutrophils and CD8⁺ T lymphocytes have a significant effect on tumor grade and progression.

Key Words: Bladder urothelial carcinoma; Tumor-associated lymphocyte; Tumor-associated neutrophil; Neutrophil-lymphocyte ratio

Received: September 7, 2022 **Revised:** October 25, 2022 **Accepted:** November 6, 2022

Corresponding Author: Wael Abdo Hassan, PhD, Department of Basic Sciences, College of Medicine, Sulaiman Al Rajhi University, Al Bukairiyah 51941, PO Box 777, Saudi Arabia
 Tel: +966-507091876, Fax: +966-163169090, E-mail: w.hassan@sr.edu.sa

Bladder cancer accounts for 3% of global cancer diagnoses and is estimated to be the 10th most common cancer worldwide [1]. Urothelial carcinoma is the most common type of bladder cancer, constituting up to 95% of bladder malignancies [2]. Most patients with urothelial carcinoma present with either non-invasive papillary neoplasms or superficially invasive tumors limited to the mucosa and submucosa. These neoplasms do not reach the muscle layer (i.e., they constitute non-muscle-invasive urothelial carcinoma [NMIUC; pTa or pT1]). For such neoplasms, transurethral resection of the bladder tumor (TURBT) is followed by adjuvant intravesical instillation therapy [3,4]. However, approximately 30% of patients present with muscle invasion (i.e., muscle-invasive urothelial carcinoma [MIUC]; pT2) [5]. The five-

year survival rate of NMIUC ranges from 50% to 70%, whereas that with MIUC, despite radical cystectomy and chemotherapy, is only 30%–40% [4,5]. Moreover, NMIUC progresses to MIUC in approximately 43% of patients [6]. Thus, despite advancements in the management of bladder carcinomas, the outcomes have remained largely unchanged over several decades [7], highlighting the need to identify additional pathological parameters and biomarkers that could affect carcinogenesis and help improve management procedures [8].

The link between tumor microenvironment inflammation and tumor progression has been reported in several malignancies [9-11]. Neutrophils and lymphocytes are the main inflammatory cells observed in the tumor microenvironment [12]. Several studies

have highlighted the significance of elevated neutrophil-to-lymphocyte ratio (NLR) in patients with urothelial carcinoma and its association with a higher risk of recurrence and progression in NMIUC, as well as increased mortality and decreased overall survival in patients with MIUC [13,14]. Moreover, tumor-associated lymphocytes (TALs) exhibit diverse functions in various subsets. CD8 T lymphocytes are primarily responsible for attacking tumor cells [15,16]. Meanwhile, CD4 T lymphocytes are considered a double-edged immunologic sword: they can initiate and maintain CD8 lymphocyte anti-cancer immune responses [17] but can also convert anti-tumor activity to pro-tumor activity [18]. This study investigated the presence of tumor-associated neutrophils (TANs) and TALs, both CD4 and CD8, in both NMIUC and MIUC and their relation to well-known clinical and pathological prognostic parameters.

MATERIALS AND METHODS

Patients and specimens

This study included 106 patients pathologically diagnosed with urothelial bladder neoplasm by TURBT at Suez Canal University and Ismailia Oncology Hospitals from December 2021 to May 2022. Only cases with bladder urothelial neoplasms were selected. Clinical and pathological data of age, sex, tumor size (maximum diameter of the tumor) and number, pathological grade, and pTNM stage were recorded. The tumors were classified and graded according to the 2016 World Health Organization/International Society of Urological Pathology classification [19].

Histopathological evaluation

The samples were fixed with 10% formalin and embedded in paraffin. From each block, histological sections of 3- μ m thickness were submitted, mounted to a glass slide, stained by hematoxylin and eosin, and reviewed to confirm the diagnosis of urothelial bladder neoplasm and to identify tumor grade, invasion depth, and presence of lympho-vascular invasion. Moreover, TANs and TALs were identified.

Immunohistochemical staining

Sections from the selected paraffin blocks were cut into 4- μ m-thick sections for immunohistochemical (IHC) staining. Slides were prepared and incubated with primary anti-CD8 antibody (anti-CD8 alpha; ab4055, Abcam, Cambridge, UK) and anti-CD4 antibody (anti-CD4; ab133616, Abcam) to further subclassify the tumor-infiltrating lymphocytes (TILs). This was followed by incubation with the appropriate secondary antibody

(anti-rabbit IgG; ab205718, Abcam). All slides were lightly counterstained with hematoxylin for 30 seconds prior to dehydration and mounting.

Histopathological and IHC scoring

TANs or TALs were defined as any neutrophils or lymphocytes that were in close proximity to the tumor base in non-invasive neoplasms or between tumor nests in invasive neoplasms. Four fields from the tumor were selected under low magnification ($\times 100$), and the neutrophils and lymphocytes were counted at high magnification ($\times 400$) using 2D image analysis software (Olympus CellSense, Tokyo, Japan) on an Olympus BX-46 microscope equipped with an Olympus SC30 digital camera. Care was taken not to count such inflammatory cells in areas of ulceration or erosion. Then, the average number was calculated and scored. TANs and TALs (either CD4 or CD8 T lymphocytes) were identified in the lamina propria just beneath the lower margin of the non-invasive urothelial neoplasm or infiltrated in the cancer nests or stroma.

Statistical analysis and data interpretation

Data were fed to a computer and analyzed using IBM SPSS Statistics for Windows ver. 27.0, released 2020 (IBM Corp., Armonk, NY). Qualitative data were described using number and percentage. The quantitative data were described using median (minimum and maximum) and interquartile range (IQR) for non-parametric data and mean and standard deviation for parametric data after determining normality using the Kolmogorov-Smirnov test. Significance of the obtained results was assigned at the (0.05) level.

Data analysis

Qualitative data were analyzed using chi-square test. If more than 25% of cells had a count less than 5 in the tables, the Monte Carlo test was used. Fisher exact test was employed when more than 25% of cells had a count less than five in 2×2 tables. The Mann-Whitney U-test was used to compare two independent groups.

RESULTS

The study included 106 patients with a median age of 58 years and an IQR of 49–66 years. There were 60 males (56.6%) and 46 females (43.4%) who were classified according to the degree of invasion into three groups (Table 1): group 1, non-invasive urothelial carcinoma (NIUC) (36 patients, 34%) (Fig. 1A);

Table 1. Numbers of tumor-associated neutrophils and lymphocytes and NLR in the studied groups classified according to tumor grade and state of tumor invasiveness

Group	No. of cases	TAN (median)	TAL (median)	NLR
Grading: Low				
Non-invasive neoplasms	12	5.5	13.5	0.6
Non-muscle-invasive neoplasms	18	8.0	41.0	0.8
Muscle-invasive neoplasms	12	4.0	35.5	1.7
Grading: High				
Non-invasive neoplasms	24	11.5	12.5	0.5
Non-muscle-invasive neoplasms	20	17.5	28.5	1.2
Muscle-invasive neoplasms	20	30.0	25.5	0.9

NLR, neutrophil-to-lymphocyte ratio; TAN, tumor-associated neutrophils; TAL, tumor-associated lymphocytes.

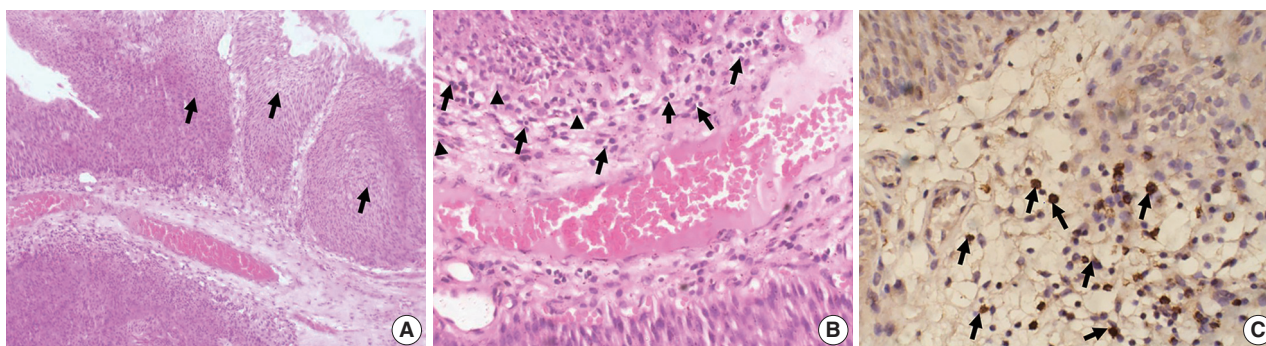


Fig. 1. Tumor-associated neutrophils and CD8⁺ lymphocytes in non-invasive urothelial carcinoma. (A) Representative hematoxylin and eosin (H&E)-stained section of a low-grade papillary (arrows) non-invasive urothelial carcinoma. (B) Higher magnification of the base of the tumor reveals an abundance of lymphocytes (arrows) with few neutrophils (arrowheads). (C) Immunohistochemically, the lymphocytes express CD8 protein (arrows).

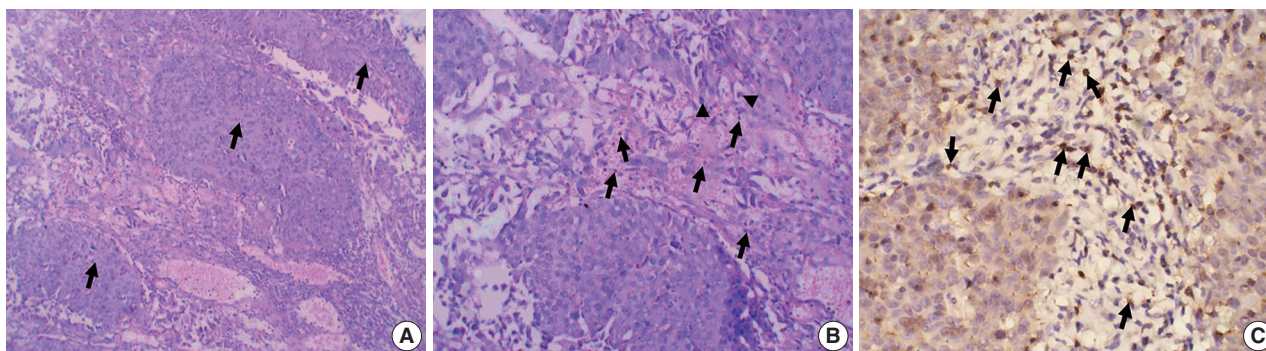


Fig. 2. Tumor-associated neutrophils and CD8⁺ lymphocytes in non-muscle-invasive urothelial carcinoma. (A) Representative hematoxylin and eosin-stained section of a lamina propria (non-muscle) invasive urothelial carcinoma. Tumor tissue grows as nests of malignant urothelial cells (arrows) infiltrating the lamina propria. (B) Higher magnification of the tumor stroma reveals an abundance of lymphocytes (arrows), with few neutrophils (arrowheads). (C) Immunohistochemically, many lymphocytes express CD8 protein (arrows).

group 2, non-muscle-invasive urothelial carcinoma (NMIUC) (38 patients, 35.8%) (Fig. 2A); group 3, MIUC (32 patients, 30.2%) (Fig. 3A).

The patients were further classified according to tumor grade: low-grade urothelial carcinoma (UC) (42 patients, 39.6%), high-grade UC (64 patients, 60.4%).

Significance of neutrophils

The presence of neutrophils correlated with high-grade urothelial neoplasms. Specifically, there was a significant increase in neutrophil number in high-grade UC cases compared to low-grade cases ($p = .005$) (Table 2).

We found a significant increase in the number of neutrophils in the MIUC (Fig. 3B) compared to the NIUC (Fig. 1B) in

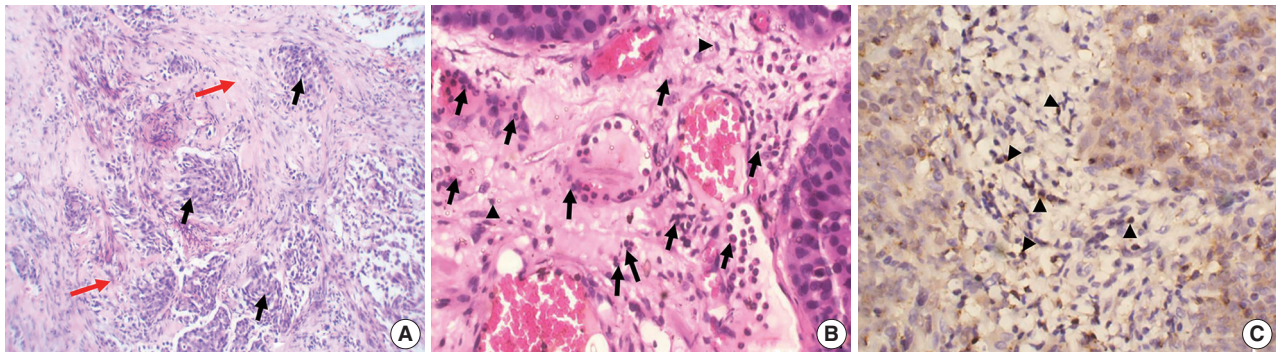


Fig. 3. Tumor-associated neutrophils and CD8⁺ lymphocytes in muscle-invasive urothelial carcinoma. (A) Representative hematoxylin and eosin-stained section of muscle-invasive urothelial carcinoma. Tumor tissue grows as nests of malignant urothelial cells (black arrows) infiltrating the muscle layer (red arrows). (B) Higher magnification of the tumor stroma reveals an abundance of neutrophils (black arrows) with few lymphocytes (arrowheads). Immunohistochemically (C), few lymphocytes express CD8 protein (arrowheads).

Table 2. Significance of tumor-associated neutrophils and lymphocytes, and NLR in the groups studied

Group	TAN	TAL	NLR
Grading: Low			
Non-invasive neoplasms vs. non-muscle-invasive neoplasms	.851	.007	.152
Non-muscle-invasive neoplasms vs. muscle-invasive neoplasms	.550	.315	>.999
Non-invasive neoplasms vs. muscle-invasive neoplasms	.460	.052	.128
Grading: High			
Non-invasive neoplasms vs. non-muscle-invasive neoplasms	.570	.013	.232
Non-muscle-invasive neoplasms vs. muscle-invasive neoplasms	.053	.913	.041
Non-invasive neoplasms vs. muscle-invasive neoplasms	.012	.005	.792

Significant at $p < .05$.

NLR, neutrophil-to-lymphocyte ratio; TAN, tumor-associated neutrophils; TAL, tumor-associated lymphocytes.

high-grade neoplasms ($p = .012$). Similarly, there was a significant increase in neutrophils in the MIUC (Fig. 3B) compared to the NMIUC (Fig. 2B) in high-grade neoplasms ($p = .053$) (Table 2).

On the other hand, the number of neutrophils increased in the NMIUC (Fig. 2B) compared to the NIUC (Fig. 1B) in both low- and high-grade neoplasms; however, the increase was not statistically significant ($p = .851$ and $p = .570$, respectively) (Table 2).

Significance of lymphocytes

The presence of lymphocytes correlated more significantly with progressive invasion of urothelial neoplasms than with neoplasm grade. Nevertheless, there was a decrease in total lymphocyte count in high-grade neoplasms compared to low-grade neoplasms. However, the decrease was not statistically significant ($p = .193$).

Moreover, we identified a significant increase in lymphocytes during progression from NIUC (Fig. 1B) to NMIUC (Fig. 2B) in both low- and high-grade neoplasms ($p = .007$ and $p = .013$, respectively). Additionally, immunohistochemistry showed that the number of CD8⁺ lymphocytes in the low-grade neoplasms was significantly increased ($p = .045$) in the NMIUC group (Fig.

2C) compared to the NIUC group (Table 2, Fig. 1C). Furthermore, we found a significant increase in the lymphocyte count in the MIUC group (Fig. 3B) compared to the NIUC group (Fig. 1B) in both low- and high-grade neoplasms ($p = .052$ and $p = .005$, respectively) (Table 2).

On the other hand, when comparing MIUC (Fig. 3B) with NMIUC (Fig. 2B), there was a decrease in lymphocyte number, although it was not statistically significant in either low- or high-grade neoplasms ($p = .315$ and $p = .913$, respectively) (Table 2). However, there was a significant decrease in CD8⁺ lymphocytes in low-grade MIUC (Fig. 3C) compared to low-grade NMIUC ($p = .052$) (Table 3, Fig. 2C).

Significance of neutrophil-lymphocyte ratio

The NLR correlated with tumor grade; specifically, there was a significant increase in the ratio in high-grade urothelial neoplasms compared to low-grade neoplasms ($p = .003$) (Table 2). We found a significant increase in the NLR in the MIUC cases compared to the NMIUC cases in the high-grade neoplasms ($p = .041$), whereas we found no significant change in the ratio in the low-grade neoplasms (Table 2).

Table 3. Significance of numbers of tumor-associated CD4⁺ and CD8⁺ T lymphocytes in the groups studied

Group	CD4 ⁺ T lymphocytes	CD8 ⁺ T lymphocytes
Grading: Low		
Non-invasive neoplasms vs. non-muscle-invasive neoplasms	.552	.045
Non-muscle-invasive neoplasms vs. muscle-invasive neoplasms	.471	.052
Non-invasive neoplasms vs. muscle-invasive neoplasms	.932	.812
Grading: High		
Non-invasive neoplasms vs. non-muscle-invasive neoplasms	.864	.220
Non-muscle-invasive neoplasms vs. muscle-invasive neoplasms	.425	.821
Non-invasive neoplasms vs. muscle-invasive neoplasms	.791	.335

Significant at $p < .05$.

Meanwhile, there was a non-significant decrease in the NLR in the NMIUC cases compared to the NIUC cases in both low- and high-grade neoplasms ($p = .152$ and $p = .232$, respectively) (Table 2). Similarly, there was a non-significant decrease in the NLR when comparing the NIUC group to the MIUC group in both low- and high-grade neoplasms ($p = .128$ and $p = .792$, respectively) (Table 2).

DISCUSSION

Inflammation within a tumor microenvironment plays an important role in tumor progression. Neutrophils are recognized for their antimicrobial activities and are found in many types of tumors. Early studies have suggested that TANs, which are short-lived, have no role in cancer progression. However, it has recently become evident that TANs with associated inflammation play a significant role in malignancy progression [20]. Neutrophils within tumor nests can induce anti-tumoral immune memory. Alternatively, they may have a pro-tumoral phenotype that promotes angiogenesis, invasion, metastasis, and immunosuppression [21]. This study revealed that the presence of neutrophils correlated with high-grade urothelial neoplasms, as there was a significant increase in neutrophil count in high-grade UC cases compared to low-grade cases ($p = .005$). There was also a significant increase in the number of neutrophils in MIUC cases compared to NIUC cases in high-grade neoplasms ($p = .012$). Similarly, there was a significant increase in neutrophil count in MIUC cases compared to NMIUC cases in high-grade neoplasms ($p = .053$).

The increased number of neutrophils in high-grade tumors and deeply invasive tumors may suggest that TANs are related to a poorer prognosis. Liu et al. [21] revealed similar results in their study on localized bladder cancer; i.e., an increased count of TANs was related to deeper tumor invasion and higher grade. This finding coincided with many studies on various tumor types in different organs, such as renal cell carcinoma, head and neck

squamous cell carcinoma, and pancreatic adenocarcinoma [22-24]. Such pro-tumor activity of neutrophils could be attributed to released matrix of metalloproteinase 9, which frees vascular endothelial growth factor from the extracellular matrix to enhance angiogenesis, and to secreted arginase 1, which suppresses CD8 T lymphocytes. Moreover, TANs generate reactive oxygen species, which induce tumor progression [25,26]. Similarly, TALs have a dual regulatory role as they can induce an anti-tumor immune response by inhibiting tumor growth and tumor progression by creating a microenvironment that stimulates tumor outgrowth [27].

We found a significant increase in lymphocytes during progression from NIUC to NMIUC in both low- and high-grade neoplasms. This finding coincides with a previous study that reported an association between the adaptive immune response and tumor progression [28,29]. Regarding the lymphocyte population, we found that the number of CD8⁺ lymphocytes in low-grade neoplasms was significantly increased in the NMIUC group compared to the NIUC group. Similarly, Pichler et al. [30] and Masson-Lecomte et al. [31] reported an increased number of CD8⁺ lymphocytes in T1 bladder cancer compared to Ta bladder cancer. Moreover, we found a significant decrease in CD8⁺ lymphocytes in low-grade MIUC compared to low-grade NMIUC, indicating a possible role of CD8⁺ lymphocytes in hindering the progression to muscle invasion. This finding coincides with a recent review that evaluated the prognostic role of CD8⁺ TILs in cancer patients treated with immune checkpoint inhibitors. That review showed that CD8⁺ T cells at the invasive margin of tumors were negatively correlated with depth of invasion, and that high CD8⁺ TALs led to a 48% reduction in risk of disease progression compared with low CD8⁺ TILs [32].

On the other hand, Faraj et al. [33] found no significant relation between CD8-expressing T lymphocytes and any clinicopathological parameters; however, they did report a significant correlation with overall survival and disease-specific survival. Unlike our results, Hulsén et al. [34] found significantly higher

values for CD8⁺ T-cell infiltration in grade 3 tumors. They also found that increased CD8 expression was related to decreased survival and increased recurrence and was associated with poor prognosis. They only included specimens were of patients diagnosed with T1 urothelial carcinoma, preventing comparison between tumor stages or relation of their findings to tumor progression [34]. Regarding CD4⁺ lymphocytes, we could not find a significant relation between their number and any of the groups studied. Similar results were obtained by previous studies, which could not show an association between CD4⁺ T cell density and any of the studied clinicopathological variables, including tumor stage and histological grade [35-37]. The relation between neutrophil counts in blood and lymphocytes has been correlated to clinicopathological parameters and has been suggested as a prognostic factor for urothelial carcinoma in many studies [38-40].

In the present study, we investigated the NLR at the tissue level. We found that the ratio correlated with tumor grade, as there was a significant increase in the ratio in high-grade urothelial neoplasms compared to low-grade neoplasms. We found a significant increase in this ratio in the MIUC cases compared to the NMIUC cases in high-grade neoplasms, confirming the tumor-promoting effect of neutrophils. It has been suggested that TANs are different from circulating neutrophils. Specifically, cytokines within the tumor microenvironment induce a population of neutrophils that have a pro-tumor phenotype that inhibits CD8⁺ T cells, and its tumor promotion increases with tumor progression [20]. However, Mandelli et al. [41] found no significant association between the tissue NLR and any of the studied clinicopathological variables, including tumor stage and grade. Such a discrepancy in the results highlights the complexity of the inflammatory response in urothelial carcinogenesis, and that other factors can potentiate or attenuate the role of inflammatory cells as anti- or pro-tumor cells. The importance of TALs is clearly demonstrated by the relation between elevated expression of programmed death-ligand 1 by tumor cells and higher TIL density, as well as by the association with higher histological grade and higher pT category [42].

In summary, this study highlighted the significance of inflammatory cells within the tumor environment of bladder urothelial carcinoma. TANs correlated with tumor grade and stage, whereas TALs, especially CD8⁺ T cells, and the NLR were more likely to be associated with progression of tumor invasion rather than tumor grade. Further prospective multicenter studies with prolonged follow-up are recommended to confirm our results and to elucidate the prognostic role of inflammatory cells in the progression of urothelial carcinoma.

Ethics Statement

All procedures performed in the current study were approved by the Institutional Ethics Review Board of Suez Canal University (4687-5/12/2021) in accordance with the 1964 Helsinki declaration and its later amendments. Informed consent was obtained from all individual participants included in the study. A copy of the written consent is available for review by the Editor-in-Chief of the journal.

Availability of Data and Material

The datasets generated or analyzed during the study are available from the corresponding author on reasonable request.

Code Availability

Not applicable.

ORCID

Wael Abdo Hassan	https://orcid.org/0000-0003-0613-9161
Ahmed Kamal ElBanna	https://orcid.org/0000-0003-2296-5957
Noha Noufal	https://orcid.org/0000-0002-0032-4203
Mohamed El-Assmy	https://orcid.org/0000-0003-3798-5811
Hany Lotfy	https://orcid.org/0000-0002-5743-872X
Rehab Ibrahim Ali	https://orcid.org/0000-0003-0567-6969

Author Contributions

Conceptualization: WAH. Data curation: AKE, NN, MEA, HL. Methodology: WAH, MEA, RIA. Project administration: WAH. Resources: WAH, NN, RIA. Supervision: WAH. Validation: WAH, RIA, NN. Visualization: HL, MEA, AKE. Writing—original draft: WAH, NN, RIA, MEA. Writing—review & editing: HL, AKE. Approval of final manuscript: all authors.

Conflicts of Interest

The authors declare that they have no potential conflicts of interest.

Funding Statement

No funding to declare.

References

- Bray F, Ferlay J, Soerjomataram I, Siegel RL, Torre LA, Jemal A. Global cancer statistics 2018: GLOBOCAN estimates of incidence and mortality worldwide for 36 cancers in 185 countries. *CA Cancer J Clin* 2018; 68: 394-424.
- Miyazaki J, Nishiyama H. Epidemiology of urothelial carcinoma. *Int J Urol* 2017; 24: 730-4.
- Kamat AM, Hahn NM, Efstathiou JA, et al. Bladder cancer. *Lancet* 2016; 388: 2796-810.
- Chang SS, Boorjian SA, Chou R, et al. Diagnosis and treatment of non-muscle invasive bladder cancer: AUA/SUO guideline. *J Urol* 2016; 196: 1021-9.
- Mathieu R, Lucca I, Klatte T, Babjuk M, Shariat SF. Trimodal therapy for invasive bladder cancer: is it really equal to radical cystectomy? *Curr Opin Urol* 2015; 25: 476-82.
- Ceylan C, Doluoglu OG, Keles I, et al. Importance of the neutrophil-to-lymphocyte ratio in muscle-invasive and non-muscle invasive bladder tumors. *Urologia* 2014; 81: 120-4.
- Abdou Hassan W, Shalaby E, Abo-Hashesh M, Ibrahim Ali R. Evaluation of the expression of HER2 and c-KIT proteins as prognostic markers in superficial bladder urothelial carcinoma. *Res Rep Urol* 2021; 13: 197-206.
- Lobo N, Mount C, Omar K, Nair R, Thurairaja R, Khan MS. Landmarks in the treatment of muscle-invasive bladder cancer. *Nat Rev*

- Urol 2017; 14: 565-74.
9. Gakis G, Todenhofer T, Stenzl A. The prognostic value of hematological and systemic inflammatory disorders in invasive bladder cancer. *Curr Opin Urol* 2011; 21: 428-33.
 10. Schepisi G, Santoni M, Massari F, et al. Urothelial cancer: inflammatory mediators and implications for immunotherapy. *BioDrugs* 2016; 30: 263-73.
 11. Cavallo F, De Giovanni C, Nanni P, Forni G, Lollini PL. 2011: the immune hallmarks of cancer. *Cancer Immunol Immunother* 2011; 60: 319-26.
 12. Amulic B, Cazalet C, Hayes GL, Metzler KD, Zychlinsky A. Neutrophil function: from mechanisms to disease. *Annu Rev Immunol* 2012; 30: 459-89.
 13. Mano R, Baniel J, Shoshany O, et al. Neutrophil-to-lymphocyte ratio predicts progression and recurrence of non-muscle-invasive bladder cancer. *Urol Oncol* 2015; 33: 67.
 14. Gondo T, Nakashima J, Ohno Y, et al. Prognostic value of neutrophil-to-lymphocyte ratio and establishment of novel preoperative risk stratification model in bladder cancer patients treated with radical cystectomy. *Urology* 2012; 79: 1085-91.
 15. Ho WY, Yee C, Greenberg PD. Adoptive therapy with CD8(+) T cells: it may get by with a little help from its friends. *J Clin Invest* 2002; 110: 1415-7.
 16. Sato E, Olson SH, Ahn J, et al. Intraepithelial CD8+ tumor-infiltrating lymphocytes and a high CD8+/regulatory T cell ratio are associated with favorable prognosis in ovarian cancer. *Proc Natl Acad Sci U S A* 2005; 102: 18538-43.
 17. Sheu BC, Hsu SM, Ho HN, Lin RH, Torng PL, Huang SC. Reversed CD4/CD8 ratios of tumor-infiltrating lymphocytes are correlated with the progression of human cervical carcinoma. *Cancer* 1999; 86: 1537-43.
 18. Sharma MD, Hou DY, Liu Y, et al. Indoleamine 2,3-dioxygenase controls conversion of Foxp3+ Tregs to TH17-like cells in tumor-draining lymph nodes. *Blood* 2009; 113: 6102-11.
 19. Comperat EM, Burger M, Gontero P, et al. Grading of urothelial carcinoma and the new "World Health Organisation classification of tumours of the urinary system and male genital organs 2016". *Eur Urol Focus* 2019; 5: 457-66.
 20. Uribe-Querol E, Rosales C. Neutrophils in cancer: two sides of the same coin. *J Immunol Res* 2015; 2015: 983698.
 21. Liu K, Zhao K, Wang L, Sun E. The prognostic values of tumor-infiltrating neutrophils, lymphocytes and neutrophil/lymphocyte rates in bladder urothelial cancer. *Pathol Res Pract* 2018; 214: 1074-80.
 22. Jensen HK, Donskov F, Marcussen N, Nordmark M, Lundbeck F, von der Maase H. Presence of intratumoral neutrophils is an independent prognostic factor in localized renal cell carcinoma. *J Clin Oncol* 2009; 27: 4709-17.
 23. Trellakis S, Bruderek K, Dumitru CA, et al. Polymorphonuclear granulocytes in human head and neck cancer: enhanced inflammatory activity, modulation by cancer cells and expansion in advanced disease. *Int J Cancer* 2011; 129: 2183-93.
 24. Naso JR, Topham JT, Karasinska JM, et al. Tumor infiltrating neutrophils and gland formation predict overall survival and molecular subgroups in pancreatic ductal adenocarcinoma. *Cancer Med* 2021; 10: 1155-65.
 25. Lin C, Lin W, Yeh S, Li L, Chang C. Infiltrating neutrophils increase bladder cancer cell invasion via modulation of androgen receptor (AR)/MMP13 signals. *Oncotarget* 2015; 6: 43081-9.
 26. Joseph M, Enting D. Immune responses in bladder cancer-role of immune cell populations, prognostic factors and therapeutic implications. *Front Oncol* 2019; 9: 1270.
 27. Schreiber RD, Old LJ, Smyth MJ. Cancer immunoeediting: integrating immunity's roles in cancer suppression and promotion. *Science* 2011; 331: 1565-70.
 28. Kim HS, Ku JH. Prognostic impact of tumor infiltrating lymphocytes in bladder urothelial carcinoma. *Transl Androl Urol* 2019; 8(Suppl 3): S291-2.
 29. Rouanne M, Betari R, Radulescu C, et al. Stromal lymphocyte infiltration is associated with tumour invasion depth but is not prognostic in high-grade T1 bladder cancer. *Eur J Cancer* 2019; 108: 111-9.
 30. Pichler R, Fritz J, Zavadil C, Schafer G, Culig Z, Brunner A. Tumor-infiltrating immune cell subpopulations influence the oncologic outcome after intravesical bacillus Calmette-Guerin therapy in bladder cancer. *Oncotarget* 2016; 7: 39916-30.
 31. Masson-Lecomte A, Maille P, Pineda S, et al. CD8+ cytotoxic immune infiltrate in non-muscle invasive bladder cancer: a standardized methodology to study association with clinico-pathological features and prognosis. *Bladder Cancer* 2019; 5: 159-69.
 32. Li F, Li C, Cai X, et al. The association between CD8+ tumor-infiltrating lymphocytes and the clinical outcome of cancer immunotherapy: a systematic review and meta-analysis. *EClinicalMedicine* 2021; 41: 101134.
 33. Faraj SE, Munari E, Guner G, et al. Assessment of tumoral PD-L1 expression and intratumoral CD8+ T cells in urothelial carcinoma. *Urology* 2015; 85: 703.
 34. Hulsen S, Lippolis E, Ferrazzi F, et al. High stroma T-cell infiltration is associated with better survival in stage pT1 bladder cancer. *Int J Mol Sci* 2020; 21: 8407.
 35. Zhang Q, Hao C, Cheng G, et al. High CD4(+) T cell density is associated with poor prognosis in patients with non-muscle-invasive bladder cancer. *Int J Clin Exp Pathol* 2015; 8: 11510-6.
 36. Yu A, Mansure JJ, Solanki S, et al. Presence of lymphocytic infiltrate cytotoxic T lymphocyte CD3+, CD8+, and immunoscore as prognostic marker in patients after radical cystectomy. *PLoS One* 2018; 13: e0205746.
 37. Shi MJ, Meng XY, Wu QJ, Zhou XH. High CD3D/CD4 ratio predicts better survival in muscle-invasive bladder cancer. *Cancer Manag Res* 2019; 11: 2987-95.
 38. Favilla V, Castelli T, Urzi D, et al. Neutrophil to lymphocyte ratio, a biomarker in non-muscle invasive bladder cancer: a single-institutional longitudinal study. *Int Braz J Urol* 2016; 42: 685-93.
 39. Kawahara T, Furuya K, Nakamura M, et al. Neutrophil-to-lymphocyte ratio is a prognostic marker in bladder cancer patients after radical cystectomy. *BMC Cancer* 2016; 16: 185.
 40. Tazeh NN, Canter DJ, Damodaran S, et al. Neutrophil to lymphocyte ratio (NLR) at the time of transurethral resection of bladder tumor: a large retrospective study and analysis of racial differences. *Bladder Cancer* 2017; 3: 89-94.
 41. Mandelli GE, Missale F, Bresciani D, et al. Tumor infiltrating neutrophils are enriched in basal-type urothelial bladder cancer. *Cells* 2020; 9: 291.
 42. Nukui A, Kamai T, Arai K, et al. Association of cancer progression with elevated expression of programmed cell death protein 1 ligand 1 by upper tract urothelial carcinoma and increased tumor-infiltrating lymphocyte density. *Cancer Immunol Immunother* 2020; 69: 689-702.

Current state of cytopathology residency training: a Korean national survey of pathologists

Uiju Cho¹, Tae Jung Kim², Wan Seop Kim³, Kyo Young Lee⁴, Hye Kyoung Yoon⁵, Hyun Joo Choi¹,
The Fellowship Council and Committee of Quality Improvement of the Korean Society for Cytopathology

¹Department of Pathology, St. Vincent's Hospital, The College of Medicine, The Catholic University of Korea, Seoul;

²Department of Pathology, Yeouido St. Mary's Hospital, College of Medicine, The Catholic University of Korea, Seoul;

³Department of Pathology, Konkuk University School of Medicine, Seoul;

⁴Department of Pathology, Konkuk University Chungju Hospital, Chungju;

⁵Department of Pathology, Inje University Busan Paik Hospital, Inje University College of Medicine, Busan, Korea

Background: Although the Korean Society for Cytopathology has developed educational goals as guidelines for cytopathology education in Korea, there is still no systematic approach to cytopathology education status for pathology residents. Furthermore, satisfaction with cytopathology education and with the outcome of the current training/educational program has not been investigated in Korea. This study aimed to obtain comprehensive data on the current state of cytopathology education for residents and evaluate education outcomes. **Methods:** An online survey was conducted in December 2020 for the board-certified pathologists and training residents registered as members of the Korean Society for Cytopathology. The questionnaire comprised questions that investigated the current status of cytopathology at each training institution, the degree of satisfaction with the work and education related to cytopathology, outcomes of cytopathology training, and educational accomplishments. **Results:** Of the participants surveyed, 12.3% (132/1,075) completed the questionnaire, and 36.8% (32/87) of cytopathology residents participated. The mean overall satisfaction with cytopathology education was 3.1 points (on a 1- to 5-point scale, 5: very satisfied). The most frequent suggestion among the free description format responses was to expand educational opportunities, such as online education opportunities, outside of the individual institutions. **Conclusions:** Our results showed that cytopathology training in Korea needs further improvement. We expect that this study will inform systematic training of competent medical personnel armed with broad cytopathology knowledge and strong problem-solving abilities.

Key Words: Cytopathology; Education; Residents; Statistics; Surveys

Received: December 9, 2022 **Revised:** December 19, 2022 **Accepted:** January 6, 2023

Corresponding Author: Hyun Joo Choi, MD, Department of Pathology, St. Vincent's Hospital, College of Medicine, The Catholic University of Korea, 93 Jungbu-daero, Paldal-gu, Suwon 16247, Korea
Tel: +82-31-249-7592, Fax: +82-31-244-6786, E-mail: chj0103@catholic.ac.kr

Cytopathology is important not only for disease diagnosis and healthcare but also for the Korean National Cancer Screening and Prevention Program [1,2]. The field of cytopathology has been a major component of pathology since its inception. The Korean Society for Cytopathology (KSC) was established nearly 40 years ago for quality control, development, and education in the field of cytopathology [3].

Although the KSC develops educational goals as a guideline for cytopathology education in Korea, there has been no systematic approach to understanding the current cytopathology training status for pathology residents. In addition, satisfaction with cytopathology education and with the outcomes of the current

training/educational program has not been investigated in Korea. There is also a concern that the current training program for pathology residents does not focus sufficiently on cytopathology, especially because the field is so clinically diverse and continues to play an important role in patient management and cancer screening.

As an initial step to ensure higher standards of cytopathology training, we conducted a survey among pathology residents and pathologists to obtain their views on the current status of cytopathology education and training. With the support of the KSC, this research aimed to obtain comprehensive data on the current state of cytopathology education for residents and to evaluate

educational outcomes as a baseline evaluation for further improvement of cytopathology training in Korea.

MATERIAL AND METHODS

Survey participants and implementation

The survey was conducted among 988 board-certified pathologists and 87 training residents registered as members of the KSC. A series of questions addressing cytopathology residency training were developed, edited, and revised according to the KSC mission on clarity, quality, appropriateness, and importance. In December 2020, we conducted an online, confidential survey of KSC members. The questionnaire was uploaded onto an online survey site. KSC members were invited by email to participate, and an additional invitation was posted on social media for non-responsive residents.

Survey instrument and statistical analysis

The survey questionnaire included both closed- and open-ended questions. The questionnaire was divided into the following five sections: (1) general information, (2) current resident cytopathology training curriculum, (3) degree of resident satisfaction with the cytopathology training curriculum, (4) performance prediction and directions for improvement, and (5) training transfer. A total of 62 questions were included in the survey. Section 3 was filled out only by the pathology residents. These questions were rated on a 5-point Likert scale (5, strongly agree; 4, agree; 3, neutral; 2, disagree; and 1, strongly disagree). Residents who responded with 3, 4, or 5 were considered “satisfied”, and those who responded with 1 or 2 were considered “unsatisfied”. There were also open-ended questions about why responders were unsatisfied with the training curriculum and suggestions for improvements were requested (see Supplementary Data S1 for full survey and response statistics). Descriptive statistics were used to summarize demographics and outcome measures.

RESULTS

General information

The response rate for the survey was 12.3% ($n=132/1,075$). The respondents were 32 training residents (24.2%) and 100 board-certified pathologists (75.8%). The response rate among the residents was 36.8% ($n=32/87$). However, one of the resident responders did not participate in section 3; therefore, the total number of responses to this section was 31. Twenty-five of the board-certified pathologists were currently directors of the de-

partments where they worked. By practice experience, 57% of the pathologists had more than 16 years, 9% had 11 to 15 years, 21% had 6 to 10 years, and 13% had less than 5 years. Furthermore, 29% of their institutions had residents in training at the time of the survey.

Current resident cytopathology training curriculum

This section was answered by residents and pathologists who had pathology residents in their institution. The proportion of respondents who answered that there was no training period exclusively dedicated to cytopathology was 52.5%. The proportion of those who had more than 3 months of cytopathology training was 36.1%. Regarding the percentage of training time allocated to cytopathology training or work time, 49.2% answered that cytopathology training comprised 10%–25% of the training period. The beginning of cytopathology education was most often in the second year of residency (59.0%), followed by the first (31.1%) and third years (9.8%). Most hospitals (63.9%) did not further divide the training program according to specific cytopathology fields (e.g., gynecologic vs. non-gynecologic). Of the respondents, 77.1% answered that the frequency of diagnosing cytopathology slides (i.e., signing-out) with the residents was more than 4 times per month. The following knowledge and skills were studied in Korean pathology departments: (1) screening of marked cytopathology slides, 85.2%; (2) preparing draft reports, 80.3%; (3) attending onsite rapid assessment of fine needle aspiration (FNA) or endobronchial ultrasound FNA, 44.3%; (4) screening of unmarked cytopathology slides, 41.0%; and (5) performing FNA, 1.6%. The majority of the institutions did not have designated conference time for cytopathology education (78.7%). In terms of the frequency of cytopathology education sessions, in 47.5% they occurred less than 3 times a year, and 31.1% reported none each year. Furthermore, regarding the frequency with which residents attended cytopathology conferences, seminars, or workshops held by the cytopathology society or other external organizations, 67.2% attended 2–6 times a year.

In the open-ended question, respondents were asked to express their opinion on the current cytopathology training program in Korea. Overall, 12% (16/132) of the respondents left comments, and the most common opinion was that the cytopathology society needed to organize more educational programs, especially further implementation of online education (from 10 respondents) (see Supplementary Data S1 for the other responses).

Degree of resident satisfaction with the cytopathology training curriculum

This section was answered only by residents who were in training at the time of the survey. This section asked questions that concerned three areas: (1) overall satisfaction with the cytopathology training program, (2) satisfaction with the training practices and specific training fields, and (3) satisfaction with the training environment. The mean overall satisfaction with the cytopathology training program was 3.1 (Fig. 1). Satisfaction with training practice and specific training fields ranged from 2.7 to 3.5 (Fig. 2). Sign-out with a senior pathologist was rated as the most satisfactory field of the training (average rating, 3.5). Training and on-site assessment of FNA specimens was rated as the most unsatisfactory field of the training (average rating, 2.7). Pathology residents rated satisfaction with the cytopathology training environment (e.g., number of teaching pathologists, reference bibliographies, and teaching or reference slides) as 3.2–3.3 (Fig. 3).

Performance prediction and directions for the improvement

All the respondents answered questions in this section. We first asked whether practicing pathologists and residents were familiar with the current cytopathology training guidelines that were established by the KSC [4]. According to the survey results, 41.7% of the participants acknowledged being aware of the guidelines, albeit not entirely familiar, while 46.2% reported not knowing the guideline. When the residents were asked whether the current education and training system could help them accomplish the training goals suggested by the KSC guidelines, 44.7% were neutral and 32.5% answered that they were likely to accomplish the training goal. Among the 42 responders who did not feel they would gain the ability to competently make a cytopathology diagnosis upon completion of training, lack of specific curriculum and training time (57.1%) and lack of diverse cytopathology cases during training (23.8%) were selected as the main reasons.

Questionnaire items	Frequencies of satisfaction scores ^a					Average of satisfaction scores	Percentage of satisfaction
	1, strongly disagree	2, disagree	3, neutral	4, agree	5, strongly agree		
Q1. I am satisfied with the current overall cytopathology training	12.9%	16.1%	32.3%	29.0%	9.7%	3.1	71.0%
Q2. I am satisfied with the current overall gynecologic cytopathology training	19.4%	22.6%	22.6%	22.6%	12.9%	2.9	58.1%
Q3. I am satisfied with the current overall non-gynecologic cytopathology training	16.1%	19.4%	19.4%	32.3%	12.9%	3.1	64.5%
Q4. I am satisfied with the training hours occupied by the cytopathology during pathology resident training period	19.4%	9.7%	32.3%	29.0%	9.7%	3.0	71.0%

Fig. 1. Overall satisfaction ratings provided by residents. ^a31 Responders answered.

Questionnaire items	Frequencies of satisfaction scores ^a					Average of satisfaction scores	Percentage of satisfaction
	1, strongly disagree	2, disagree	3, neutral	4, agree	5, strongly agree		
Q1. I am satisfied with the training practice - slide screening and preparing draft reports	9.7%	12.9%	35.5%	25.8%	16.1%	3.3	77.4%
Q2. I am satisfied with the training practice -sign out reports to diagnose with pathologist	6.5%	6.5%	38.7%	25.8%	22.6%	3.5	87.1%
Q3. I am satisfied with the training practice - institutional education sessions (e.g., lecture)	19.4%	19.4%	32.3%	19.4%	9.7%	2.8	61.3%
Q4. I am satisfied with the education on criteria and guidelines	16.1%	12.9%	38.7%	22.6%	9.7%	3.0	71.0%
Q5. I am satisfied with the case conferences	16.1%	16.1%	38.7%	19.4%	9.7%	2.9	67.7%
Q6. I am satisfied with the education and conferences provided by society or other institutions	12.9%	9.7%	35.5%	29.0%	12.9%	3.2	77.4%
Q7. I am satisfied with the training on FNA and on-site rapid assessment	25.8%	12.9%	35.5%	16.1%	9.7%	2.7	61.3%
Q8. I am satisfied with the training on quality control and laboratory management	19.4%	3.2%	45.2%	19.4%	12.9%	3.0	77.4%
Q9. I am satisfied with the training on digital pathology and automated screening system	25.8%	9.7%	32.3%	22.6%	9.7%	2.8	64.5%
Q10. I am satisfied with cytopathology research participation	25.8%	9.7%	32.3%	19.4%	12.9%	2.8	64.5%

Fig. 2. Satisfaction with cytopathology training practices and specific training fields. FNA, fine needle aspiration. ^a31 Responders answered.

The second group of questions was about fields of training that needed strengthening. Among gynecologic and several non-gynecologic fields, gynecologic cytopathology and thyroid FNA were chosen as the training sectors that needed to be strengthened (average rating, 3.8) (Fig. 4).

The third group of questions was about the predicted performance of the cytopathology training. The respondents expected that the current cytopathology training system would most likely enhance cytopathology diagnostic skills (average rating, 3.4) but was unlikely to enhance understanding and skills regarding digital pathology and automated screening systems (average rating, 2.8) (Fig. 5).

In the open-ended question, respondents expressed the need for more exposure to diverse specimens, the need for an improved cytopathology training program, and continuing education for the pathologists who train residents. More opinions are provided in Supplementary Data S1.

Training transfer

Respondents mostly stated that they applied what they learned during cytopathology training in real-world practice (average

rating, 3.7), that their cytopathology training enhanced their performance at work (average rating, 3.7), and that they have tried to apply what they learned in the training process to their actual work tasks (average rating, 3.8). Also, most residents stated that the cytopathology training program has enhanced their job expertise (average rating, 3.7) (Fig. 6).

DISCUSSION

This study is the first survey addressing the current status and perspectives on cytopathology training in Korea. Globally, reports or surveys on the status of cytopathology training are scarce [5-8]. Based on the survey results, most institutions did not have an exclusive cytopathology training period for the residents (52.5% of respondents), and the training period was approximately 10%–20% of the workload. Mostly, the training comprised drafting a diagnosis in cytopathology cases (80.3%) that was prescreened and marked by cytotechnicians (85.2%). The residents had sign-out sessions with board-certified pathologists once (27.9%) or more than twice (49.2%) per week. There were very few intra-institutional cytopathology conferences or educa-

Questionnaire items	Frequencies of satisfaction scores ^a					Average of satisfaction scores	Percentage of satisfaction
	1, strongly disagree	2, disagree	3, neutral	4, agree	5, strongly agree		
Q1. There are enough pathologists who direct or teach cytopathology	16.1%	16.1%	19.4%	25.8%	22.6%	3.2	67.7%
Q2. There are sufficient cytopathology references and books	9.7%	16.1%	22.6%	35.5%	16.1%	3.3	74.2%
Q3. There are sufficient educational or reference slides	12.9%	16.1%	29.0%	22.6%	19.4%	3.2	71.0%

Fig. 3. Satisfaction with the training environment. ^a31 Responders answered.

Questionnaire items	Frequencies of satisfaction scores ^a					Average of agreement
	1, strongly disagree	2, disagree	3, neutral	4, agree	5, strongly agree	
Q1. Gynecologic cytopathology training should be strengthened	0.0%	6.8%	37.1%	28.8%	27.3%	3.8
Q2. Non-gynecologic: respiratory cytopathology training should be strengthened	0.0%	6.8%	40.2%	31.8%	21.2%	3.7
Q3. Non-gynecologic: urine cytopathology training should be strengthened	0.8%	5.3%	37.1%	35.6%	21.2%	3.7
Q4. Non-gynecologic: salivary gland, lymph node, and pancreaticobiliary cytopathology training should be strengthened	0.8%	6.1%	33.3%	38.6%	21.2%	3.7
Q5. Non-gynecologic: thyroid gland cytopathology training should be strengthened	0.8%	4.5%	34.1%	31.1%	29.5%	3.8
Q6. Non-gynecologic: other areas (e.g., cerebrospinal fluid and breast) of cytopathology training should be strengthened	4.5%	6.1%	48.5%	26.5%	14.4%	3.4

Fig. 4. Areas of cytopathology training that should be strengthened. ^a132 Responders answered.

tion sessions, less than three sessions per year.

The overall satisfaction rating on cytopathology education was 3.1 among the pathology residents. In specific fields, sign out sessions with board-certified pathologists were rated as the most satisfactory of the training program (average rating, 3.5), while training on the FNA technique was rated as the least sat-

isfactory (average rating, 2.7). We found that the traditional training approach, which requires enhancing the experience through co-sign-out of the diagnosis and is often called apprenticeship education, was satisfactory and necessary. However, there seems to be little training time or education resources allocated to cytopathology training. The reality is that many board-certi-

Questionnaire items	Frequencies of satisfaction scores ^a					Average of agreement
	1, strongly disagree	2, disagree	3, neutral	4, agree	5, strongly agree	
Q1. Current cytopathology training will improve cytopathology diagnostic skills	4.5%	7.6%	42.4%	36.4%	9.1%	3.4
Q2. Current cytopathology training will improve the ability to analyze differences between histologic and cytopathologic findings	5.3%	7.6%	45.5%	34.1%	7.6%	3.3
Q3. Current cytopathology training will improve communication skills with colleagues, including clinicians	6.1%	9.1%	47.0%	31.8%	6.1%	3.2
Q4. Current cytopathology training will improve the ability to apply ancillary staining methods in cytopathology	4.5%	12.1%	41.7%	34.1%	7.6%	3.3
Q5. Current cytopathology training will improve the understanding of pre-analytical conditions	5.3%	15.9%	45.9%	28.8%	4.5%	3.1
Q6. Current cytopathology training will improve basic knowledge on cytopathology	4.5%	12.9%	40.9%	34.8%	6.8%	3.3
Q7. Current cytopathology training will improve research ability in cytopathology	9.1%	20.5%	37.9%	28.0%	4.5%	3.0
Q8. Current cytopathology training will improve quality control and laboratory management abilities	5.3%	15.9%	40.2%	32.6%	6.1%	3.2
Q9. Current cytopathology training will improve understanding and use of diagnostic systems, such as, the cervical pap smear Bethesda system	5.3%	7.6%	35.6%	39.4%	12.1%	3.5
Q10. Current cytopathology training will improve understanding and use of diagnostic systems, such as, the thyroid Bethesda, salivary Milan, and urine Paris systems	3.8%	6.8%	40.2%	42.4%	6.8%	3.4
Q11. Current cytopathology training will improve understanding and use of digital pathology and automated screening system	15.2%	20.5%	37.9%	22.7%	3.8%	2.8
Q12. Current cytopathology training will improve the use of molecular cytopathology	12.1%	21.2%	37.9%	25.8%	3.0%	2.9
Q13. Upon completion of a four-year training, the residents will have the ability to independently and competently make a cytopathology diagnosis	10.6%	21.2%	34.8%	28.8%	4.5%	3.0

Fig. 5. Performance prediction. ^a132 Responders answered.

Questionnaire items	Frequencies of satisfaction scores ^a					Average of agreement
	1, strongly disagree	2, disagree	3, neutral	4, agree	5, strongly agree	
Q1. I am using what I learned in cytopathology training in real-time work	2.3%	5.3%	30.3%	41.7%	20.5%	3.7
Q2. What I learned during cytopathology training has improved my performance	3.0%	3.8%	32.6%	43.2%	17.4%	3.7
Q3. I am applying what I have learned in the cytopathology training to real work	3.8%	1.5%	26.5%	46.2%	22.0%	3.8
Q4. After the cytopathology training, I receive positive evaluation from the seniors or colleagues about my improved work performance	3.8%	7.6%	49.2%	30.3%	9.1%	3.3
Q5. What I learned during the cytopathology training helped me solve problems in real-time work that deals with patients	3.0%	4.5%	40.9%	39.4%	12.1%	3.5
Q6. Cytopathology training has improved my job expertise	3.0%	2.3%	35.6%	43.9%	15.2%	3.7
Q7. Cytopathology training has improved my communication skills with the patients and clinicians	5.3%	6.1%	39.4%	39.4%	9.8%	3.4

Fig. 6. Training transfer. ^a132 Responders answered.

fied pathologists have an excessive workload; thus, it may be difficult for them to dedicate additional time for residency training and co-sign-out. Our study underlines the importance of education through personal teaching and a co-sign out approach; therefore, a systematic effort to provide sufficient educational opportunities is needed.

The field of education that needs to be strengthened the most is gynecologic cytopathology and thyroid FNA cytopathology (average rating, 3.8). According to nationwide survey data, gynecology and thyroid FNA are the most frequently performed cytopathology examinations [3]. The reason they were selected as an area that needed to be strengthened may be because of the high demand for those areas in real-time diagnostic work. Generally, most residents expected that they would be able to work independently and proficiently diagnose cases related to cytopathology after completing residency training (average rating, 3.0). However, many opinions have suggested that the lack of specific cytopathology training curricula and training time may affect residents' competence in cytopathology. A lack of training time was noted in a European cytopathology training survey [6]. The KSC developed training performance and goals for pathology residents, but few pathologists and residents were familiar with these guidelines (average rating, 2.5). It is necessary to reflect on the extent to which these guidelines have been used in individual institutions.

Even though there were many opinions that highlighted the lack of education and training time for cytopathology, the respondents rated training transfer questions as 3.0 or more. This suggests that cytopathology training has been useful and effective in the daily work of the respondents. Cytopathology training will progress if the results from this survey are reflected in future training development.

The low response rate is the major limitation of this survey. The response rate among residents (36.8%) was higher than that of board-certified pathologists (10.1%), but the responses may not fully reflect the opinions of all residents.

In this survey, there were several suggestions for improving cytopathology education in the future that seemed necessary. First, the respondents suggested that a systematic residency training program should be implemented at each institution. It is necessary to consider the strengths and weaknesses of the current training system and to reinforce areas with low satisfaction. Second, they suggested that guidelines for a systematic residency training program should be provided by the KSC. The goals and guidelines of current residency training state the depth of experience in diagnosis and fields that the residents should be trained in.

However, there is no specific action plan, such as how the residents should be taught or the minimum training period required. This guide does not need to be regulatory or mandatory; however, it will still be helpful to each institution that attempts to improve their cytopathology training program [7,9]. Currently, the qualification requirement for pathology board certification does not include minimum educational participation hours in the field of cytopathology. Creating such a requirement could be one approach to increasing educational opportunities, such as intradepartmental cytopathology conferences or society education, and to encourage participation of residents in these educational opportunities. Lastly, the respondents suggested that more diverse educational programs should be provided by the academic society. Online education, case galleries, and clinical case-oriented education sessions were suggested as solutions. This survey was conducted at a time when most academic events were suspended due to the coronavirus disease 2019 (COVID-19) pandemic. Therefore, the lack of educational opportunities reported may have been due to the COVID-19 situation. With these results, we hope that institutions and the KSC can develop more diverse educational programs, such as an on-demand online educational program. The KSC is currently developing an online educational site that reflects the study suggestions, and the site will be launched soon.

This study is expected to improve the quality of cytopathology education, provide opportunities to standardize cytopathology education for residents, and to serve as a basis for improvement in cytopathology education for both residents and practicing pathologists. We expect that this study will inform systematic training for competent medical personnel armed with broad knowledge of cytopathology and strong problem-solving abilities.

Supplementary Information

The Data Supplement is available with this article at <https://doi.org/10.4132/jptm.2023.01.06>.

Ethics Statement

All procedures performed in the current study were approved by the Institutional Review Board of St. Vincent's Hospital (VC20QCDI0083) in accordance with the 1964 Helsinki Declaration and its later amendments. The need for formal written informed consent was waived by the institutional review board.

Availability of Data and Material

The datasets generated or analyzed during the study are available from the corresponding author on reasonable request.

Code Availability

Not applicable.

ORCID

Uiju Cho <https://orcid.org/0000-0002-6229-8418>
 Tae Jung Kim <https://orcid.org/0000-0003-3140-3681>
 Wan Seop Kim <https://orcid.org/0000-0001-7704-5942>
 Kyo Young Lee <https://orcid.org/0000-0001-9954-8583>
 Hye Kyung Yoon <https://orcid.org/0000-0003-0714-8537>
 Hyun Joo Choi <https://orcid.org/0000-0003-2292-424X>

Author Contributions

Conceptualization: HJC, TJK. Data curation: UC. Formal analysis: UC. Funding acquisition: HJC. Investigation: HJC, UC. Methodology: HJC, UC, TJK. Project administration: HJC. Resources: UC. Software: UC. Supervision: HJC. Validation: HJC, UC. Visualization: HJC, UC. Writing—original draft: UC. Writing—review & editing: HJC, TJK, WSK, KYL, HKY. Approval of final manuscript: all authors.

Conflicts of Interest

The authors declare that they have no potential conflicts of interest.

Funding Statement

This study was funded by the Korean Society for Cytopathology, Korea (Grant number: 2017-02).

Acknowledgments

The authors would like to acknowledge the Korean Society for Cytopathology for providing the funding necessary to conduct this study. We also thank the Fellowship Council and the Committee of Quality Improvement of the Korean Society for Cytopathology for its guidance in preparing and

conducting this survey.

References

1. Lim SC, Yoo CW. Current status of and perspectives on cervical cancer screening in Korea. *J Pathol Transl Med* 2019; 53: 210-6.
2. Min KJ, Lee YJ, Suh M, et al. The Korean guideline for cervical cancer screening. *J Gynecol Oncol* 2015; 26: 232-9.
3. Oh EJ, Jung CK, Kim DH, et al. Current cytology practices in Korea: a nationwide survey by the Korean Society for Cytopathology. *J Pathol Transl Med* 2017; 51: 579-87.
4. Korean Society for Cytopathology [Internet]. Seoul: Korean Society for Cytopathology, 2022 [cited 2022 Aug 3]. Available from: https://www.cytopathol.or.kr/resident_01.asp.
5. Cohen MB, Perez-Reyes N, Stoloff AC. The status of residency training in cytopathology. *Diagn Cytopathol* 1995; 12: 186-7.
6. Anshu, Herbert A, Cochand-Priollet B, et al. Survey of medical training in cytopathology carried out by the Journal Cytopathology. *Cytopathology* 2010; 21: 147-56.
7. Yu GH; Accreditation Council for Graduate Medical Education. Goals and guidelines for residency training in cytopathology. *Diagn Cytopathol* 2011; 39: 455-60.
8. Gill B, Slater S. What should be done to improve cytopathology training in the UK? *Cytopathology* 2010; 21: 142-4.
9. Tambouret R, Nayar R, Pitman MB, Ehya H. Standardized cytopathology training through accreditation in the United States. *Cytopathology* 2010; 21: 139-41.

Postmortem lung and heart examination of COVID-19 patients in a case series from Jordan

Maram Abdaljaleel^{1,2}, Isra Tawalbeh³, Malik Sallam^{1,2,4}, Amjad Bani Hani⁵, Imad M. Al-Abdallat^{1,2}, Baheth Al Omari^{1,2}, Sahar Al-Mustafa^{1,2}, Hasan Abder-Rahman^{1,2}, Adnan Said Abbas³, Mahmoud Zureigat³, Mousa A. Al-Abbadi^{1,2}

¹Department of Pathology, Microbiology and Forensic Medicine, School of Medicine, The University of Jordan, Amman;

²Department of Clinical Laboratories and Forensic Medicine, Jordan University Hospital, Amman;

³Department of Forensic Pathology, Ministry of Health, Amman, Jordan;

⁴Department of Translational Medicine, Faculty of Medicine, Lund University, Malmö, Sweden;

⁵Department of General Surgery, School of Medicine, The University of Jordan, Amman, Jordan

Background: Coronavirus disease 2019 (COVID-19) has emerged as a pandemic for more than 2 years. Autopsy examination is an invaluable tool to understand the pathogenesis of emerging infections and their consequent mortalities. The aim of the current study was to present the lung and heart pathological findings of COVID-19-positive autopsies performed in Jordan. **Methods:** The study involved medicolegal cases, where the cause of death was unclear and autopsy examination was mandated by law. We included the clinical and pathologic findings of routine gross and microscopic examination of cases that were positive for COVID-19 at time of death. Testing for severe acute respiratory syndrome coronavirus 2 (SARS-CoV-2) was confirmed through molecular detection by real-time polymerase chain reaction, serologic testing for IgM and electron microscope examination of lung samples. **Results:** Seventeen autopsies were included, with male predominance (76.5%), Jordanians (70.6%), and 50 years as the mean age at time of death. Nine out of 16 cases (56.3%) had co-morbidities, with one case lacking such data. Histologic examination of lung tissue revealed diffuse alveolar damage in 13/17 cases (76.5%), and pulmonary microthrombi in 8/17 cases (47.1%). Microscopic cardiac findings were scarcely detected. Two patients died as a direct result of acute cardiac disease with limited pulmonary findings. **Conclusions:** The detection of SARS-CoV-2 in postmortem examination can be an incidental or contributory finding which highlights the value of autopsy examination to determine the exact cause of death in controversial cases.

Key Words: Postmortem examination; Forensic medicine; Betacoronavirus; Virology; Diffuse alveolar damage

Received: November 27, 2022 **Revised:** January 6, 2023 **Accepted:** January 30, 2023

Corresponding Author: Malik Sallam, MD, PhD, Department of Clinical Laboratories and Forensic Medicine, Jordan University Hospital, Queen Rania Al-Abdullah Street-Aljubeiha/P.O. Box 13046, Amman, Jordan
 Tel: +962-6-5353666 (ext. 2811), E-mail: malik.sallam@ju.edu.jo

Since the declaration of coronavirus disease 2019 (COVID-19) as a pandemic, several parameters have been used to measure its public health impact [1]. These statistical measures include the rate of detected cases, rate of critical cases, and importantly the rate of death as a result of the disease [2]. The case fatality ratio (CFR) can be used to evaluate the severity among the detected cases; nevertheless, this parameter is prone to inherent bias in light of the following factors: (1) the guidelines for COVID-19 testing vary in different countries, with subsequent underestimation of true number of cases; (2) the postmortem detection of severe acute respiratory syndrome coronavirus 2 (SARS-CoV-2) does not necessarily indicate its causal role in death which may

cause an overestimation of the CFR; and (3) the time lags in handling and reporting of recovery and mortality from the disease which can lead to an under- or overestimation of the CFR [3-5].

Autopsy examination is the definitive method to establish the cause of death, particularly in the context of a novel infectious disease such as COVID-19 [6,7]. It can be chiefly beneficial to identify the causal relationship between death and infectious diseases in pandemic setting [8]. In addition, autopsy examination can provide important clues to understand the mechanisms of SARS-CoV-2-induced organ damage and its underlying mechanisms [9]. Forensic examination is a central step in a multidisciplinary approach to determine the cause of death in medicolegal

cases positive for COVID-19 [10,11]. Thus, autopsy examination is invaluable in resolving disputes in medicolegal cases with legal liability of health professionals in the context of COVID-19–related deaths, especially in the hospitals and nursing homes [12,13]. The utility of autopsy examination has also been emphasized in cases of breakthrough infection post–COVID-19 vaccination [10]. In the absence of suitable precautionary measures, autopsy examination can be done using the minimally invasive approach, which can provide important clues to data on deaths attributed to COVID-19 [14].

More than 2 years have passed amid COVID-19 pandemic, and much has been known regarding its epidemiology, pathophysiology, and clinical manifestations [15]. Specifically, it is well-known now that there is a wide variability in clinical presentation of the disease with a majority of cases being asymptomatic or mild-to-moderate in clinically apparent infections [16]. Nevertheless, a substantial number of COVID-19 cases evolve into severe or critical disease with respiratory failure, septic shock, and/or multiple-organ failure and death from the disease [17,18].

Despite the rapid availability of extensive and comprehensive research on COVID-19, several aspects of the disease have not been fully elucidated yet, one of which is labeling the deaths with positive SARS-CoV-2 testing results as COVID-19–related mortalities despite the absence of typical findings of the disease [11,19,20]. Thus, autopsy examination can be the sole method to reach a definitive conclusion about the genuine cause of death in such a scenario [21].

In COVID-19, the causative agent is SARS-CoV-2, which utilizes angiotensin-converting enzyme 2 receptors to enter the target cells [22]. Although COVID-19 is primarily a respiratory disease, extrapulmonary manifestations including cardiovascular effects are commonplace especially in severe and critical cases [23]. Hypercoagulability state in association with COVID-19 has been observed frequently and could be linked to dual effect of direct virus damage and activation of various host inflammatory mediators [24]. Subsequently, the hypercoagulability can give rise to acute coronary syndrome (ACS) as a cardiac manifestation of the disease [25].

For the diagnosis of COVID-19, molecular detection by nucleic acid amplification testing including real-time polymerase chain reaction (qPCR) can be considered the gold standard laboratory diagnostic method [26]. Another diagnostic approach, which can be helpful in COVID-19 cases with late presentation include serologic testing for IgM antibodies [27]. The use of electron microscopy (EM) is considered a reliable tool to delineate the ultra-structural details of viruses, including SARS-CoV-2;

however, its use in clinical practice has been limited by cost issues besides the need for technical expertise and tedious procedure compared to molecular detection techniques [28].

Histopathologic findings in autopsies from COVID-19–positive cases include the detection of diffuse alveolar damage (DAD) in a vast majority of cases [28,29], with frequent detection of microthrombi. The spectrum of findings ranges from alveolar hyaline membranes formation, interstitial edema, necrosis of type 1 pneumocytes and endothelial cells in the exudative phase to hyperplasia of type II pneumocytes, and interstitial myofibroblasts with lymphocytic infiltration in the organizing phase and eventually collagenous fibrosis and end-stage lung changes in the fibrotic phase [29]. Despite the view that COVID-19 pneumonia is a heterogeneous disease, from a histopathologic point of view, there is previous evidence that acute and organizing DAD can be considered the primary cause of mortality due to SARS-CoV-2 infection [29,30].

In spite of the growing number of case series describing the autopsy findings in COVID-19–positive deaths, there is a general lack of reports describing the pathophysiology and histopathologic examination of autopsies in the Middle East region to the best of our knowledge [6,7,31]. Thus, such an investigation can be considered necessary to supplement the previous literature with more insights that can be helpful to better define the histopathologic changes that occur in the context of COVID-19 and to establish the cause of death in cases with atypical presentation. Therefore, the current study aimed to evaluate the histopathologic findings in autopsies in a case series from individuals who were positive for COVID-19 at time of death in Jordan.

MATERIALS AND METHODS

Study design

The current study was based on conducting a serial postmortem examination in COVID-19–positive patients at time of death among medicolegal cases in which autopsies are mandatory by Jordanian law to determine the cause of death. Testing for SARS-CoV-2 for all cases of death was mandatory by law before burial in Jordan. Autopsies were conducted at Jordan University Hospital (JUH) and Zarqa Hospital. Forensic gross assessment was done for specimens from the lungs, heart, among other organs. Postmortem specimens were tested for SARS-CoV-2 by qPCR, serologic testing, or both. The final confirmation of SARS-CoV-2 detection in autopsies was done through examining lung specimens under EM, which was conducted at the Department of Pathology, Microbiology and Forensic Medicine at the School

of Medicine, University of Jordan.

Testing for COVID-19

The postmortem detection of SARS-CoV-2 was based on three approaches as follows: (1) qPCR of nasopharyngeal swabs, with RNA purification using the automated Zybio Nucleic Acid Isolation System EXM3000 (Zybio, Chongqing, China), with reverse-transcriptase qPCR being done using SARS-CoV-2 Nucleic Acid Detection Kit (Zybio) targeting three genomic regions (Envelope, ORF1ab, and Nucleocapsid) with interpretation according to manufacturer's instructions; (2) serologic testing to detect IgM/IgG; (3) EM examination of autopsies with lung tissue.

Initially, all cases were identified through either a positive qPCR testing result or serologic testing, while EM examination was conducted among all cases.

Autopsy examination

Autopsies carried out on COVID-19–positive dead bodies were done by authority of the District Attorney since all cases were labeled as medicolegal cases. Such cases are considered medicolegal due to the sudden and unexpected death with no clear causes, with consent to conduct autopsy examination being waived in such cases. Most included autopsies were limited to the chest and abdomen, but some cases were examined fully according to the circumstances of their death. Personal protective equipment was used among all staff members. The procedures involved the minimum needed number of staff. Full external inspection of the body as it was received was conducted initially, followed by midline chest and abdomen incision with extraction of the lungs and heart with full inspection and documentation by “inspection report and photographing of all positive findings.” Tissue sampling was limited to the lungs and heart.

Histopathologic examination

Tissue specimens were fixed in 10% formalin for 72 hours, dehydrated by ethanol, and cleared twice by xylene, then embedded in paraffin, and sectioned as 5 µm sections. The prepared sections were dried and stained by hematoxylin and eosin full final histopathologic examination, which was conducted by the first authors and the senior author (M.A. and M.A.A.-A.), who are consultant histopathologists at JUH.

The differentiation between “death from COVID-19” vs. “death with SARS-CoV-2 infection” was based on the presence of DAD in the former group in contrast to its total absence in the later group.

EM examination

The procedure of EM was adopted from a previous publication by Shatarat et al. [32]. Briefly, the extracted tissues from autopsies were fixed for one hour in buffered 1%–2% osmium tetroxide followed by gradual dehydration in ethanol/propylene oxide and embedding in epoxy resin media mixture. The U7 ultra-cut was used to obtain sections with a range of 70–90 nm, followed by mounting on 200 mesh copper grids, and contrasted with uranyl acetate and lead citrate [32]. The FEI Morgagni Transmission Electron Microscope was used for image acquisition and analysis.

Criteria for identification of “death from COVID-19” vs. “death with SARS-CoV-2 infection”

As previously stated, we used histopathologic findings as the sole criterion to define death from COVID-19 if DAD was found while its absence, was used to denote death with SARS-CoV-2 infection.

Statistical analysis

Based on the small sample size, two-sided Fisher exact test was used to investigate categorical variables, while assessment of the association between age as a continuous variable with dichotomous categorical variables was done using the Mann-Whitney U test. Statistical analysis was done using IBM SPSS Statistics for Windows ver. 22.0 (IBM Corp., Armonk, NY, USA).

RESULTS

Characteristics of the included cases

The study cohort comprised 17 individuals who were positive for COVID-19 at postmortem SARS-CoV-2 assessment by qPCR testing of nasopharyngeal swabs ($n = 4$), serologic testing for SARS-CoV-2 IgM ($n = 3$) or confirmed by both methods ($n = 10$). Two individuals were diagnosed with COVID-19 by qPCR several days prior to death (5 days and 12 days antemortem), whereas the remaining cases had positive test results within 24 hours from being declared dead. The majority of cases were males (76.5%), Jordanians (70.6%), and the average age at time of death was 50 years (Table 1).

The majority of cases were declared dead at home ($n = 11$, 64.7%). Eight cases were diagnosed during the first COVID-19 wave in Jordan, while the remaining nine cases were diagnosed during the second wave of COVID-19 in the country.

The most frequent co-morbidities in the study cohort were hypertension and obesity ($n = 5$ for both). Previous emergency

Table 1. Summary of the clinical features of the study cohort (n=17)

Variable	No. (%)
Mean age (range, yr)	50 (27–77)
Sex	
Male	13 (76.5)
Female	4 (23.5)
Nationality	
Jordanian	12 (70.6)
Non-Jordanian	5 (29.4)
Co-morbidity	
Obesity	5 (29.4)
Hypertension	5 (29.4)
Type 2 DM	3 (17.6)
Obstructive sleep apnea	2 (11.8)
Allergy	1 (5.9)
Cerebrovascular accident	1 (5.9)
Depression on treatment	1 (5.9)
Medically free	4 (23.5)
Information is not available	1 (5.9)
Pronounced cause of death ^a	
Pneumonia	7 (41.2)
Pulmonary embolism	4 (23.5)
Coronary artery thrombus	4 (23.5)
Multiorgan failure	1 (5.9)
Intracranial hemorrhage	1 (5.9)

DM, diabetes mellitus.

^aPronounced cause of death: before autopsy examination.

department visits were recorded for eight cases (four of which were for respiratory symptoms including shortness of breath and cough).

Four cases died with SARS-CoV-2 infection compared to 13 dying from COVID-19

Evidence of the presence of SARS-CoV-2 with the absence of DAD was found in four cases (23.5%). Based on that, the case series was divided into two groups “death with SARS-CoV-2 infection” vs. “death from COVID-19.” In the former group, two cases were presumptively diagnosed with pneumonia at death, one with ACS and the last case was diagnosed with subdural and subarachnoid hemorrhage. For the “death from COVID-19” group, six were diagnosed with pneumonia, four were diagnosed with pulmonary embolism, and three were diagnosed with acute coronary syndrome. The mean age of individuals within the “death with SARS-CoV-2 infection” was younger than the mean age of those within the “death from COVID-19” group (39 years vs. 54 years, $p = .078$, Mann-Whitney U test).

Absence of co-morbidities was recorded among all cases in the “death with SARS-CoV-2 infection” (0/4) in contrast to (9/11, 81.8%) having at least one co-morbid condition in the “death

from COVID-19” group with missing data in two cases ($p = .011$, Fisher exact test).

Autopsy findings from lung tissues

Gross examination of the lungs in the study cohort revealed the common occurrence of congestion and edema followed by hepatization of lungs (Table 2).

On histopathologic examination, DAD was detected in 13/17 cases (76.5%), which was sub-classified into exudative DAD ($n = 5$), proliferative DAD ($n = 7$), and a single case of evolving fibrosing DAD. All cases with exudative DAD showed hyaline membrane formation, denudation and/or necrosis of type 1 pneumocytes (Fig. 1).

Variable degrees of hyaline membrane organization and type II pneumocytes hyperplasia were noted in the seven proliferative DAD cases (Fig. 2).

A majority of cases displayed evidence of interstitial and intra-alveolar edema (64.7%), lymphocytic infiltration of the alveoli (64.7%), and pulmonary capillaries congestion (100%). Microthrombi were found in eight cases (47%), of which two cases showed no DAD, two cases displayed exudative DAD, and four cases showed proliferative DAD. Emphysematous changes were noted in eight cases (Table 2, Fig. 3).

In the absence of co-morbidities, no specific histologic changes were noticed in alveoli ($n = 4$), compared to the presence of lymphocytic infiltration in 8/9 of the cases with co-morbidities ($p = .011$, Fisher exact test). All cases in the “died with COVID-19” group lacked alveolar changes by definition ($n = 4$), compared to 11/13 with lymphocytic infiltration in the “died from COVID-19” group ($p = .006$, Fisher exact test).

Autopsy findings from heart tissues

Gross examination of the heart in this case series revealed the relatively high prevalence of atherosclerotic changes in coronary arteries ($n = 8$, 47.1%). Histopathologic changes were scarcely detected. Fibrosis in intima and thickening of media were detected in a single case, while myocardial cell necrosis was found in another single case (Table 2).

EM findings

All cases were examined using EM, and spherical structures with surface spikes were found in all cases ($n = 17$, 100%) (Fig. 4).

DISCUSSION

This study represents the first description of autopsy findings

Table 2. Autopsy lung and heart findings in the study cohort (n= 17)

Finding	Total cases (n= 17)	Died of COVID-19 (n= 13)	Died with SARS-CoV-2 infection (n=4)
Lung			
Gross			
Congestion and edema	12 (70.6)	10 (76.9)	2 (50.0)
Hepatization	10 (58.8)	7 (53.8)	3 (75.0)
Hemorrhage	10 (58.8)	9 (69.2)	1 (25.0)
Vascular thrombosis	3 (17.6)	3 (23.1)	0
Pleural adhesions	3 (17.6)	3 (23.1)	0
Saddle pulmonary embolism	2 (11.8)	2 (15.4)	0
Pleural effusion	1 (5.9)	1 (7.7)	0
Histopathologic			
Alveolar congestion only	4 (23.5)	0	4 (100)
Exudative diffuse alveolar damage	5 (29.4)	5 (38.5)	0
Proliferative diffuse alveolar damage	7 (41.2)	7 (53.8)	0
Early fibrosing diffuse alveolar damage	1 (5.9)	1 (7.7)	0
Specific microscopic findings			
Hyaline membranes with type I pneumocytes necrosis or denudation	5 (29.4)	5 (38.5)	0
Organizing or remnants of hyaline membrane and type II pneumocytes hyperplasia	7 (41.2)	7 (53.8)	0
Early and focal fibrosis	1 (5.9)	1 (7.7)	0
Diffuse collagenous fibrosis	0	0	0
Interstitial and intra-alveolar edema	17 (100)	13 (100)	4 (100)
Microscopic honeycomb-like change	0	0	0
Collapsed alveoli	0	0	0
Lymphocytic infiltration	11 (64.7)	11 (84.6)	0
Traction bronchiectasis	0	0	0
Pneumocytes			
No change	4 (23.5)	0	4 (100)
Denudation and necrosis of type I pneumocytes	4 (23.5)	4 (30.8)	0
Proliferation of type II pneumocyte	3 (17.6)	3 (23.1)	0
Denudation and necrosis of type I pneumocytes and proliferation of type II pneumocyte	6 (35.3)	6 (46.2)	0
Necrosis of endothelial cells			
No	16 (94.1)	12 (92.3)	4 (100)
Yes	1 (5.9)	1 (7.7)	0
Neutrophil aggregation			
No	16 (94.1)	12 (92.3)	4 (100)
Yes	1 (5.9)	1 (7.7)	0
Microthrombi			
Absent	9 (52.9)	6 (46.2)	3 (75.0)
Present	8 (47.1)	7 (53.8)	1 (25.0)
Hemorrhage			
Absent	5 (29.4)	3 (23.1)	2 (50.0)
Present	12 (70.6)	10 (76.9)	2 (50.0)
Pulmonary capillary congestion			
Absent	0	0	0
Present	17 (100)	13 (100)	4 (100)
Reactive pneumocytes and syncytial cells			
Absent	7 (41.2)	4 (30.8)	3 (75.0)
Present	10 (58.8)	9 (69.2)	1 (25.0)
Focal emphysema			
Absent	9 (52.9)	7 (53.8)	2 (50.0)
Present	8 (47.1)	6 (46.2)	2 (50.0)

(Continued to the next page)

Table 2. Continued

Finding	Total cases (n=17)	Died of COVID-19 (n=13)	Died with SARS-CoV-2 infection (n=4)
Vasculitis			
Absent	17 (100)	13 (100)	4 (100)
Present	0	0	0
Heart			
Gross			
No significant changes	5 (29.4)	4 (30.8)	1 (25.0)
Coronary arteries atherosclerosis	8 (47.1)	6 (46.2)	2 (50.0)
Cardiac hypertrophy	3 (17.6)	1 (7.7)	2 (50.0)
Cardiomegaly	3 (17.6)	1 (7.7)	2 (50.0)
Acute thrombus	2 (11.8)	0	2 (50.0)
Fibrosis	1 (5.9)	1 (7.7)	0
Specific microscopic findings			
Fibrosis in intima			
Absent	16 (94.1)	12 (92.3)	4 (100)
Present	1 (5.9)	1 (7.7)	0
Thickening of media			
Absent	16 (94.1)	12 (92.3)	4 (100)
Present	1 (5.9)	1 (7.7)	0
Myocardial hypertrophy			
Absent	17 (100)	13 (100)	4 (100)
Present	0	0	0
Senile amyloidosis			
Absent	17 (100)	13 (100)	4 (100)
Present	0	0	0
Myocardial cell necrosis			
Absent	16 (94.1)	12 (92.3)	4 (100)
Present	1 (5.9)	1 (7.7)	0

Values are presented as number (%). COVID-19, coronavirus disease 2019; SARS-CoV-2, severe acute respiratory syndrome coronavirus 2.

from individuals positive for COVID-19 in Jordan, and Arab countries to the best of our knowledge. Previously, a majority of autopsy case series in the context of COVID-19 were mostly conducted in the United States, Europe, and China [21]. Such a study appears of prime importance in the Middle East region for a number of reasons. First, challenges were posed to forensic pathologists considering the controversies around the Islamic burial rituals and handling of corpses if autopsies revealed the presence of SARS-CoV-2 [33,34]. This is particularly relevant considering the evidence suggesting the presence of replicative SARS-CoV-2 a few days postmortem as shown in the study by Grassi et al. [35] that involved 29 autopsies examined in Italy. Our findings confirmed the presence of the virus in all cases included in this study. The diagnosis of COVID-19 in this case series was established by postmortem molecular or serologic testing for SARS-CoV-2 even in the absence of typical clinical presentation of COVID-19 at time of death. Second, this study is important in Jordan considering the previous evidence of high prevalence of embracing conspiratorial beliefs towards emerging virus infec-

tions that could entail irrational COVID denialism [36]. The findings of this study add an explicit proof of the presence of the virus among autopsies that tested positive for the virus through direct EM visualization. The confirmation of coronavirus presence by EM examination added further proof of virus presence in all included cases despite the variability in laboratory testing approach initially used in this case series (qPCR vs. serologic testing).

Macroscopic and microscopic findings in the majority of cases (13/17, 76.5%) in this study were consistent with previous literature suggesting the crucial role of DAD as the hallmark of acute respiratory distress syndrome complicating COVID-19 infections [37-39]. The predominance of proliferative DAD in this case series indicates the late presentation of a substantial number of cases with subsequent ominous outcome. The wide prevalence of DAD as the predominant feature in lung parenchyma among COVID-19-positive autopsies was reported previously in various reports from the United States [40,41], Germany [30,42], Spain [43], Italy [44], and China [45]. An early

case series from Switzerland that involved 21 autopsies examined following COVID-19–related mortalities revealed that the major cause of death was respiratory insufficiency due to exudative DAD and massive capillary congestion [46]. In addition, the

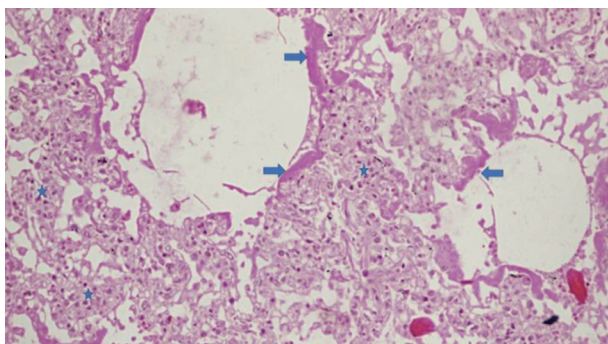


Fig. 1. The histopathologic changes of a case with exudative phase of diffuse alveolar damage with hyaline membrane formation (arrows) and lymphocytic infiltrate (star).

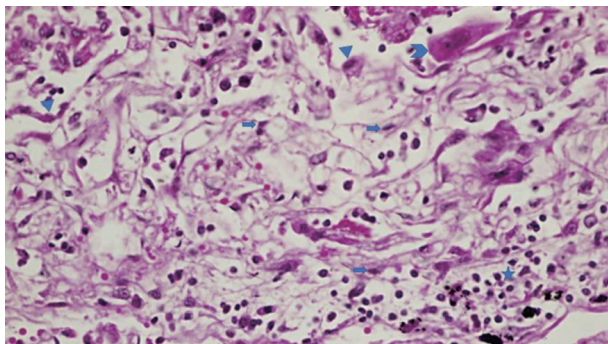


Fig. 2. The histopathologic changes of a case with evolving fibrotic changes with type II pneumocytes hyperplasia (arrowhead), squamous metaplasia (chevron), expansion of septum with interstitial fibroblastic and myofibroblast proliferation (arrows), edema, and lymphocytic infiltrate (star).

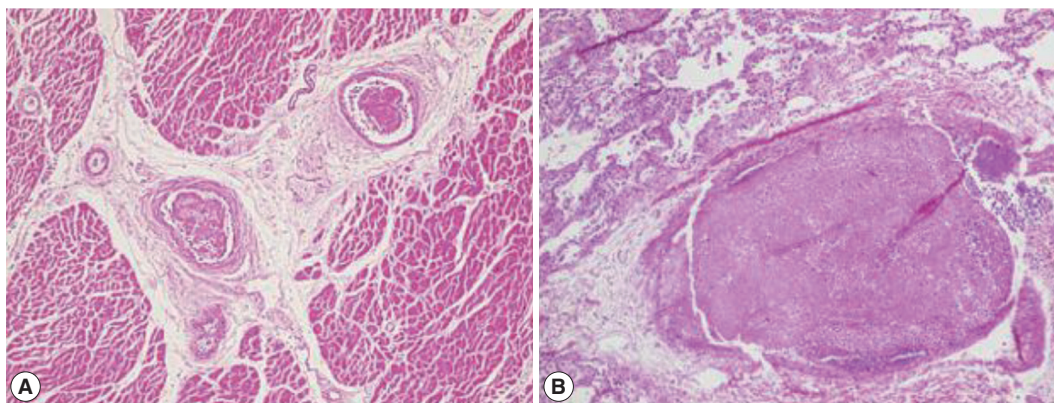


Fig. 3. Intravascular microthrombi. (A) Heart tissue showing two intravascular microthrombi. (B) Lung with large thrombus occupying a medium sized vessel.

Swiss case series reported the detection of microthrombi despite the intake of anticoagulation prior to death [46].

The role of coagulopathy in the pathophysiology of COVID-19 was manifested by the frequent detection of microthrombi in lungs (8/17, 47.1%) in the study cohort. Likewise, and indicative of the central role of thrombotic microangiopathy in critical cases of COVID-19, a study from Iran reported the presence of thrombotic microangiopathy in 60% of 31 lung biopsies from patients who passed away due to COVID-19 [47]. Additional reports on autopsy findings amid COVID-19 pandemic found a high incidence of thromboembolic events suggesting its role in the fatal outcome of COVID-19 [39,48]. A recent comprehensive review for autopsic investigations from 749 COVID-19 mortalities in 14 studies revealed the presence of pulmonary embolism-related findings in 30% of cases, with venous thromboembolic events as the cause of death 25% of the cases [49]. An early Austrian study involving 11 autopsies showed that thrombosis in small pulmonary arteries was a fundamental finding resulting in mortality due to COVID-19 [50].

The frequency of co-morbidities was high in this case series among mortalities that were linked directly to SARS-CoV-2 infection in contrast to its total absence among those who died with the disease. Conditions like hypertension, obesity, and type 2 diabetes mellitus were previously linked to excess mortality among SARS-CoV-2 infected patients [51]. In line with this observation, co-morbidities in this cohort were linked to death from COVID-19 rather than death with the virus.

A novel finding of this study was the observation that four out of 17 individuals died without significant histopathologic pulmonary changes. This observation was made despite the presence of SARS-CoV-2 as evidenced by qPCR, serology, and EM findings. One important parameter in the assessment of infec-

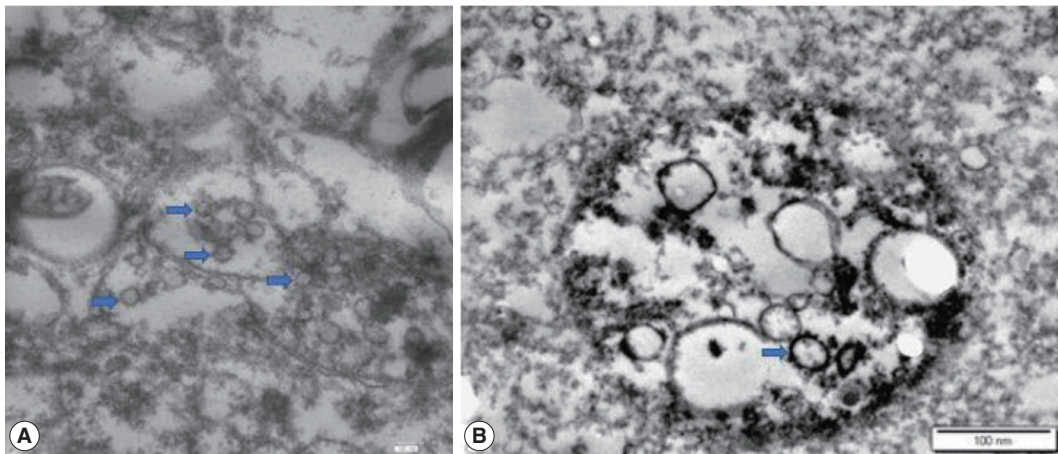


Fig. 4. The electron microscopic findings from two cases. Intracellular coronavirus particles, some of which showing delicate surface spikes (scale bar = 100 nm): $\times 20,000$ (A), $\times 98,000$ (B).

tious disease is the CFR, which is defined as “the proportion of individuals diagnosed with a disease who die from that disease” [3]. The aspects of bias in the efforts to estimate COVID-19 CFR appear to cause an underestimation through time lags in reporting of death, and overestimation through underreporting of asymptomatic and mild cases [5]. Another important cause of bias, which was noticed in this study, is the overestimation of fatalities due to COVID-19. This can happen as a result of reporting any death with a positive SARS-CoV-2 testing result as a COVID-19 case, even in the absence of sufficient evidence that the individual died as a result of virus infection, which might be present as an incidental finding [52]. Such a scenario can frequently occur in the course of COVID-19 epidemic waves with a high proportion of asymptomatic cases/mild disease [16]. Hence, sub-clinical cases are rarely tested and consequently are missed.

In this study, even with a small sample size, the proportion of death with SARS-CoV-2 infection appears relatively high 4/17 (23.5%). In line with this finding, a study from Italy reported on the causes of death among nine cases that tested positive for COVID-19 at time of death, with five cases dying as a result of carbon monoxide poisoning in a nursing home (death with SARS-CoV-2 infection) [11]. In an earlier study from Germany, Edler et al. [42] found a similar observation; however, at a much smaller scale with only 5% out of 80 autopsies that were labeled as “non-COVID-19 deaths.”

It is important to note that the incidental finding of SARS-CoV-2 in autopsies can be higher in outbreak situation. The current study took place during the first and second waves of COVID-19 in Jordan, with more than several thousand of newly diagnosed cases at waves’ peaks [53]. Several differential diagnoses should be considered in outbreak setting with community

spread of SARS-CoV-2, including other viral infections, previously undiagnosed heart disease, and drug toxicity among other conditions [54]. Despite the absence of DAD in four cases, the role of SARS-CoV-2 in mortality cannot be ruled out, particularly in the cases with ACS and this issue could be viewed as a caveat in our stratification approach. This is evidenced by the previous studies linking COVID-19 with direct cardiac damage and indirect involvement through the thrombotic complications [55]. However, we are inclined to believe that the cases in the “death with SARS-CoV-2 infection” group did not pass away due to SARS-CoV-2 complications since the subjects in this group lacked co-morbidities and were younger compared to those with histopathologic evidence of death due to the infection.

Finally, the findings in this case series should be interpreted in light of several limitations that included: (1) the small sample size, which was mostly related to restriction of autopsy examination to medicolegal cases; (2) potential selection bias since all deaths were considered as medicolegal cases; (3) missing of full clinical history data in a few cases, including the history of COVID-19 vaccine uptake among the four cases included following the start of vaccination campaign in Jordan, besides the lack of data on microbiologic testing to rule out bacterial superinfections; (4) the approach used to stratify the cases into “died of COVID-19” vs. “died with SARS-CoV-2 infection” depended on the detection of DAD solely. Thus, future studies should benefit from a refined approach of classification including consideration of detailed medical records from the included cases, as well as the full utility of postmortem radiology, besides toxicologic investigations [20]; and finally (5) virtual autopsy (virtopsy) was not conducted in this study and should be considered in the future studies considering its promising role for postmortem investigation

in the context of resolving disputed cases of COVID-19 deaths.

To conclude, in this case series, we described the histopathologic findings of COVID-19–related mortalities and explored the distinction between death due to COVID-19 as opposed to dying with SARS-CoV-2 infection. This disparity might be supported by the younger age and absence of co-morbidities in the “died with COVID-19” group; however, this observation is pending further evidence from studies with larger samples. Besides DAD as the primary histopathologic finding among the “death from COVID-19” group, microthrombi were frequently detected. This microthrombi can be indicative of a hypercoagulability state. Such a state appears to play a prominent role in the pathophysiology of severe and critical cases of COVID-19, which can be implicated in the mortality from the disease.

Ethics Statement

This study was approved by the Institutional Review Board of Jordan University Hospital (JUH–IRB, decision No. 78/2021, reference No. 10/2021/5885, issued on 14 March 2021). The written informed consent from the next of kin was waived based on the medico-legal status of the cases.

Availability of Data and Material

The datasets generated or analyzed during the study are available from the corresponding author on reasonable request.

Code Availability

Not applicable.

ORCID

Maram Abdaljaleel	https://orcid.org/0000-0002-9257-2596
Isra Tawalbeh	https://orcid.org/0000-0001-6977-0650
Malik Sallam	https://orcid.org/0000-0002-0165-9670
Amjad Bani Hani	https://orcid.org/0000-0003-1671-4991
Imad M. Al-Abdallat	https://orcid.org/0000-0002-0260-6204
Baheth Al Omari	https://orcid.org/0000-0001-7561-7708
Sahar Al-Mustafa	https://orcid.org/0000-0001-9969-3983
Hasan Abder-Rahman	https://orcid.org/0000-0003-1230-6691
Adnan Said Abbas	https://orcid.org/0000-0001-7625-9041
Mahmoud Zureigat	https://orcid.org/0000-0001-8461-2757
Mousa A. Al-Abadi	https://orcid.org/0000-0002-0467-8244

Author Contributions

Conceptualization: MA, MAAA. Data curation: MA, IT, MS, ABH, IMAA, BAO, SAM, HAR, ASA, MZ, MAAA. Formal analysis: MA, MS. Funding acquisition: MA. Investigation: MA, IT, MS, ABH, IMAA, BAO, SAM, HAR, ASA, MZ, MAAA. Methodology: MA, IT, MS, ABH, IMAA, BAO, SAM, HAR, ASA, MZ, MAAA. Project administration: MA. Resources: MA, IT, MS, ABH, IMAA, BAO, SAM, HAR, ASA, MZ, MAAA. Supervision: MA, MAAA. Validation: MA, MS. Visualization: MA, MS. Writing—original draft preparation: MA, MS. Writing—review & editing: MA, IT, MS, ABH, IMAA, BAO, SAM, HAR, ASA, MZ, MAAA. Approval of final manuscript: all authors.

Conflicts of Interest

The authors declare that they have no potential conflicts of interest.

Funding Statement

This research was funded by Deanship of Scientific Research at the University of Jordan, grant number: 498/2021/19; (24/2020–2021), granted on 21 April 2021.

References

- Gallo LG, Oliveira AF, Abrahao AA, et al. Ten epidemiological parameters of COVID-19: use of rapid literature review to inform predictive models during the pandemic. *Front Public Health* 2020; 8: 598547.
- Onder G, Rezza G, Brusaferro S. Case-fatality rate and characteristics of patients dying in relation to COVID-19 in Italy. *JAMA* 2020; 323: 1775–6.
- World Health Organization. Estimating mortality from COVID-19: scientific brief [Internet]. Geneva: World Health Organization, 2020 [cited 2022 Oct 29]. Available from: <https://www.who.int/publications/i/item/WHO-2019-nCoV-Sci-Brief-Mortality-2020.1>.
- Schwab N, Nienhold R, Henkel M, et al. COVID-19 autopsies reveal underreporting of SARS-CoV-2 infection and scarcity of co-infections. *Front Med (Lausanne)* 2022; 9: 868954.
- Grande E, Fedeli U, Pappagallo M, et al. Variation in cause-specific mortality rates in Italy during the first wave of the COVID-19 pandemic: a study based on nationwide data. *Int J Environ Res Public Health* 2022; 19: 805.
- Sessa F, Bertozzi G, Cipolloni L, et al. Clinical-forensic autopsy findings to defeat COVID-19 disease: a literature review. *J Clin Med* 2020; 9: 2026.
- Maiese A, Manetti AC, La Russa R, et al. Autopsy findings in COVID-19-related deaths: a literature review. *Forensic Sci Med Pathol* 2021; 17: 279–96.
- Kim MY, Cheong H, Kim HS; Working Group for Standard Autopsy Guideline for COVID-19 from the Korean Society for Legal Medicine. Proposal of the autopsy guideline for infectious diseases: preparation for the post-COVID-19 era (abridged translation). *J Korean Med Sci* 2020; 35: e310.
- Salerno M, Sessa F, Piscopo A, et al. No autopsies on COVID-19 deaths: a missed opportunity and the lockdown of science. *J Clin Med* 2020; 9: 1472.
- Filograna L, Manenti G, Grassi S, et al. Virtual autopsy in SARS-CoV-2 breakthrough infection: a case report. *Forensic Imaging* 2022; 30: 200520.
- De-Giorgio F, Grassi VM, Bergamin E, et al. Dying “from” or “with” COVID-19 during the pandemic: medico-legal issues according to a population perspective. *Int J Environ Res Public Health* 2021; 18: 8851.
- Esposito M, Salerno M, Scoto E, Di Nunno N, Sessa F. The impact of the COVID-19 pandemic on the practice of forensic medicine: an overview. *Healthcare (Basel)* 2022; 10: 319.
- Filograna L, Manenti G, Arena V, et al. Claimed medical malpractice in fatal SARS-CoV-2 infections: the importance of combining ante- and post-mortem radiological data and autopsy findings for correct forensic analysis. *Forensic Imaging* 2021; 25: 200454.
- Rakislova N, Marimon L, Ismail MR, et al. Minimally invasive autopsy practice in COVID-19 cases: biosafety and findings. *Pathogens* 2021; 10: 412.
- Harapan H, Itoh N, Yufika A, et al. Coronavirus disease 2019 (COVID-19): a literature review. *J Infect Public Health* 2020; 13: 667–73.
- Sah P, Fitzpatrick MC, Zimmer CF, et al. Asymptomatic SARS-

- CoV-2 infection: a systematic review and meta-analysis. *Proc Natl Acad Sci U S A* 2021; 118: e2109229118.
17. Wiersinga WJ, Rhodes A, Cheng AC, Peacock SJ, Prescott HC. Pathophysiology, transmission, diagnosis, and treatment of coronavirus disease 2019 (COVID-19): a review. *JAMA* 2020; 324: 782-93.
 18. Grippo F, Navarra S, Orsi C, et al. The role of COVID-19 in the death of SARS-CoV-2-positive patients: a study based on death certificates. *J Clin Med* 2020; 9: 3459.
 19. Slater TA, Straw S, Drozd M, Kamalathasan S, Cowley A, Witte KK. Dying 'due to' or 'with' COVID-19: a cause of death analysis in hospitalised patients. *Clin Med (Lond)* 2020; 20: e189-90.
 20. Giorgetti A, Oraziotti V, Busardo FP, Pirani F, Giorgetti R. Died with or died of? Development and testing of a SARS CoV-2 significance score to assess the role of COVID-19 in the deaths of affected patients. *Diagnostics (Basel)* 2021; 11: 190.
 21. Spherhake JP. Autopsies of COVID-19 deceased? Absolutely! *Leg Med (Tokyo)* 2020; 47: 101769.
 22. Hoffmann M, Kleine-Weber H, Schroeder S, et al. SARS-CoV-2 cell entry depends on ACE2 and TMPRSS2 and is blocked by a clinically proven protease inhibitor. *Cell* 2020; 181: 271-80.
 23. Gupta A, Madhavan MV, Sehgal K, et al. Extrapulmonary manifestations of COVID-19. *Nat Med* 2020; 26: 1017-32.
 24. Abou-Ismaïl MY, Diamond A, Kapoor S, Arafah Y, Nayak L. The hypercoagulable state in COVID-19: Incidence, pathophysiology, and management. *Thromb Res* 2020; 194: 101-15.
 25. Nishiga M, Wang DW, Han Y, Lewis DB, Wu JC. COVID-19 and cardiovascular disease: from basic mechanisms to clinical perspectives. *Nat Rev Cardiol* 2020; 17: 543-58.
 26. Bohn MK, Mancini N, Loh TP, et al. IFCC interim guidelines on molecular testing of SARS-CoV-2 infection. *Clin Chem Lab Med* 2020; 58: 1993-2000.
 27. Pan Y, Li X, Yang G, et al. Serological immunochromatographic approach in diagnosis with SARS-CoV-2 infected COVID-19 patients. *J Infect* 2020; 81: e28-32.
 28. Brahim Belhaouari D, Fontanini A, Baudoin JP, et al. The strengths of scanning electron microscopy in deciphering SARS-CoV-2 infectious cycle. *Front Microbiol* 2020; 11: 2014.
 29. Hanley B, Lucas SB, Youd E, Swift B, Osborn M. Autopsy in suspected COVID-19 cases. *J Clin Pathol* 2020; 73: 239-42.
 30. Schaller T, Hirschbuhl K, Burkhardt K, et al. Postmortem examination of patients with COVID-19. *JAMA* 2020; 323: 2518-20.
 31. Satturwar S, Fowkes M, Farver C, et al. Postmortem findings associated with SARS-CoV-2: systematic review and meta-analysis. *Am J Surg Pathol* 2021; 45: 587-603.
 32. Shatarat A, Alzghoul H, Al-Qattan D, Elbeltagy M. Anatomical and ultrastructural sex differences in mean diameter and thickness of myelinated axons in adult rat corpus callosum. *Int J Morphol* 2020; 38: 505-12.
 33. Nurhayati N, Purnama TB. Funeral processes during the COVID-19 pandemic: perceptions among Islamic religious leaders in Indonesia. *J Relig Health* 2021; 60: 3418-33.
 34. Al-Dawoody A, Finegan O. COVID-19 and Islamic burial laws: safeguarding dignity of the dead [Internet]. Geneva: International Committee of the Red Cross, 2020 [cited 2020 Apr 30]. Available from: <https://blogs.icrc.org/law-and-policy/2020/04/30/covid-19-islamic-burial-laws/>.
 35. Grassi S, Arena V, Cattani P, et al. SARS-CoV-2 viral load and replication in postmortem examinations. *Int J Legal Med* 2022; 136: 935-9.
 36. Sallam M, Dababseh D, Yaseen A, et al. COVID-19 misinformation: mere harmless delusions or much more? A knowledge and attitude cross-sectional study among the general public residing in Jordan. *PLoS One* 2020; 15: e0243264.
 37. Youd E, Moore L. COVID-19 autopsy in people who died in community settings: the first series. *J Clin Pathol* 2020; 73: 840-4.
 38. Elezkurtaj S, Greuel S, Ihlow J, et al. Causes of death and comorbidities in hospitalized patients with COVID-19. *Sci Rep* 2021; 11: 4263.
 39. Rimmelink M, De Mendonca R, D'Haene N, et al. Unspecific post-mortem findings despite multiorgan viral spread in COVID-19 patients. *Crit Care* 2020; 24: 495.
 40. Bradley BT, Maioli H, Johnston R, et al. Histopathology and ultrastructural findings of fatal COVID-19 infections in Washington State: a case series. *Lancet* 2020; 396: 320-32.
 41. Barton LM, Duval EJ, Stroberg E, Ghosh S, Mukhopadhyay S. COVID-19 autopsies, Oklahoma, USA. *Am J Clin Pathol* 2020; 153: 725-33.
 42. Edler C, Schroder AS, Aepfelbacher M, et al. Dying with SARS-CoV-2 infection-an autopsy study of the first consecutive 80 cases in Hamburg, Germany. *Int J Legal Med* 2020; 134: 1275-84.
 43. The COVID-19 Autopsy. The first COVID-19 autopsy in Spain performed during the early stages of the pandemic. *Rev Esp Patol* 2020; 53: 182-7.
 44. Carsana L, Sonzogni A, Nasr A, et al. Pulmonary post-mortem findings in a series of COVID-19 cases from northern Italy: a two-centre descriptive study. *Lancet Infect Dis* 2020; 20: 1135-40.
 45. Ding Y, Wang H, Shen H, et al. The clinical pathology of severe acute respiratory syndrome (SARS): a report from China. *J Pathol* 2003; 200: 282-9.
 46. Menter T, Haslbauer JD, Nienhold R, et al. Postmortem examination of COVID-19 patients reveals diffuse alveolar damage with severe capillary congestion and variegated findings in lungs and other organs suggesting vascular dysfunction. *Histopathology* 2020; 77: 198-209.
 47. Sadegh Beigee F, Pourabdollah Toutkaboni M, Khalili N, et al. Diffuse alveolar damage and thrombotic microangiopathy are the main histopathological findings in lung tissue biopsy samples of COVID-19 patients. *Pathol Res Pract* 2020; 216: 153228.
 48. Caramaschi S, Kapp ME, Miller SE, et al. Histopathological findings and clinicopathologic correlation in COVID-19: a systematic review. *Mod Pathol* 2021; 34: 1614-33.
 49. Zuin M, Engelen MM, Bilato C, et al. Prevalence of acute pulmonary embolism at autopsy in patients with COVID-19. *Am J Cardiol* 2022; 171: 159-64.
 50. Lax SF, Skok K, Zechner P, et al. Pulmonary arterial thrombosis in COVID-19 with fatal outcome: results from a prospective, single-center, clinicopathologic case series. *Ann Intern Med* 2020; 173: 350-61.
 51. Bhaskaran K, Bacon S, Evans SJ, et al. Factors associated with deaths due to COVID-19 versus other causes: population-based cohort analysis of UK primary care data and linked national death registrations within the OpenSAFELY platform. *Lancet Reg Health Eur* 2021; 6: 100109.
 52. Niforatos JD, Melnick ER, Faust JS. Covid-19 fatality is likely overestimated. *BMJ* 2020; 368: m1113.
 53. Sallam M, Mahafzah A. Molecular analysis of SARS-CoV-2 genetic lineages in Jordan: tracking the introduction and spread of COV-

- ID-19 UK variant of concern at a country level. *Pathogens* 2021; 10: 302.
54. Geller RL, Aungst JL, Newton-Levinson A, et al. Is it COVID-19? The value of medicolegal autopsies during the first year of the COVID-19 pandemic. *Forensic Sci Int* 2022; 330: 111106.
55. Schoene D, Schnekenberg LG, Pallesen LP, et al. Pathophysiology of cardiac injury in COVID-19 patients with acute ischaemic stroke: what do we know so far?: a review of the current literature. *Life (Basel)* 2022; 12: 75.

Clinicopathologic significance of the delta-like ligand 4, vascular endothelial growth factor, and hypoxia-inducible factor-2 α in gallbladder cancer

Sujin Park¹, Junsik Kim², Woncheol Jang², Kyoung-Mee Kim¹, Kee-Taek Jang¹

¹Department of Pathology and Translational Genomics, Samsung Medical Center, Sungkyunkwan University School of Medicine, Seoul;

²Department of Statistics, Duksung Women's University, Seoul, Korea

Background: Gallbladder cancer (GBC) is usually detected in advanced stages with a low 5-year survival rate. Delta-like ligand 4 (DLL4), vascular endothelial growth factor (VEGF), and hypoxia-inducible factor-2 α (HIF2 α) have been studied for their role in tumorigenesis and potential for therapeutic target, and multiple clinical trials of the agents targeting them are ongoing. We investigated the expression of these markers in surgically resected GBC and tried to reveal their association with the clinicopathologic features, mutual correlation of their expression, and prognosis of the GBC patients by their expression. **Methods:** We constructed the tissue microarray blocks of 99 surgically resected GBC specimens and performed immunohistochemistry of DLL4, VEGF, and HIF2 α . We used the quantitative digital image analysis to evaluate DLL4 and VEGF expression, while the expression of HIF2 α was scored manually. **Results:** The expression of VEGF and HIF2 α showed a significant trend with tumor differentiation ($p = .028$ and $p = .006$, respectively). We found that the high DLL4 and VEGF expression were significantly correlated with lymph node metastasis ($p = .047$, both). The expression of VEGF and HIF2 α were significantly correlated ($p < .001$). The GBC patients with low HIF2 α expression showed shorter recurrence-free survival than those with high HIF2 α expression. **Conclusions:** This study suggested the possibility of the usage of DLL4 and VEGF to predict the lymph node metastasis and the possibility of VEGF and HIF2 α to predict the expression level mutually. Further studies may be needed to validate our study results and eventually accelerate the introduction of the targeted therapy in GBC.

Key Words: Gallbladder neoplasms; DLL4; Vascular endothelial growth factor; HIF2 α ; Targeted therapy

Received: November 19, 2022 **Revised:** February 1, 2023 **Accepted:** February 1, 2023

Corresponding Author: Kee-Taek Jang, MD, PhD, Department of Pathology and Translational Genomics, Samsung Medical Center, Sungkyunkwan University School of Medicine, 81 Irwon-ro, Gangnam-gu, Seoul 06351, Korea

Tel: +82-2-3410-2763, Fax: +82-2-3410-0025, E-mail: kt12.jang@samsung.com

Gallbladder cancer (GBC) ranks in the top 10 for both incidence and mortality in South Korea [1]. GBC is known as a deadly disease because only 21.8% of the patients are diagnosed at a localized stage, while near half (41.0%) present distant metastasis at the time of diagnosis in Korea [2,3]. The recently reported 5-year survival rate of total Korean GBC patients was 28.7%, and in cases with distant metastasis, it was even lower as 2.5% [2]. The poor prognosis of Korean GBC patients suggests the limited efficacy of conventional systemic treatments such as gemcitabine plus cisplatin, 5-fluorouracil, etc. It implicates the need to develop other treatment modalities for advanced-stage patients [4]. In the era of molecular pathology, there have been many attempts to discover actionable targets in GBC, and there

are several ongoing clinical trials with novel therapeutic agents including tyrosine kinase inhibitors and immunotherapeutic agents [5,6].

Delta-like ligand 4 (DLL4) is one of the transmembrane agonistic ligands of Notch receptors [7,8] which is induced by vascular endothelial growth factor (VEGF). It plays a role as a negative feedback regulator to prevent over-exuberant angiogenesis and promote the proper formation of vascular structures [9]. Furthermore, DLL4 in vasculature cells is also involved in tumor angiogenesis through interactions with the VEGF pathway [9,10]. Previous studies demonstrated that high DLL4 expression was correlated with or predicted poor prognosis in gastric cancer and pancreatic cancer patients [11,12]. In other cancer types, includ-

ing breast cancer and head and neck squamous cell carcinoma, several studies were executed regarding DLL4 as a potential therapeutic target [13-15]. In more recent years, there have been multiple clinical trials for the efficacy of anti-DLL4 antibodies and anti-DLL4/anti-VEGF bispecific antibodies in advanced solid tumors [16,17].

Hypoxia-inducible factor-2 α (HIF2 α) is a transcription factor that is stabilized in hypoxic conditions and activates multiple downstream genes, including VEGF [18,19]. Hypoxia, in turn, increases the expression of Notch ligands, including DLL4, whereas Notch signaling regulates the response for hypoxia in multiple cancers by controlling the expression of HIF2 α [18]. It is well known that the VHL-HIF2 α -VEGF axis is involved in tumor development and progression of conventional clear cell type renal cell carcinoma (RCC), and the treatment options that target the molecules in this pathway have progressed in recent years. The target therapies for RCC include: targeting angiogenesis through VEGF inhibitors, anti-proliferative agents targeting the mammalian target of rapamycin pathway, immune-checkpoint inhibitor, and novel HIF2 α inhibitors [20,21].

Based on the accumulated data about the interactions and associations of DLL4, VEGF, and HIF2 α , we assumed that it is worthy of analyzing the association between the expression of these markers in GBC. We aimed first to find out whether the expression levels are associated with the clinicopathologic characteristics and prognosis of the patients and whether there is an association between the expressions of the three markers. On the therapeutic aspect, if substitution between an anti-DLL4 antibody or anti-DLL4/anti-VEGF bispecific antibody and HIF2 α -inhibitor would be proved possible in the future based on our results, it would be a benefit for patients considering possible adverse effects or resistance [16,20].

MATERIALS AND METHODS

Patient selection and tissue samples

We collected the tissues of the GBC patients that underwent surgical resection between January 2010 and December 2017 from the surgical pathology database of Samsung Medical Center (Seoul, Korea). Initially, 101 cases were found, but one was excluded because the tumor was a metastatic tumor from the liver, and another one was excluded due to pre-operative chemotherapy. Finally, we enrolled a total study population of 99 GBC cases. Clinical data, including age, sex, date of surgery, history of post-operative chemotherapy, recurrence-free survival (RFS), overall survival, and duration of follow-up, were extracted from

electronic medical records. As all hematoxylin and eosin (H&E)-stained slides were reviewed by two pathologists (K.T.J. and S.P.), the histologic type and differentiation were reviewed for all tumor tissues. We checked the tumor staging according to the American Joint Committee on Cancer staging system (8th edition) [22].

Tissue microarray construction and immunohistochemistry

Representative tumor areas confirmed for the absence of hemorrhage or necrosis were marked on the formalin-fixed paraffin-embedded blocks. Two tissue cores with a diameter of 2.0 mm were acquired from each donor block and were arranged in the recipient paraffin blocks. Each tissue microarray (TMA) block contained up to 40 tumor tissue cores and two control tissue cores. One normal pancreas tissue core and one normal tonsil tissue core were used as control cores.

Immunohistochemistry (IHC) was performed on 4- μ m-thick tissue sections obtained from TMA blocks. For detection of DLL4 and HIF2 α , automated Ventana BenchMark Ultra instrument (Ventana Medical Systems, Tucson, AZ, USA) was used for antigen retrieval and primary antibody reaction. After the antigen retrieval for 92 minutes with CC1 in Ventana BenchMark Ultra, the sections were incubated with anti-DLL4 antibody (HPA023392, 1:50, Sigma-Aldrich, St. Louis, MO, USA) for 60 minutes in 37°C and with EPAS-1 (sc-46691, 1:50, Santa Cruz Biotechnology, Santa Cruz, CA, USA) for HIF2 α detection for 120 minutes in 37°C, respectively. For EPAS-1, the chromogenic reactions were carried out for 12 minutes with OptiView Amplification Kit (860-099, Ventana Medical Systems) and OptiView DAB IHC Detection kit (760-700, Ventana Medical Systems), but for anti-DLL4 antibody, with OptiView DAB IHC Detection kit (760-700, Ventana Medical Systems) only. For VEGF protein detection, the sections were incubated with a mouse monoclonal anti-VEGF antibody (sc-7269, 1:500, Santa Cruz Biotechnology) for 20 minutes in a Bond-max autoimmunostainer (Leica Biosystems, Melbourne, Australia) after antigen retrieval with ER1 buffer (pH 6.0, Leica Biosystems) in 100°C. Antigen-antibody chromogenic reactions were developed for 10 minutes using the Bond Polymer refine detection kit, DS9800 (Vision Biosystems, Melbourne, Australia).

Quantitative digital image analysis and manual scoring

The TMA slide stained with H&E and IHC was digitized by Aperio AT2 scanner (Leica Biosystems, Buffalo Grove, IL, USA) at 20 \times magnification. For DLL4 and VEGF expression analysis, Aperio ImageScope software (ver. 12.4.2, Leica Biosystems, Buffalo Grove, IL, USA) was used. All tumor cells except those

in lymphocyte-rich areas were exclusively annotated in each TMA core. According to the expression patterns of the antibodies, DLL4 expression and VEGF expression were analyzed with membrane v9 algorithm and cytoplasm v2 algorithm (Fig. 1), respectively. The algorithms were available as a component in the commercial version of Aperio ImageScope software. Both algorithms automatically counted the VEGF- or DLL4-positive cells based on their staining intensity (0, 1+, 2+, and 3+). The annotation was performed by one pathologist (S.P.), and reviewed by an additional pathologist (K.T.J.) before the automatic analysis. Two pathologists (S.P. and K.T.J.) jointly reviewed the digitally scanned slides and results of the automatic analysis to confirm its performance. The H-scores could be automatically derived from the results (cytoplasm v2), or be calculated from the values of the results (membrane v9).

Due to the extensive background staining of HIF2 α compared to DLL4 and VEGF (Fig. 2), the expression of HIF2 α was manually scored according to the staining intensity (0, 1+, 2+, and 3+) (Fig. 3) to calculate the H-scores, by one pathologist (S.P.). As an additional pathologist (K.T.J.) reviewed, consensus was

achieved between two pathologists for any discrepancy.

Statistical analysis

As appropriate, Pearson's chi-square test or Cochran-Armitage test was used to analyze the correlation between DLL4, VEGF, and HIF2 α expression and clinicopathologic parameters. Pearson's chi-square test and Spearman's ρ rank correlation test were used to analyze the correlations between the expression levels of three markers. The Kaplan-Meier survival method was used to analyze survival rates. The Cox proportional hazard regression was used to describe the effects of one or more predictors on survival time or time-to-event outcomes. In all statistical analyses, IBM SPSS ver. 27.0 for Windows (IBM Corp., Armonk, NY, USA) and R software (R Foundation for Statistical Computing, Vienna, Austria) were used.

RESULTS

Clinicopathologic features of the GBC patients

The clinicopathologic features of the GBC patients and the

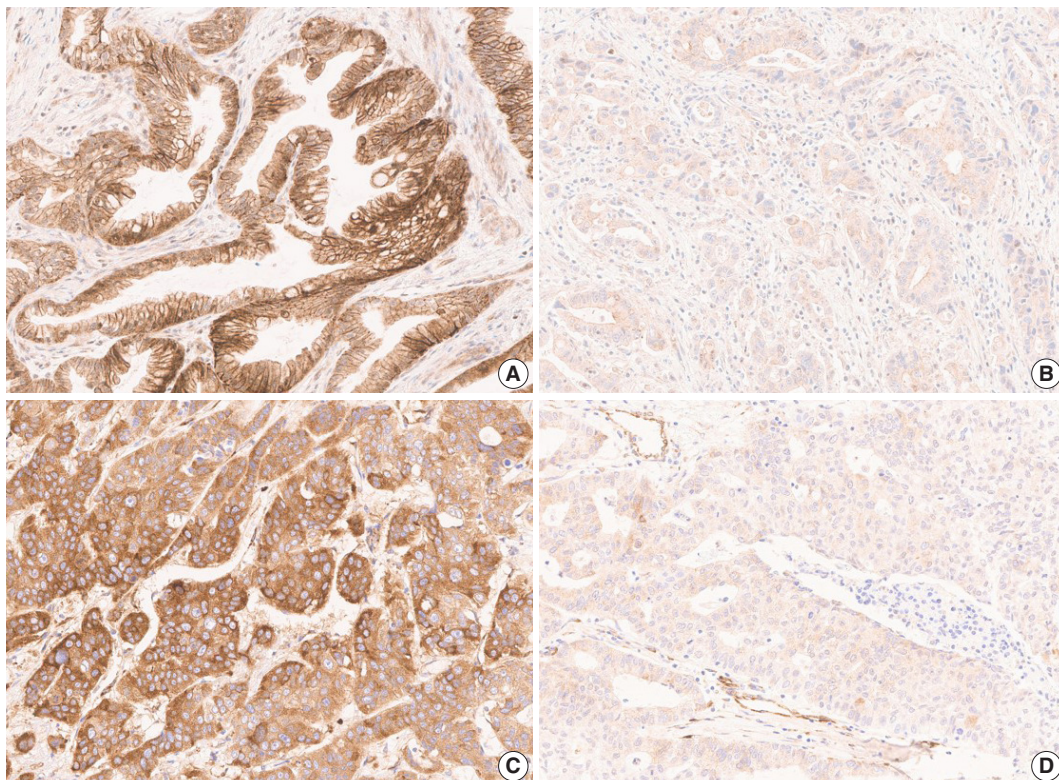


Fig. 1. Representative images of expression of anti-DLL4 and anti-VEGF antibodies in gallbladder cancer of each group, according to the H-score calculated via Aperio ImageScope software. (A) High membranous expression of anti-DLL4 antibody (H-score 208.43). (B) Low membranous expression of anti-DLL4 antibody (H-score 40.28). (C) High cytoplasmic expression of anti-VEGF antibody (H-score 214.01). (D) Low cytoplasmic expression of anti-VEGF antibody (H-score 34.36). DLL4, delta-like ligand 4; VEGF, vascular endothelial growth factor.

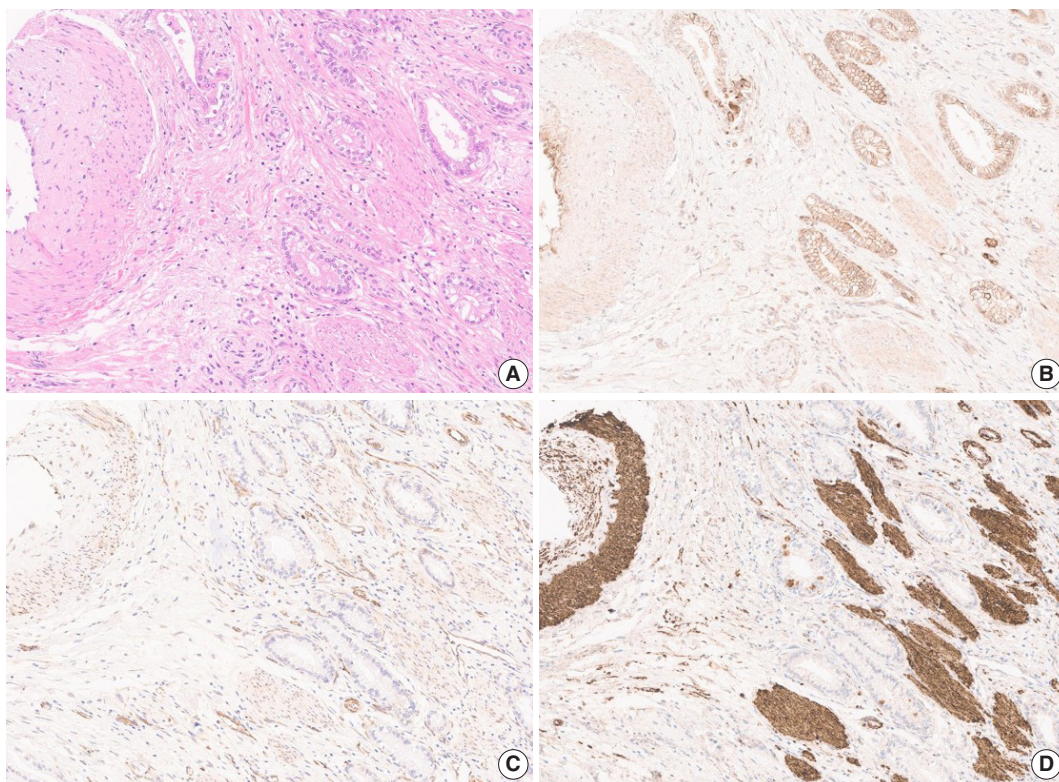


Fig. 2. Images of hematoxylin and eosin stain (A) and expression of anti-DLL4 (B), anti-VEGF (C), and anti-HIF2 α (D) antibodies in the corresponding area, showing tumor and surrounding soft tissue, including vessel, muscle, and nerve. Expression of anti-HIF2 α antibody shows extensive background stain compared to other markers, which led to manual scoring of H-score. Digital image analysis would mistake the background staining and overestimate the H-score of such cases. DLL4, delta-like ligand 4; VEGF, vascular endothelial growth factor; HIF2 α , hypoxia-inducible factor-2 α .

association of these features with DLL4, VEGF, and HIF2 α expression are summarized in Table 1. For the chi-square test, the expression levels of the markers were divided into two groups: high when the H-score ≥ 120 , low when < 120 (Fig. 1). Among the 99 patients, 40 patients (40.4%) were male, and 59 patients (59.6%) were female, and their age at the time of diagnosis ranged widely from 31 to 85 years (median age, 63 years). All tumors were primary GBCs, consist of conventional adenocarcinoma (81 cases, 81.8%), adenosquamous carcinoma (8 cases, 8.1%), neuroendocrine carcinoma (5 cases, 5.1%), mixed neuroendocrine carcinoma and adenocarcinoma, hepatoid adenocarcinoma (1 case, 1.0%), and undifferentiated carcinoma (3 cases, 3.0%, respectively). About half of the cases were well, moderately, or well to moderately differentiated tumors (56 cases, 56.6%). Forty cases (40.4%) had any proportion of poor differentiation, and the remaining three cases (3.0%) were classified as undifferentiated tumors. As a result of surgical resection, most cases were T3 (88 cases, 88.9%). Lymph node metastasis was present in 68 cases (68.7%), and distant metastasis was present in 11 cases (11.1%).

Recurrence occurred in 53 cases (53.5%) during the follow-up period (median, 11.6 months; range, 0.7 to 126.9 months) and 36 patients (36.4%) died during the follow-up period (median, 20.0 months; range, 0.7 to 126.9 months).

The chi-square test showed that lower DLL4 expression and VEGF expression was associated with lymph node metastasis ($p = .047$, both). The Cochran-Amitage test revealed that there is a statistically significant linear-trend between the degree of differentiation and VEGF or HIF2 α expression ($p = .028$ and $p = .006$, respectively). The test suggests strong evidence of a linearity between the expression of these markers and the tumor differentiation.

Expression of DLL4, VEGF, and HIF2 α

When compared by the chi-square test as described above, DLL4 expression did not correlate with the expression of other markers. VEGF and HIF2 α expression, however, was significantly correlated ($p < .001$), tumors with high VEGF expression would display higher expression of HIF2 α , vice versa.

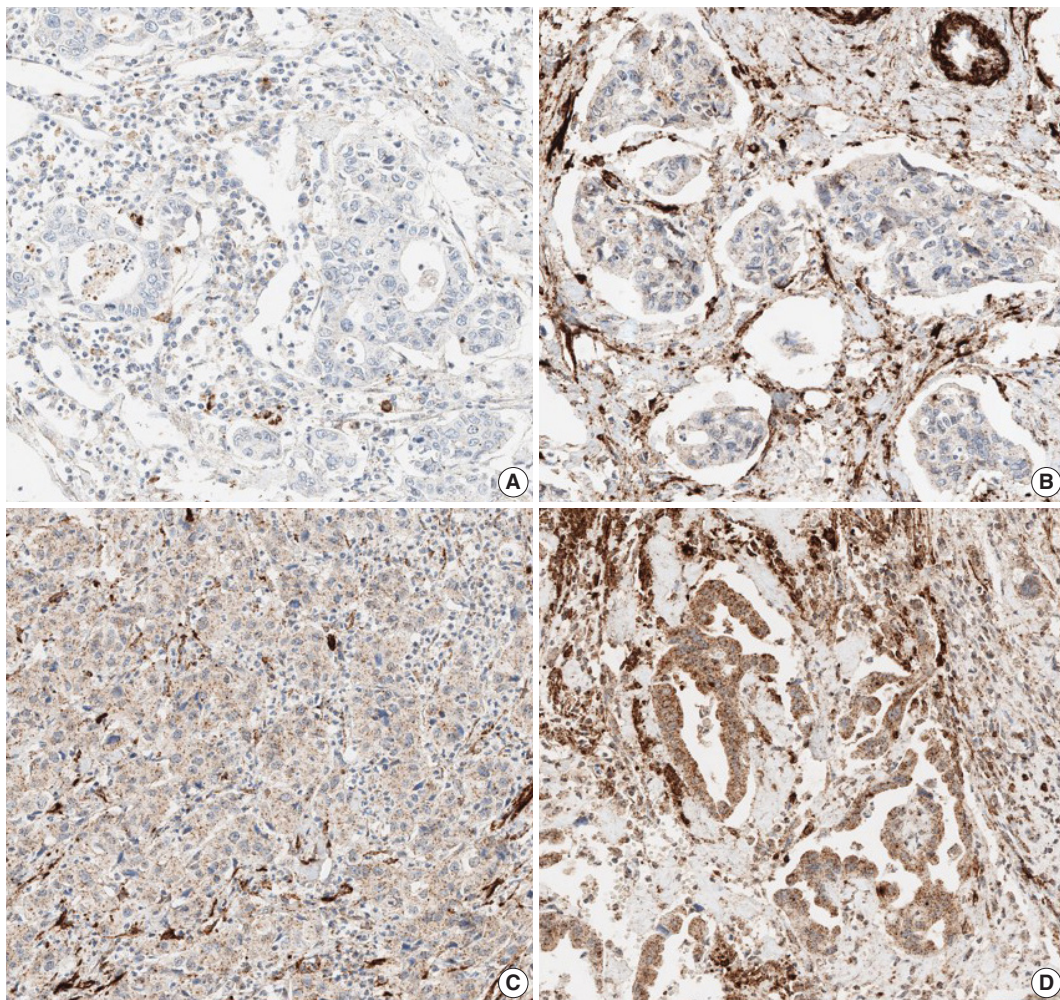


Fig. 3. Representative images of HIF2 α immunohistochemistry according to intensity score: (A) score 0, (B) score 1, (C) score 2, and (D) score 3. Background staining was intense in smooth muscles and lymphocytes. HIF2 α , hypoxia-inducible factor-2 α .

To further confirm the statistical significance of the correlation between expressions of the three markers, we performed an additional statistical analysis. By correlation matrix, the correlations were visualized, showing weak correlations between DLL4 vs. VEGF, and DLL4 vs. HIF2 α , but a relatively strong correlation between VEGF vs. HIF2 α (Fig. 4).

Considering that the H-score values of three makers are not normally distributed, we used Spearman's ρ rank correlation coefficient to test the significances of correlations between the H-score values of three makers. Between DLL4 and VEGF, and between DLL4 and HIF2 α , the Spearman's rank correlation coefficients are 0.09 ($p = .356$) and 0.34 ($p < .001$), respectively, which is consistent with the insignificant results obtained with previous chi-square test. Between H-score values of VEGF and HIF2 α , there was a statistically significant positive correlation, with correlation coefficient of 0.57 ($p < .001$). The Spearman's

rank correlation coefficient values between each marker are reflected in Fig. 4.

Impact of DLL4, VEGF, and HIF2 α expression on the prognosis

According to the Kaplan-Meier survival analysis result, expression of DLL4 and VEGF did not affect recurrence or death. According to HIF2 α expression, however, recurrence rates showed a statistically significant difference. When the cutoff for high or low expression was set as H-score = 150, patients with low HIF2 α expression ($n = 74$) showed shorter RFS than the patients with higher HIF2 α expression ($n = 25$) ($p = .048$). When the high expression group was defined as the tumor with more than 30% of 2+ and 3+ cells, patients with low HIF2 α expression ($n = 70$), again, showed shorter RFS than those with higher HIF2 α expression ($n = 29$) ($p = .011$) (Fig. 5). By performing Cox proportional

Table 1. The clinicopathologic features and association with DLL4, VEGF, and HIF2 α expression

	Total (n=99)	DLL4 expression		p-value	VEGF expression		p-value	HIF2 α expression		p-value
		Low (n=65, 65.7%)	High (n=34, 34.3%)		Low (n=56, 56.6%)	High (n=43, 43.4%)		Low (n=65, 65.7%)	High (n=34, 34.3%)	
Age (yr)				.654			.410			.648
\geq 60	67 (67.7)	43 (64.2)	24 (35.8)		36 (53.7)	31 (46.3)		45 (67.2)	22 (32.8)	
< 60	32 (32.3)	22 (68.8)	10 (31.3)		20 (62.5)	12 (37.5)		20 (62.5)	12 (37.5)	
Sex				.159			.796			.023
Female	59 (59.6)	42 (71.2)	17 (28.8)		34 (57.6)	25 (42.4)		44 (74.6)	15 (25.4)	
Male	40 (40.4)	23 (57.5)	17 (42.5)		22 (55.0)	18 (45.0)		21 (52.5)	19 (47.5)	
Diagnosis				NA			NA			NA
Adenocarcinoma	81 (81.8)	48 (59.3)	33 (40.7)		51 (63.0)	30 (37.0)		52 (64.2)	29 (35.8)	
Adenosquamous carcinoma	8 (8.1)	7 (87.5)	1 (12.5)		2 (25.0)	6 (75.0)		6 (75.0)	2 (25.0)	
NEC	5 (5.1)	5 (100)	0		1 (20.0)	4 (80.0)		4 (80.0)	1 (20.0)	
Mixed NEC and adenocarcinoma	1 (1.0)	1 (100)	0		0	1 (100)		1 (100)	0	
Hepatoid adenocarcinoma	1 (1.0)	1 (100)	0		1 (100)	0		1 (100)	0	
Undifferentiated carcinoma	3 (3.0)	3 (100)	0		1 (33.3)	2 (66.7)		1 (33.3)	2 (66.7)	
Differentiation ^a				.068			.028			.006
WD, MD	56 (56.6)	33 (58.9)	23 (41.1)		37 (66.1)	19 (33.9)		43 (76.8)	13 (23.2)	
PD	40 (40.4)	29 (72.5)	11 (27.5)		18 (45.0)	22 (55.0)		21 (52.5)	19 (47.5)	
UD	3 (3.0)	3 (100)	0		1 (33.3)	2 (66.7)		1 (33.3)	2 (66.7)	
T category ^a				.827			.792			.827
1b, 2a, 2b	5 (5.1)	1 (20.0)	4 (80.0)		3 (60.0)	2 (40.0)		4 (80.0)	1 (20.0)	
3	88 (88.9)	62 (70.5)	26 (29.5)		49 (55.7)	39 (44.3)		56 (63.6)	32 (36.4)	
4	6 (6.1)	2 (33.3)	4 (66.7)		4 (66.7)	2 (33.3)		5 (83.3)	1 (16.7)	
N category				.047			.047			.872
N0	31 (31.3)	16 (51.6)	15 (48.4)		13 (41.9)	18 (58.1)		20 (64.5)	11 (35.5)	
N1, N2	68 (68.7)	49 (72.1)	19 (27.9)		43 (63.2)	25 (36.8)		45 (66.2)	23 (33.8)	
M category				.410			.616			.410
M0	88 (88.9)	59 (67.0)	29 (33.0)		49 (55.7)	39 (44.3)		59 (67.0)	29 (33.0)	
M1	11 (11.1)	6 (54.5)	5 (45.5)		7 (63.6)	4 (36.4)		6 (54.5)	5 (45.5)	
AJCC stage				.112			.155			.772
I-III	71 (71.7)	50 (70.4)	21 (29.6)		37 (52.1)	34 (47.9)		46 (64.8)	25 (35.2)	
IV	28 (28.3)	15(53.6)	13 (46.4)		19 (67.9)	9 (32.1)		19 (67.9)	9 (32.1)	
Recurrence				.610			.690			.174
Yes	46 (46.5)	29 (63.0)	17 (37.0)		27 (58.7)	19 (41.3)		27 (58.7)	19 (41.3)	
No	53 (53.5)	36 (67.9)	17 (32.1)		29 (54.7)	24 (45.3)		38 (71.7)	15 (28.3)	
Death				.873			.789			.549
Yes	63 (63.6)	41 (65.1)	22 (34.9)		35 (55.6)	28 (44.4)		40 (63.5)	23 (36.5)	
No	36 (36.4)	24 (66.7)	12 (33.3)		21 (58.3)	15 (41.7)		25 (69.4)	11 (30.6)	
DLL4 expression							.340			.054
Low	65 (65.7)				39 (60.0)	26 (40.0)		47 (72.3)	18 (27.7)	
High	34 (34.3)				17 (50.0)	17 (50.0)		18 (52.9)	16 (47.1)	
VEGF expression				.340						<.001
Low	56 (56.6)	39 (69.6)	17 (30.4)					49 (87.5)	7 (12.5)	
High	43 (43.4)	26 (60.5)	17 (39.5)					16 (37.2)	27 (62.8)	
HIF2 α expression				.054			<.001			
Low	34 (34.3)	47 (72.3)	18 (27.7)		49 (75.4)	16 (24.6)				
High	65 (65.7)	18 (52.9)	16 (47.1)		7 (20.6)	27 (79.4)				

Values are presented as number (%).

DLL4, delta-like ligand 4; VEGF, vascular endothelial growth factor; HIF2 α , hypoxia-inducible factor-2 α ; NEC, neuroendocrine carcinoma; WD, well differentiated; MD, moderately differentiated; PD, poorly differentiated; UD, undifferentiated; AJCC, American Joint Committee on Cancer.

^aBy Cochran-Armitage trend test, otherwise by chi-square test.

hazard regression, HIF2 α expression was confirmed to be a significant predictive factor of the time to recurrence ($p = .020$), along with the presence of nodal metastasis of the patients ($p < .001$). The result regarding HIF2 α expression shows consistency with the result of Kaplan-Meier survival analysis. Overall survival rate

did not differ among patients according to HIF2 α expression by Kaplan-Meier survival analysis, and all the negative results were consistent with the result of Cox proportional hazard regression model.

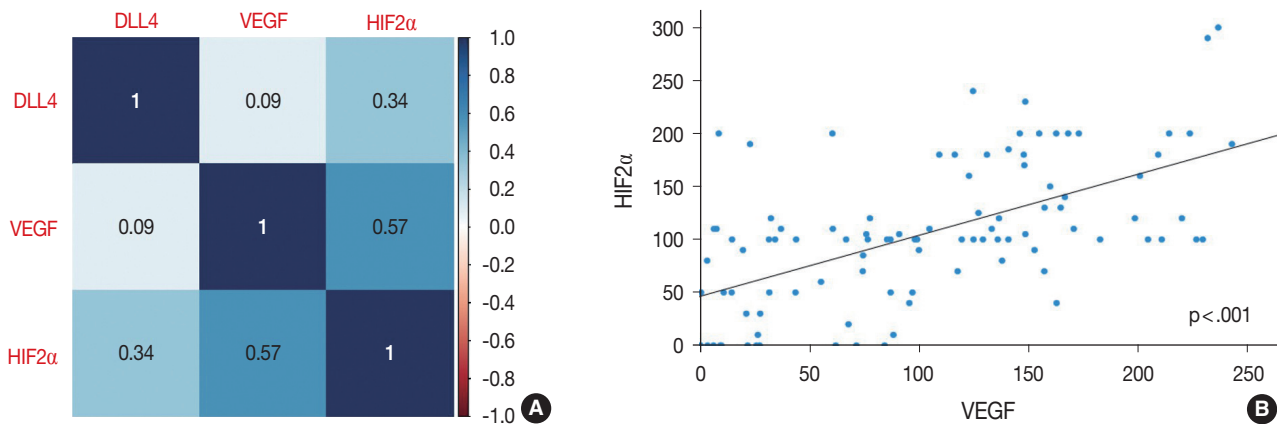


Fig. 4. The correlation matrix visualizing the correlation between the expression levels of DLL4, VEGF, and HIF2 α (A). The Spearman correlation coefficients are recorded in the center of each box. The scatter plot showing the positive correlation between VEGF and HIF2 α (B). DLL4, delta-like ligand 4; VEGF, vascular endothelial growth factor; HIF2 α , hypoxia-inducible factor-2 α .

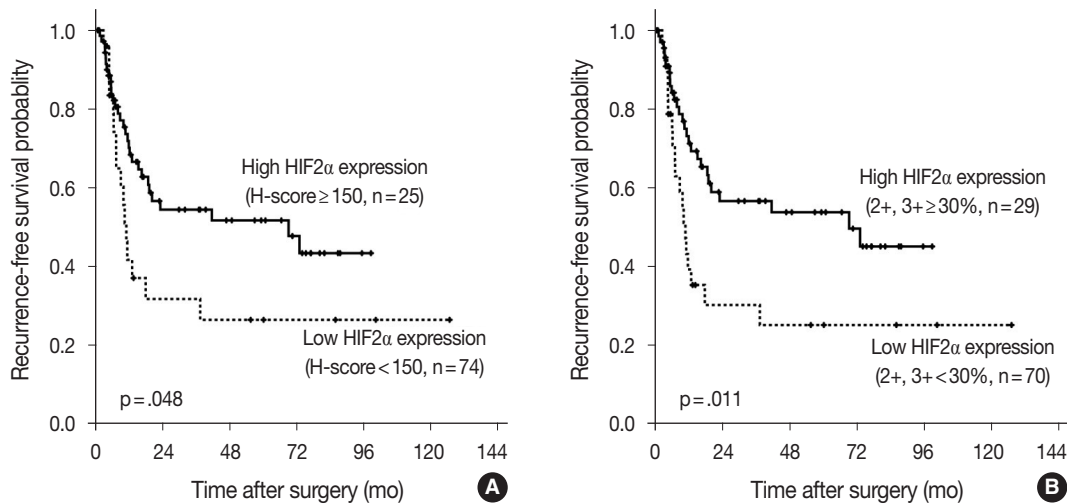


Fig. 5. Kaplan-Meier survival curves according to HIF2 α expression. (A, B) Recurrence-free survival curves for differently defined high/low expression groups. HIF2 α , hypoxia-inducible factor-2 α .

DISCUSSION

Although several previous studies investigated the expression of DLL4, VEGF, or HIF2 α in GBC separately [23-27], this is the first study to perform the IHC of these three markers coincidentally, attempting to integrate and confirm the results of the previous studies. As the study material, we used the TMA constructed with 99 surgically resected gallbladder cases from a single institution. These cases were followed up for a relatively long period of time – at least 0.7 months to a maximum of 11 years. For analysis of IHC, we digitized the slides and utilized a digital image analysis platform. Complete annotation of tumor area of 99 cases was laborious and time-consuming, but with this tool, we could assure the objectivity of the analysis. Most of the pre-

vious studies scored the IHC stain manually with a light microscope, which is inevitably subjective, and this might affect the study results. With digital image analysis, we attempted to overcome such limitations on the aspect of DLL4 and VEGF, but still not for the analysis related to HIF2 α , due to the background staining (Fig. 2D). Quantitative digital image analysis has been used in multiple previous studies in various platforms such as Aperio ImageScope, QuPath, ASAP, etc. Since subjectivity of interpretation has long been a hurdle to be overcome and a task for pathologists to conquer, we believe this can be achieved in part by digital image analysis.

The tumors were divided into three groups according to the degree of differentiation. The tumors that consisted of only well-differentiated and/or moderately differentiated portions were clas-

sified as the first group, and the tumors with any poorly differentiated portion were the second group. Only three undifferentiated tumors were classified as the third group. As a result, there was a positive trend between the differentiation and the expression of VEGF or HIF2 α ; the worse the differentiation tumors showed, the lower expression they exhibited. This trend was not consistent with the results of previous studies: some studies showed that VEGF expression was higher in poorly differentiated tumors compared to more differentiated tumors [25,27], and in other studies, no association was revealed [23,24]. To our knowledge, there have been no previous studies to report the significant association of degree of tumor differentiation and HIF2 α expression. Although this study demonstrated a different result than the previous ones because the expression of VEGF and HIF2 α are positively correlated, which is consistent with what is stated in other studies. Therefore, the result regarding the trend with differentiation might not be discarded. Instead, such conflicting results should be explained by investigating underlying mechanisms in future studies.

As stated above, VEGF and HIF2 α expression were significantly correlated – the tumors with higher VEGF expression tend to show higher HIF2 α expression, vice versa. In a study by Giatromanolaki et al. [23], IHC was performed in 60 GBC samples and showed a similar result compared to ours. Since the data showing the association between VEGF and HIF2 α expression are being accumulated, the application of these data onto the therapeutic aspects of these markers could be considered. VEGF has long been regarded as a well-established anti-neoplastic therapy. Several anti-VEGF inhibitors have been developed and are currently used, including bevacizumab [28]. Anti-VEGF inhibitor inhibits angiogenesis by reducing endothelial cell proliferation and thus tumor growth. Recently, anti-DLL4/anti-VEGF bispecific monoclonal antibody has been developed to enhance the anti-neoplastic activity and avoid the cardiac toxicity observed in patients when treated with anti-DLL4 inhibitors [16]. HIF2 α , on the other hand, playing a pivotal role in tumor progression and metastasis [19], and being the main driver in the development of clear cell RCC [29], is an attractive therapeutic target. Multiple agents have been designed, and some have shown promising results in preclinical level and clinical trials [30,31]. Since the role of both VEGF and HIF2 α and drugs that inhibit their action are being vigorously investigated, if VEGF and HIF2 α could work as surrogate markers for each other or helps predict the expression level of each other, it might be considerably useful and convenient, in possible future occasions that expression level of these markers may work as a treatment indication.

By chi-square test, we found that DLL4 and VEGF are correlated with lymph node metastasis status. DLL4 and VEGF expression tended to be lower in cases with lymph node metastasis ($p = .047$). Although our result did not reveal any prognostic significance of DLL4 and VEGF, because lymph node metastasis is determining factor for TNM stage that reflects patient survival, this correlation may point to the potential prognostic implication. In the cases that show low expression when stained with DLL4 and VEGF and if it is detected in biopsy sample prior to surgical resections, surgeons should perform meticulous lymph node dissection considering the higher possibility of lymph node metastasis. The pathologists should also spend more time evaluating the presence of tumor cells in dissected lymph nodes. If such a patient is subject to concurrent chemotherapy and radiotherapy, it would provide information for oncologists or radiologists' decision. Low expression groups of DLL4 and VEGF, however, account for more than half of the patients (65.7% and 56.6%, respectively), there is the possibility that they might not work as the effective screening tool. A study by Liu et al. [32] showed a relevant result in non-small cell lung cancer cases, stating that low DLL4 expression was significantly correlated with lymph node metastasis. A study with a conflicting result compared to ours [33] revealed that high DLL4 expression predicted pelvic lymph node metastasis in early cervical cancer patients. Moreover, high DLL4 expression was an independent predictor of poor survival in these cervical cancer patients. Such conflict is possibly due to the bi-functional cellular responses that Notch signaling pathway may induce during tumorigenesis in different tumors [17]. DLL4, working as a ligand in the Notch signal pathway, may either promote or inhibit tumor cell proliferation or survival, and this might be different according to tumor cell origin of tumor cell types. Further studies are necessary to clarify the underlying mechanism of DLL4 activity in GBC to confirm our results on lymph node metastasis.

Except for HIF2 α , two other markers did not show any correlation with prognosis. The correlation of HIF2 α with recurrence was not clear when the patients were divided into two groups: high as H-score ≥ 120 or low as H-score < 120 . When the high group was set with more conservative criteria (higher H-score) or the proportion of 2+ and 3+ cells, patients with lower HIF2 α expression showed shorter RFS than those with higher HIF2 α expression. By Cox proportional hazard regression model, HIF2 α expression was confirmed as a significant predictive factor for recurrence. High HIF2 α expression, therefore, may help to expect a better prognosis regarding recurrence, but the threshold for "high" expression should be relatively high to gain

reliable results. In our study cohort, some of the patients were transferred to different hospitals right after surgery for subsequent treatment and follow-up. The data regarding recurrence, death, and additional treatment could be incomplete, which might have affected our results.

In this study, multiple cutoffs for statistical analysis was used. For example, H-score = 120, H-score = 150 or the tumor with more than 30% of 2+ and 3+ cells, in each analysis. In studies using quantitative measuring of expression level, especially regarding the studies using immunohistochemical stain, a certain cutoff is needed for grouping the patients. The gold standard for setting the cutoff value, however, is not established or even recommended for pathologists. H-score = 120 was helpful in dividing the patients into two groups with adequate population in each group, for all three markers (DLL4: n = 65 in low group, n = 34 in high group; VEGF: n = 56 in low group, n = 43 in high group; HIF2 α : n = 65 in low group, n = 34 in high group). For survival analysis, however, with the same cutoff no statistically significant result was yielded, so that other cutoff values were adopted and utilized in this study. Considering that all researchers should report any meaningful data they obtained during the analysis, it was unavoidable to report the statistically significant results with multiple cutoffs.

In a previous study that demonstrated DLL4 expression was a prognostic marker and predicted gemcitabine effect in pancreatic cancer [34], two cohorts of patients, total 154, were enrolled and their clinicopathologic and treatment data for at least 6 years were collect. When a larger number of patients with complete data for survival and post-operative treatment is available in our study, DLL4 expression is worth being re-evaluated for its prognostic significance in association with treatment effect like the study by Drouillard et al. [34]. Our study has other limitations. The study cohort only includes surgically resected cases. Although 25 cases were advanced diseases as to be staged surgically as IVB, including 11 cases with distant metastasis and 14 cases without distant metastasis but with N2 lymph node metastasis, the majority of this cohort was relatively early GBC cases. Because GBC is one of the lately detected cancers, most of the patients are subject to systemic treatment rather than surgical resection at the time of diagnosis. Our cohort, therefore, may not represent the whole GBC patients. Another limitation is that we could not evaluate the HIF2 α expression digitally. Objectivity gained by quantitative digital image analysis for DLL4 and VEGF is one of the strengths of our study. However, due to the intensive background stain of HIF2 α (Fig. 2), there was no available tool to annotate and evaluate the intensity of staining exactly. Although

the consensus was made between two pathologists, manual evaluation might be relatively crude and subjective compared to digitized analysis.

In conclusion, this study studied the expression patterns and levels of DLL4, VEGF, and HIF2 α in surgically resected GBC. We demonstrated that VEGF and HIF2 α expression intensity is positively correlated, suggesting the possibility for these markers to work as mutually substitutable markers. Low DLL4 and VEGF expression levels were significantly associated with the status of lymph node metastasis, presumably with prognosis, although such a result was not yielded in this study. Lastly, patients with lower HIF2 α expression showed shorter RFS in our cohort. The cellular mechanisms of DLL4, VEGF, and HIF2 α in GBC are worth further investigating to explain these results, to accelerate the application the target therapy for these molecules to treat GBC patients.

Ethics Statement

The institutional review board of Samsung Medical Center approved this study (2021-10-053) and waived informed consent.

Availability of Data and Material

The datasets generated or analyzed during the study are available from the corresponding author on reasonable request.

Code Availability

Not applicable.

ORCID

Sujin Park	http://orcid.org/0000-0002-0804-2219
Junsik Kim	http://orcid.org/0000-0003-1428-8909
Kyoung-Mee Kim	http://orcid.org/0000-0002-1162-9205
Kee-Taek Jang	http://orcid.org/0000-0001-7987-4437

Author Contributions

Conceptualization: KMK, KTJ. Data curation: SP. Formal analysis: SP, JK. Investigation: SP. Methodology: SP, KMK. Resources: KMK, KTJ. Software: SP, JK. Supervision: KTJ. Visualization: SP, JK. Writing—original draft: SP. Writing—review & editing: KTJ.

Conflicts of Interest

The authors declare that they have no potential conflicts of interest.

Funding Statement

No funding to declare.

References

1. Jung KW, Won YJ, Hong S, Kong HJ, Im JS, Seo HG. Prediction of cancer incidence and mortality in Korea, 2021. *Cancer Res Treat* 2021; 53: 316-22.
2. Wi Y, Woo H, Won YJ, Jang JY, Shin A. Trends in gallbladder cancer incidence and survival in Korea. *Cancer Res Treat* 2018; 50: 1444-51.

3. Ministry of Health and Welfare, Korea Central Cancer Registry, National Cancer Center. Annual report of cancer statistics in Korea in 2018. Sejong: Ministry of Health and Welfare, 2020.
4. Tajima H, Ohta T, Shinbashi H, et al. Successful treatment of unresectable gallbladder cancer with low-dose paclitaxel as palliative chemotherapy after failure of gemcitabine and oral S-1: a case report. *Oncol Lett* 2012; 4: 1281-4.
5. Mishra SK, Kumari N, Krishnani N. Molecular pathogenesis of gallbladder cancer: an update. *Mutat Res* 2019; 816-818: 111674.
6. Neyaz A, Husain N, Gupta S, et al. Investigation of targetable predictive and prognostic markers in gallbladder carcinoma. *J Gastrointest Oncol* 2018; 9: 111-25.
7. D'Souza B, Miyamoto A, Weinmaster G. The many facets of Notch ligands. *Oncogene* 2008; 27: 5148-67.
8. Ranganathan P, Weaver KL, Capobianco AJ. Notch signalling in solid tumours: a little bit of everything but not all the time. *Nat Rev Cancer* 2011; 11: 338-51.
9. Lobov IB, Renard RA, Papadopoulos N, et al. Delta-like ligand 4 (DLL4) is induced by VEGF as a negative regulator of angiogenic sprouting. *Proc Natl Acad Sci U S A* 2007; 104: 3219-24.
10. Li JL, Sainson RC, Shi W, et al. Delta-like 4 Notch ligand regulates tumor angiogenesis, improves tumor vascular function, and promotes tumor growth in vivo. *Cancer Res* 2007; 67: 11244-53.
11. Kim Y, Byeon SJ, Hur J, et al. High delta-like ligand 4 expression correlates with a poor clinical outcome in gastric cancer. *J Cancer* 2019; 10: 3172-8.
12. Chen HT, Cai QC, Zheng JM, et al. High expression of delta-like ligand 4 predicts poor prognosis after curative resection for pancreatic cancer. *Ann Surg Oncol* 2012; 19 Suppl 3: S464-74.
13. Kontomanolis E, Panteliadou M, Giatromanolaki A, et al. Delta-like ligand 4 (DLL4) in the plasma and neoplastic tissues from breast cancer patients: correlation with metastasis. *Med Oncol* 2014; 31: 945.
14. Xiao M, Yang S, Ning X, Huang Y. Aberrant expression of delta-like ligand 4 contributes significantly to axillary lymph node metastasis and predicts postoperative outcome in breast cancer. *Hum Pathol* 2014; 45: 2302-10.
15. Koukourakis MI, Giatromanolaki A, Sivridis E, Gatter KC, Harris AL. High DLL4 expression in tumour-associated vessels predicts for favorable radiotherapy outcome in locally advanced squamous cell head-neck cancer (HNSCC). *Angiogenesis* 2013; 16: 343-51.
16. Jimeno A, Moore KN, Gordon M, et al. A first-in-human phase 1a study of the bispecific anti-DLL4/anti-VEGF antibody navicixizumab (OMP-305B83) in patients with previously treated solid tumors. *Invest New Drugs* 2019; 37: 461-72.
17. Katoh M, Katoh M. Precision medicine for human cancers with Notch signaling dysregulation (Review). *Int J Mol Med* 2020; 45: 279-97.
18. Mutvei AP, Landor SK, Fox R, et al. Notch signaling promotes a HIF2alpha-driven hypoxic response in multiple tumor cell types. *Oncogene* 2018; 37: 6083-95.
19. Moreno Roig E, Yaromina A, Houben R, Groot AJ, Dubois L, Vooijs M. Prognostic role of hypoxia-inducible factor-2alpha tumor cell expression in cancer patients: a meta-analysis. *Front Oncol* 2018; 8: 224.
20. Wierzbicki PM, Klacz J, Kotulak-Chrzaszcz A, et al. Prognostic significance of VHL, HIF1A, HIF2A, VEGFA and p53 expression in patients with clear-cell renal cell carcinoma treated with sunitinib as first-line treatment. *Int J Oncol* 2019; 55: 371-90.
21. Choueiri TK, Kaelin WG Jr. Targeting the HIF2-VEGF axis in renal cell carcinoma. *Nat Med* 2020; 26: 1519-30.
22. Amin MB, Edge SB, Greene FL, et al. *AJCC cancer staging manual*. 8th ed. New York: Springer, 2017.
23. Giatromanolaki A, Sivridis E, Simopoulos C, et al. Hypoxia inducible factors 1alpha and 2alpha are associated with VEGF expression and angiogenesis in gallbladder carcinomas. *J Surg Oncol* 2006; 94: 242-7.
24. Giatromanolaki A, Koukourakis MI, Simopoulos C, Polychronidis A, Sivridis E. Vascular endothelial growth factor (VEGF) expression in operable gallbladder carcinomas. *Eur J Surg Oncol* 2003; 29: 879-83.
25. Letelier P, Garcia P, Leal P, et al. Immunohistochemical expression of vascular endothelial growth factor A in advanced gallbladder carcinoma. *Appl Immunohistochem Mol Morphol* 2014; 22: 530-6.
26. Luo Y, Yang ZL, Wang C, et al. The clinicopathological significance of Jagged1 and DLL4 in gallbladder cancer. *Tumori* 2017; 103: 557-65.
27. Xu D, Li J, Jiang F, Cai K, Ren G. The effect and mechanism of vascular endothelial growth factor (VEGF) on tumor angiogenesis in gallbladder carcinoma. *Iran J Public Health* 2019; 48: 713-21.
28. Ferrara N, Hillan KJ, Gerber HP, Novotny W. Discovery and development of bevacizumab, an anti-VEGF antibody for treating cancer. *Nat Rev Drug Discov* 2004; 3: 391-400.
29. Hoeflin R, Harlander S, Schafer S, et al. HIF-1alpha and HIF-2alpha differently regulate tumour development and inflammation of clear cell renal cell carcinoma in mice. *Nat Commun* 2020; 11: 4111.
30. Choueiri TK, Bauer TM, Papadopoulos KP, et al. Inhibition of hypoxia-inducible factor-2alpha in renal cell carcinoma with belzutifan: a phase 1 trial and biomarker analysis. *Nat Med* 2021; 27: 802-5.
31. Wallace EM, Rizzi JB, Han G, et al. A small-molecule antagonist of HIF2alpha is efficacious in preclinical models of renal cell carcinoma. *Cancer Res* 2016; 76: 5491-500.
32. Liu H, Peng J, Zhao M, et al. Downregulation of DLL4 predicts poor survival in non-small cell lung cancer patients due to promotion of lymph node metastasis. *Oncol Rep* 2018; 40: 2988-96.
33. Yang S, Liu Y, Xia B, et al. DLL4 as a predictor of pelvic lymph node metastasis and a novel prognostic biomarker in patients with early-stage cervical cancer. *Tumour Biol* 2016; 37: 5063-74.
34. Drouillard A, Puleo F, Bachet JB, et al. DLL4 expression is a prognostic marker and may predict gemcitabine benefit in resected pancreatic cancer. *Br J Cancer* 2016; 115: 1245-52.

Unsuspected systemic Epstein-Barr virus–positive T-cell lymphoma of childhood diagnosed at autopsy in a potential homicide case

Daniel J. Robbins, Erik A. Ranheim, Jamie E. Kallan

Department of Pathology and Laboratory Medicine, University of Wisconsin School of Medicine and Public Health, Madison, WI, USA

Systemic Epstein-Barr virus (EBV)–positive T-cell lymphoma of childhood (SETLC) is a rare, rapidly progressive, and often fatal disease of children and young adults characterized by monoclonal expansion of EBV-positive T cells in tissues or peripheral blood following infection with EBV. Its distinction from other EBV-positive T-cell lymphoproliferative disorders with overlapping features can be difficult, and particular diagnostic features may not be manifest until autopsy examination. We present the case of a 10-year-old boy with significant disability due to remote traumatic brain injury following non-accidental head trauma who died unexpectedly at home. Given the history of physical abuse and the potential for homicide charges, significant medicolegal implications arose with this case. Pathologic investigation ultimately revealed conclusive diagnostic features of SETLC including extensive proliferation of EBV-positive T cells in multiple organs. A natural manner of death was confirmed, thereby excluding delayed homicide related to complications of non-accidental head trauma.

Key Words: Lymphoma, T-cell; Epstein-Barr virus infections; Autopsy; Homicide

Received: August 12, 2022 **Revised:** September 24, 2022 **Accepted:** October 30, 2022

Corresponding Author: Daniel J. Robbins, MD, Department of Pathology and Laboratory Medicine, 3170 UW Medical Foundation Centennial Building (MFCB), 1685 Highland Avenue, Madison, WI 53705-2281, USA
 Tel: +1-608-262-7158, Fax: +1-608-265-3301, E-mail: drobbins2@uwhealth.org

Systemic Epstein-Barr virus (EBV)–positive T-cell lymphoma of childhood (SETLC) is a rare, rapidly progressive, and often fatal disease of children and young adults characterized by monoclonal expansion of EBV-positive T cells in tissues or peripheral blood following infection with EBV [1]. The disease is most prevalent in eastern Asia and has also been reported in Latin America, but it is relatively rare in western countries [2]. Patients initially experience symptoms of acute viral illness including fever and malaise with subsequent development of hepatosplenomegaly, liver failure, coagulopathy, and pancytopenia. The disease is commonly associated with hemophagocytic syndrome and leads to organ failure, sepsis, and death within days to weeks. Due to its aggressive nature, prompt diagnosis is imperative though often difficult to establish, especially given overlapping features with other EBV-associated T-cell lymphoproliferative disorders [3,4].

Given the often fatal course of SETLC, particular diagnostic features may not be manifest until autopsy examination, making consideration of this entity important in the post-mortem setting [4-7]. Consideration of such rapidly progressive, fatal diseases be-

comes particularly important in forensic cases with unique medicolegal connotations. We present the case of a 10-year-old boy with significant disability due to remote traumatic brain injury (TBI) following non-accidental head trauma who died unexpectedly at home. Due to his debilitated state, he experienced frequent aspiration pneumonia and reportedly exhibited respiratory distress in the weeks and days prior to his death. Given the history of physical abuse and the potential for homicide charges, significant medicolegal implications arose with this case and magnified the importance of accurately ascertaining the cause and manner of death.

CASE REPORT

The decedent was a 10-year-old white male who at approximately 20 months of age suffered TBI, multiple skeletal fractures, and bilateral retinal hemorrhages following non-accidental head trauma. Sequelae of the TBI included severe spastic quadriplegia and cognitive impairment in addition to multiple hospital



Fig. 1. Gross findings at autopsy. (A) Cavitory lesion in the right temporal lobe (arrow) consistent with remote blunt head trauma. (B) Pulmonary parenchyma with diffuse nodularity imparting a “cobblestone” appearance. (C) Markedly prominent pulmonary hilar and mediastinal lymphadenopathy.

admissions for acute hypoxemic respiratory failure and pneumonia related to aspiration and viral infection. He was discharged home from the most recent admission approximately 5 weeks prior to his death. While aspiration and parainfluenza infection were noted during this admission, no diagnostic testing for EBV was performed, nor was there any documentation of prior EBV infection in the medical record. On the day of his death, the decedent reportedly experienced dyspnea before becoming unresponsive. Despite cardiopulmonary resuscitative efforts, he was ultimately pronounced dead at his residence.

Given the unexpected nature of his death and the medicolegal connotations associated with the history of physical abuse, a forensic autopsy was performed to evaluate the cause and manner of death. Internal gross examination revealed cavitory lesions of the right temporal lobe and the left frontal lobe of the brain consistent with remote blunt head trauma. The lungs displayed diffuse consolidation and parenchymal nodularity imparting a “cobblestone” appearance. Marked, extensive pulmonary hilar and mediastinal lymphadenopathy was identified with the largest lymph node measuring 3.5 cm (Fig. 1). Additionally, the gastroesophageal junction showed prominent mucosal nodularity. No significant hepatosplenomegaly was observed.

Hematoxylin and eosin stained tissue sections were prepared for microscopic examination. A section of pulmonary hilar lymph node showed vague preservation of B-cell follicles and profound paracortical expansion. The expanded paracortex was comprised of a spectrum of lymphocytes, ranging from small forms to more atypical intermediate/large forms with irregular nuclear contours, dispersed chromatin, and prominent nucleoli. Histologic sections of the lungs revealed effacement of the pulmonary architecture by sheets and expanded nodules of lymphoid cells with morphology identical to that in the lymph node along with frequent mitotic figures. Immunohistochemistry (IHC) was applied and showed the majority of atypical lymphocytes to be CD4-positive

T cells that were also positive for CD2 and CD3 and showed partial, aberrant loss of CD5 and CD7. The atypical cells were negative for CD56 and CD138. A minority of cells were positive for CD8. In-situ hybridization for EBV encoded RNA (EBER ISH) was performed and showed extensive positivity within atypical lymphoid cells in the lymph node and the lungs (Fig. 2). A section of liver revealed multiple periportal lymphoid aggregates composed predominantly of atypical T cells, while the spleen also demonstrated moderate infiltration of the red pulp by atypical T cells. A diffuse T cell infiltrate with similar morphology was also observed in the stomach disrupting the mucosal architecture. EBER ISH was positive within the atypical lymphocytes in the spleen, the liver, and the gastric mucosa. IHC performed on bone marrow showed an abundance of CD163-positive histiocytes displaying readily observable hemophagocytosis and occasional small, T-cell predominant lymphoid aggregates (Fig. 3).

The gross and microscopic features were consistent with an aggressive, EBV-positive T-cell lymphoma involving multiple organs. Given the fulminant disease onset and rapid, unexpected demise of this pediatric patient, a diagnosis of SETLC was rendered.

DISCUSSION

EBV-associated lymphoproliferative diseases comprise a wide spectrum of reactive and neoplastic processes that can result in the transformation and proliferation of B, T, or natural killer (NK) cells [8]. Amongst the entities affecting T cells and NK cells specifically, disease features can overlap causing difficulty in establishing a diagnosis. To achieve an accurate diagnosis, a combination of clinical and pathologic details must be considered as key differences exist between the morphologic and temporal aspects of these processes [4,7].

In our case, several aspects aligned with a diagnosis of SETLC. From a temporal standpoint, the rapid demise of the patient was

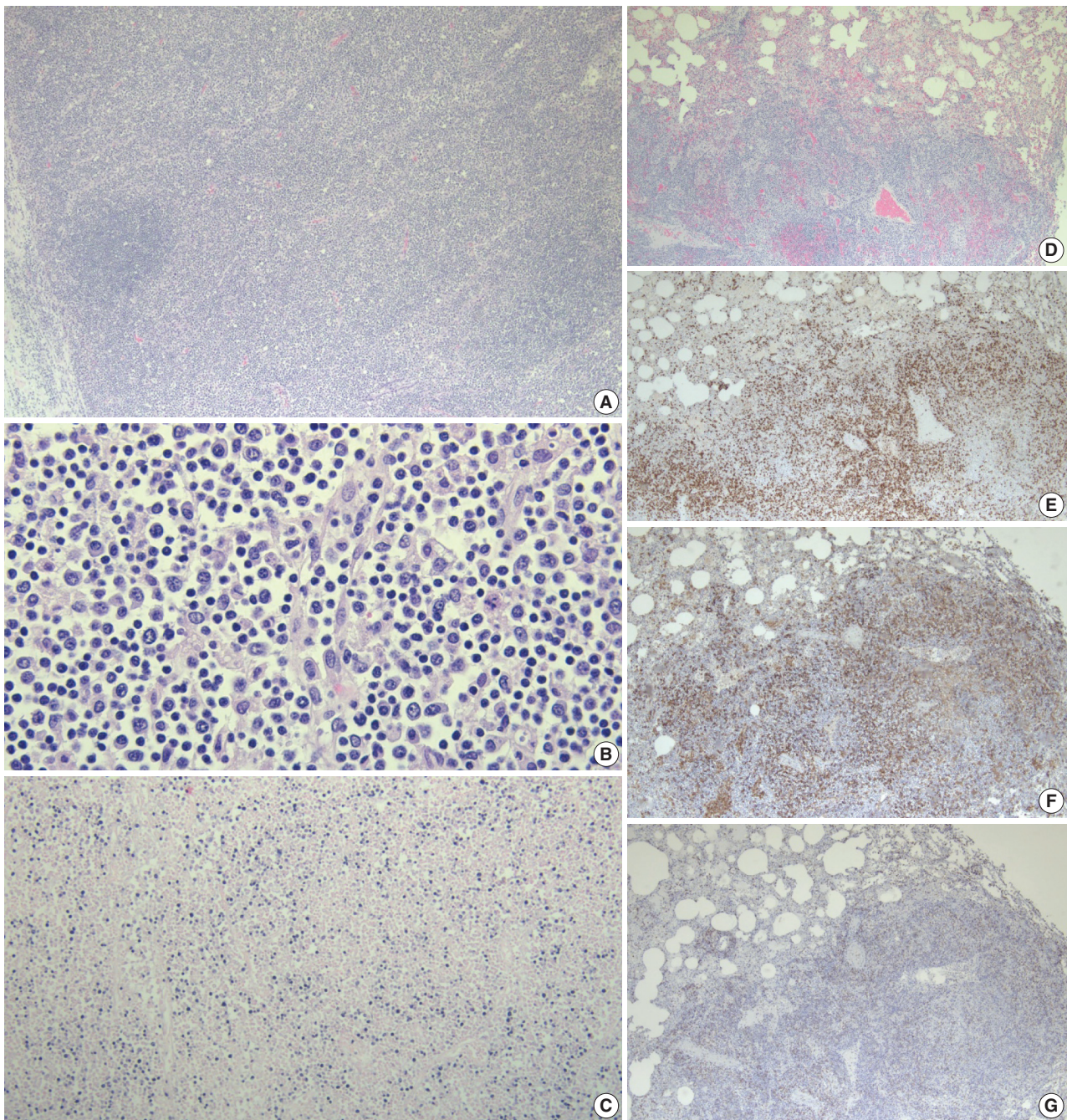


Fig. 2. Microscopic findings, pulmonary hilar lymph node (A–C) and lung (D–G). (A) Lymph node with marked paracortical expansion and vague residual follicles. (B) Neoplastic lymphocytes with a spectrum of size and morphologic atypia. (C) Positive in-situ hybridization for Epstein-Barr virus encoded RNA in neoplastic T cells. (D) Pulmonary architectural effacement by a neoplastic lymphoid infiltrate. (E) Prominent increase in T cells by immunohistochemistry (IHC) for CD3. (F) Neoplastic T cells were predominantly positive for CD4 by IHC. (G) The majority of neoplastic T cells were negative for CD8 by IHC.

consistent with the fulminant course associated with this entity. Gross and microscopic examination revealed overt T-cell lymphoma (features previously described above) with infiltration of multiple organs, demonstrating the aggressive and systemic nature of this disease. EBER ISH was positive in the T-cell infiltrates

confirming an EBV-driven etiology. Additionally, prominent hemophagocytosis was identified in the bone marrow, a finding that is often associated with SETLC [9].

Other EBV-positive T-cell and NK-cell lymphoproliferative disorders to consider along with SETLC include EBV-positive he-

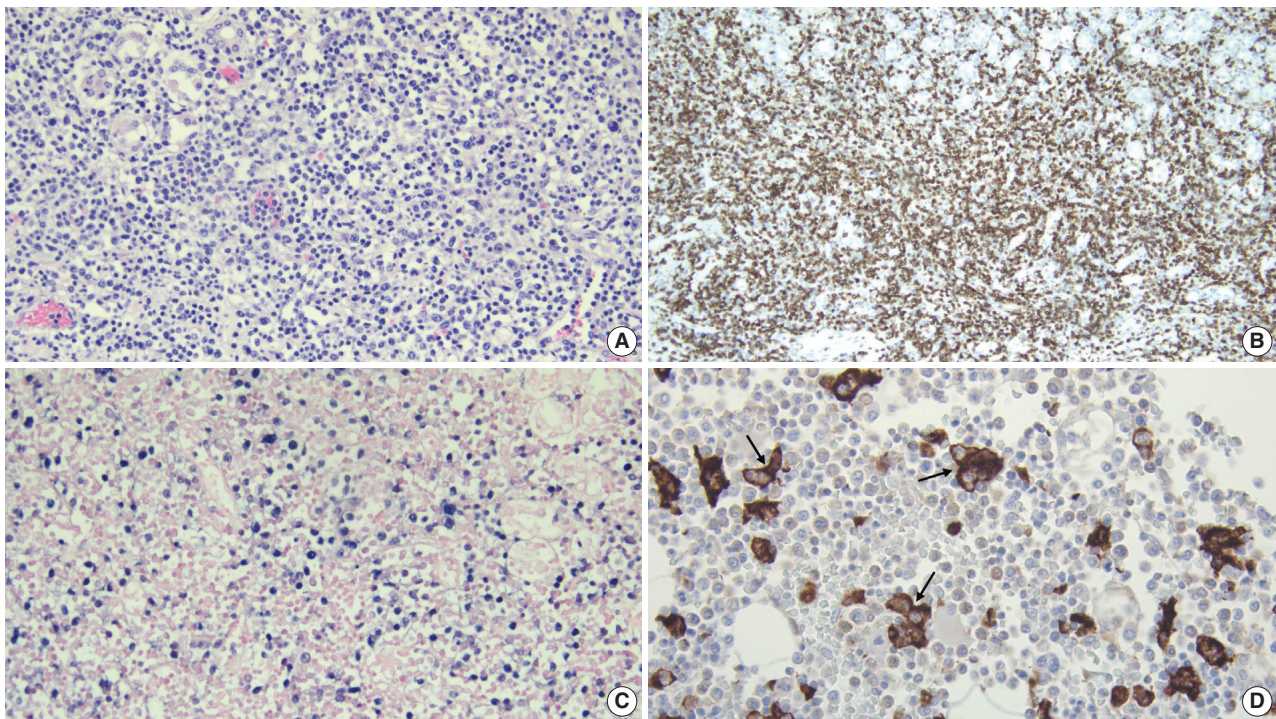


Fig. 3. Additional microscopic findings. (A) Gastric mucosa diffusely infiltrated by neoplastic lymphocytes with a spectrum of size and morphologic atypia. (B) Prominent increase in T cells within the gastric mucosa by immunohistochemistry (IHC) for CD3. (C) Positive in-situ hybridization for Epstein-Barr Virus encoded RNA within the neoplastic T cells in the gastric mucosa. (D) IHC for CD163 showing hemophagocytosis by histiocytes (arrows) in the bone marrow.

mophagocytic lymphohistiocytosis (HLH), systemic chronic active EBV infection (CAEBVI), hydroa vacciniforme-like lymphoproliferative disorder, and severe mosquito bite allergy. In our case, hydroa vacciniforme-like lymphoproliferative disorder and severe mosquito bite allergy could be excluded as these are primarily cutaneous disorders without profound systemic manifestations. EBV-positive HLH can present with clinical features similar to those of SETLC including fever, splenomegaly, and pancytopenia. However, while hemophagocytosis can be seen in the bone marrow, the spleen, or the lymph nodes, the proliferation of EBV-positive T cells is relatively small. Systemic CAEBVI can show some morphologic overlap with SETLC including paracortical expansion of lymph nodes, infiltration of multiple organs by EBV-positive T cells, and occasional hemophagocytosis. However, systemic CAEBVI displays reactive, nonspecific inflammatory changes and only subtle lymphoid infiltrates without cytologic atypia, as opposed to SETLC which is marked by neoplastic features, such as prominent lymphocytic proliferation and cytologic atypia. Additionally, systemic CAEBVI follows a more prolonged and less fulminant clinical course than SETLC with infectious symptoms persisting for greater than 3 months [1,9].

Regarding immunophenotype, the neoplastic T cells in our case

showed aberrant, partial loss of CD5 and CD7 expression by IHC. Such aberrant loss of pan T-cell antigens is a well-known feature of T-cell lymphomas in general and has been previously described in cases of SETLC specifically [4]. Cases of SETLC occurring after acute EBV infection generally show T cells with a cytotoxic CD8-positive immunophenotype, while those developing from systemic CAEBVI usually display T cells that are CD4-positive. Rarely, cases occur which exhibit both CD4-positive and CD8-positive EBV-infected T cells [2,10]. The majority of neoplastic T cells in our case were CD4-positive, but there was no evidence to suggest progression from previous systemic CAEBVI. Rather, it seems more likely that our case of SETLC is part of the unique minority that displays CD4-positive T cells following acute EBV infection.

Investigation of pediatric deaths can be a challenging aspect of forensic pathology and requires meticulous evaluation of all case aspects, particularly when there is a component of abuse or neglect [11]. This becomes particularly important when evaluating for delayed homicides which can result from complications of a remote injury inflicted by another individual. In such cases, it is crucial to determine not only the immediate cause of death but also the proximate cause of death, which is the origi-

nal injury without which the fatality would not have occurred. Infection is an immediate cause of death that can be associated with remote blunt force injuries and quadriplegia [12]. In this case, it was necessary to exclude bronchopneumonia as an immediate cause of death, especially given the reported history of dyspnea and recurrent aspiration. Since pathologic investigation revealed conclusive diagnostic features of SETLC, and excluded an etiology related to complications of non-accidental head trauma, the manner of death was determined to be natural rather than homicide.

In conclusion, we present the case of a 10-year-old boy with rapid and unexpected death due to SETLC that was diagnosed at autopsy. Our case is especially informative as it illustrates diagnostic features of SETLC that separate it from other EBV-positive lymphoproliferative disorders of T and NK cells. Additionally, it demonstrates the necessity of thorough forensic examination in the evaluation of potential homicide deaths. Finally, this case highlights the importance of considering aggressive, fulminant T-cell lymphomas as unexpected causes of death, particularly in patients with rapid deterioration and vague, nonspecific clinical presentation [5,6,13].

Ethics Statement

Given the forensic nature of this case, it did not qualify as human subject research per the Health Sciences Institutional Review Board at the University of Wisconsin-Madison, and prior approval was therefore not required. Appropriate consent was obtained from the referring medical examiner's office prior to performance of the forensic autopsy.

Availability of Data and Material

Data sharing not applicable to this article as no datasets were generated or analyzed during the study.

Code Availability

Not applicable.

ORCID

Daniel J. Robbins <https://orcid.org/0000-0003-3070-5186>

Erik A. Ranheim <https://orcid.org/0000-0002-5786-9327>

Author Contributions

Conceptualization: DJR, EAR, JEK. Investigation: DJR, EAR, JEK. Supervision: EAR, JEK. Visualization: DJR. Writing—original draft: DJR. Writing—review & editing: EAR, JEK. Approval of final manuscript: DJR, EAR, JEK.

Conflicts of Interest

The authors declare that they have no potential conflicts of interest.

Funding Statement

No funding to declare.

References

1. Kim WY, Montes-Mojarro IA, Fend F, Quintanilla-Martinez L. Epstein-Barr virus-associated T and NK-cell lymphoproliferative diseases. *Front Pediatr* 2019; 7: 71.
2. Quintanilla-Martinez L, Kumar S, Fend F, et al. Fulminant EBV(+) T-cell lymphoproliferative disorder following acute/chronic EBV infection: a distinct clinicopathologic syndrome. *Blood* 2000; 96: 443-51.
3. Tabanelli V, Agostinelli C, Sabattini E, et al. Systemic Epstein-Barr-virus-positive T cell lymphoproliferative childhood disease in a 22-year-old Caucasian man: a case report and review of the literature. *J Med Case Rep* 2011; 5: 218.
4. Coffey AM, Lewis A, Marcogliese AN, et al. A clinicopathologic study of the spectrum of systemic forms of EBV-associated T-cell lymphoproliferative disorders of childhood: a single tertiary care pediatric institution experience in North America. *Pediatr Blood Cancer* 2019; 66: e27798.
5. Kai K, Koga F, Araki N, et al. Autopsy case of systemic EBV-positive T-cell lymphoma of childhood with marked hepatomegaly in a middle-aged man. *Pathol Int* 2017; 67: 431-3.
6. Keow JY, Stecho WM, Haig AR, Sangle NA. EBV-positive T/NK-associated lymphoproliferative disorders of childhood: a complete autopsy report. *Indian J Pathol Microbiol* 2020; 63: 78-82.
7. Wang Z, Kimura S, Iwasaki H, et al. Clinicopathological findings of systemic Epstein-Barr virus-positive T-lymphoproliferative diseases in younger and older adults. *Diagn Pathol* 2021; 16: 48.
8. Kimura H, Ito Y, Kawabe S, et al. EBV-associated T/NK-cell lymphoproliferative diseases in nonimmunocompromised hosts: prospective analysis of 108 cases. *Blood* 2012; 119: 673-86.
9. Quintanilla-Martinez L, Ko YH, Kimura H, Jaffe ES. EBV-positive T-cell and NK-cell lymphoproliferative disease of childhood. In: Swerdlow SH, Campo E, Harris NL, et al., eds. *WHO classification of tumours of haematopoietic and lymphoid tissues*. Revised 4th ed. Lyon: IARC, 2017; 355-63.
10. Su IJ, Chen RL, Lin DT, Lin KS, Chen CC. Epstein-Barr virus (EBV) infects T lymphocytes in childhood EBV-associated hemophagocytic syndrome in Taiwan. *Am J Pathol* 1994; 144: 1219-25.
11. Knight LD, Collins KA. A 25-year retrospective review of deaths due to pediatric neglect. *Am J Forensic Med Pathol* 2005; 26: 221-8.
12. Lin P, Gill JR. Delayed homicides and the proximate cause. *Am J Forensic Med Pathol* 2009; 30: 354-7.
13. Alkhasawneh A, Mubeen A, Gopinath A. Lymphoma in autopsy cases. *Forensic Sci Med Pathol* 2018; 14: 327-31.

Solitary Peutz-Jeghers type hamartomatous polyp in duodenum with gastric foveolar epithelium: a case report

Eugene Choi¹, Junghwan Lee², Youngsoo Park¹

Departments of ¹Pathology and ²Gastroenterology, Asan Medical Center, University of Ulsan College of Medicine, Seoul, Korea

Peutz-Jeghers type hamartomatous polyp is known to be associated with Peutz-Jeghers syndrome, which shows characteristic multiple hamartomatous polyp involvement in the gastrointestinal tract, combined with mucocutaneous symptom, familial history of Peutz-Jeghers syndrome or *STK11/LTB1* mutation. However, some cases showing histologic appearance of the polyps discovered in Peutz-Jeghers syndrome while lacking other diagnostic criteria of the syndrome have been reported, and these are called solitary Peutz-Jeghers type polyps. Herein, we report a case of solitary Peutz-Jeghers type polyp covered with heterotopic epithelium. The patient was 47-year-old female without any mucocutaneous symptoms nor familial history of Peutz-Jeghers syndrome. Microscopic examination revealed Peutz-Jeghers type hamartomatous polyp in duodenum covered with gastric type foveolar epithelium. Considering the definition of hamartomatous polyp, which is, the abnormal overgrowth of the indigenous epithelial component, the histological feature of current case is noteworthy in a point that it shows proliferation of heterotopic component, rather than the indigenous component.

Key Words: Hamartoma; Intestinal polyps; Duodenum; Gastric mucosa; Peutz-Jeghers syndrome

Received: October 11, 2022 **Revised:** November 3, 2022 **Accepted:** November 6, 2022

Corresponding Author: Youngsoo Park, MD, Department of Pathology, Asan Medical Center, University of Ulsan College of Medicine, 88 Olympic-ro 43-gil, Songpa-gu, Seoul 05505, Korea

Tel: +82-2-3010-5608, Fax: +82-2-3010-4560, E-mail: youngspark@amc.seoul.kr

Hamartomatous polyp is defined as a polyp with disorganized growth of normal cells indigenous to the organ. Especially, Peutz-Jeghers type hamartomatous polyp represents as the arborization of smooth muscle within the lamina propria beneath pre-existing normal epithelium of the organ it involves. This polyp is known to be associated with Peutz-Jeghers syndrome, which shows characteristic multiple hamartomatous polyp involvement in the gastrointestinal (GI) tract, combined with mucocutaneous symptom, familial history of Peutz-Jeghers syndrome or *STK11/LTB1* mutation [1]. However, there have been a few cases which are histologically identical to those polyps associated with Peutz-Jeghers syndrome, without other clinical evidence diagnostic of Peutz-Jeghers syndrome. These polyps are called solitary Peutz-Jeghers type polyps [2]. We experienced a case of solitary Peutz-Jeghers type hamartomatous polyp in duodenum covered with gastric type foveolar epithelium, rather than the native intestinal columnar epithelium.

CASE REPORT

A 47-year-old woman visited outpatient clinic for incidentally discovered duodenal polyp during regular medical check-up. She did not experience any associated symptoms. She had a history of invasive ductal carcinoma of both breasts in her early to mid-30s and been treated for papillary thyroid carcinoma in her late 30s.

On initial esophagogastroduodenoscopy, a pedunculated polyp occupying half of the luminal space was found in the 2nd portion of duodenum. Histological examination of a biopsy specimen mainly showed hyperplastic gastric foveolar epithelium. Following computed tomography scan revealed a 2.9-cm-sized polypoid lesion in duodenum without any evidence of metastasis (Fig. 1A). The polyp was entirely resected by endoscopic submucosal dissection (Fig. 1B). The patient was discharged without any post-procedural complications.

Histological examination of the resected polyp showed disorganized overgrowth of epithelial cells supported by thick, branching

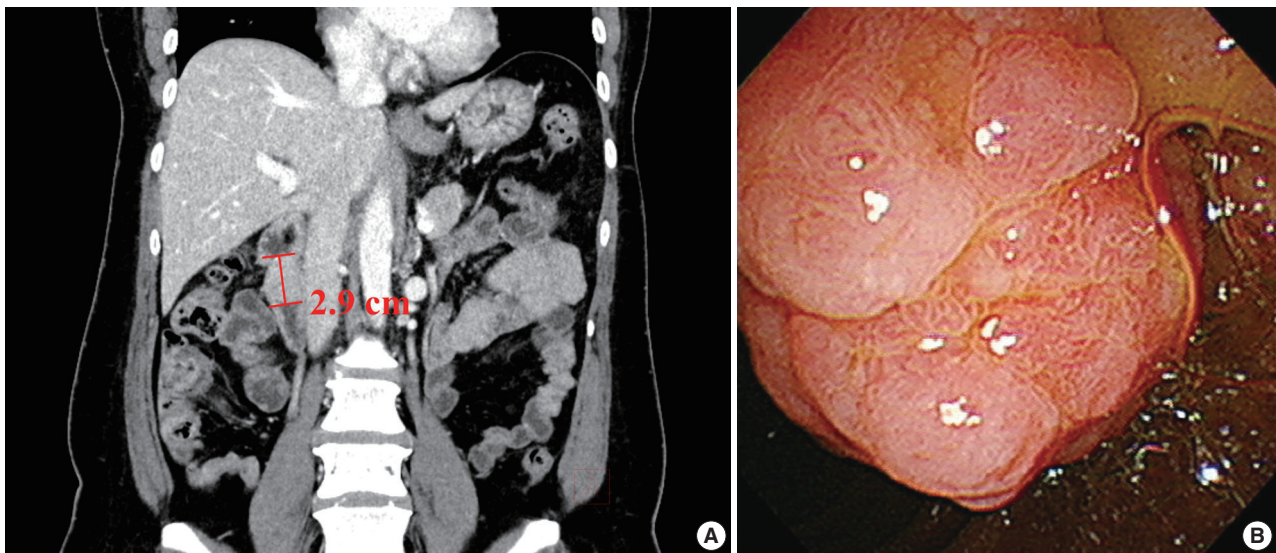


Fig. 1. Radiologic and endoscopic findings of the duodenal polyp. (A) Abdominal computed tomography image showing 2.9-cm-sized mass in duodenal 2nd portion. (B) A pedunculated polyp occupying half of the duodenal lumen discovered in endoscopic examination.

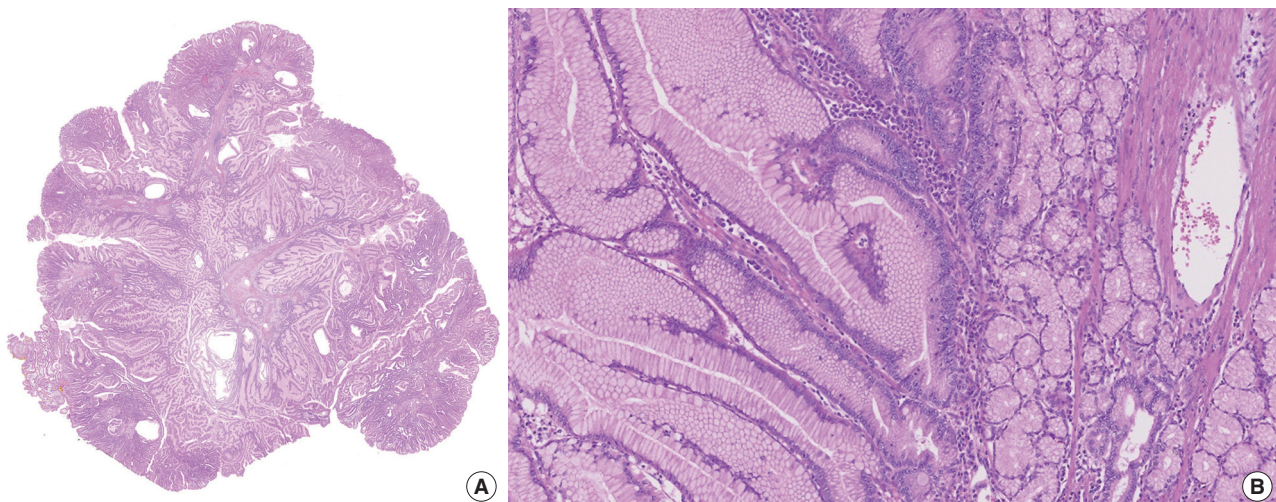


Fig. 2. Histological examination of the resected polyp. (A) Hematoxylin and eosin staining of the resected polyp showing arborizing smooth muscle bundles with overgrowth of superficial foveolar epithelium. (B) Foveolar type epithelium lying over pyloric type-like mucinous glands without dysplasia.

bundles of smooth muscles. The epithelium mainly consisted of foveolar type cells lying over mucinous glands resembling pyloric glands without dysplastic change (Fig. 2A, B). A small amount of surrounding duodenal tissue was identified at the margin of the specimen and it showed focal foveolar type epithelium among normal duodenal villous structures, suggestive of gastric metaplasia. Immunohistochemical staining for MUC5AC and MUC6 confirmed the covering hyperplastic epithelium to be gastric foveolar type with pyloric glands underneath (Fig. 3A, B).

Follow-up endoscopy after 6 months from the procedure revealed no additional polyps. In an in-depth interview after-

wards, the patient insisted she had never been diagnosed with hamartomatous polyp before and denied of any familial history nor any mucocutaneous symptoms. Genetic assessment for *STK11/LTB1* mutation was not done. According to these findings, the polyp was finally diagnosed as solitary Peutz-Jeghers type polyp with gastric foveolar epithelium.

DISCUSSION

Hamartomatous polyp is characterized by the arborization of smooth muscle bundle up to lamina propria with near-normal

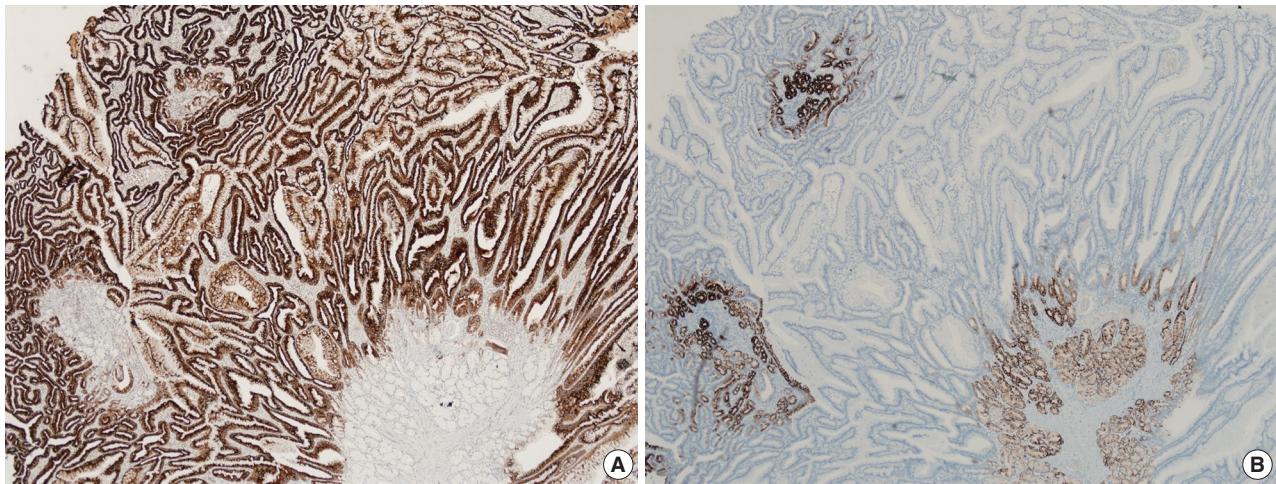


Fig. 3. Immunohistochemical stainings of the resected polyp. (A) Immunohistochemistry for MUC5AC confirms the presence of the overlying gastric type foveolar epithelium. (B) Pyloric gland-like structures showing positivity for MUC6 staining.

overlying epithelium. The surface epithelium of hamartomatous polyp is known to be identical with those of adjacent normal mucosa. Multiple hamartomatous polyps are frequently associated with various genetic syndromes, such as juvenile polyposis syndrome, Peutz-Jeghers syndrome and Cowden syndrome [1].

Of note, multiple GI tract polyps, mucocutaneous symptoms, *STK11/LTB1* mutation and familial history of Peutz-Jeghers syndrome are characteristic of Peutz-Jeghers syndrome. As this syndrome represents an increased risk of developing cancers, patient with solitary Peutz-Jeghers type hamartomatous polyp must be meticulously examined to exclude a possibility of syndromic involvement. If the polyp is proved to have no association with Peutz-Jeghers syndrome, it is defined as solitary Peutz-Jeghers type hamartomatous polyp. Although the histological aspect of solitary Peutz-Jeghers type hamartomatous polyp is indistinguishable from the polyps of Peutz-Jeghers syndrome, this solitary polyp seems to be of separated entity, as it does not show *STK11/LTB1* mutation characteristic of the syndrome. Furthermore, the frequently involved site is quite different. The polyp of the syndrome mostly occurs in small intestine, whereas the solitary counterpart develops mostly in sigmoid colon, followed by duodenum, rectum, jejunum, and stomach, according to the previously published literatures [2,3].

Solitary Peutz-Jeghers type hamartomatous polyp itself can provoke GI bleeding and intussusception, which may manifest as acute GI symptoms in some patients [4-6]. Some cases represented with dysplasia and even carcinogenesis [7,8]. Thus, complete resection of the polyp by either endoscopic or surgical procedure should be considered.

In our case, the patient was asymptomatic, and the polyp was

found during routine health check-up. The resected polyp showed hamartomatous proliferation of gastric foveolar epithelium over pyloric gland-like structures in the duodenum. Whether this aspect is related to prior gastric metaplasia or abnormal differentiation of endoderm is unclear at this moment. To date, a case of pyloric metaplasia involving multiple hamartomatous jejunal polyps in a patient with Peutz-Jeghers syndrome and a case of solitary Peutz-Jeghers type polyp with gastric antral and fundic gland mucosa have been reported [6,9]. Considering the definition of hamartomatous polyp, which is, the abnormal overgrowth of the indigenous epithelial component, the histological feature of current case is noteworthy in a point that it shows proliferation of heterotopic component, rather than the indigenous component.

Ethics Statement

Formal written informed consent was not required with a waiver by the appropriate IRB (Asan Medical Center IRB No. 2022-1339).

Availability of Data and Material

Data sharing not applicable to this article as no datasets were generated or analyzed during the study.

Code Availability

Not applicable.

ORCID

Eugene Choi <https://orcid.org/0000-0002-0457-7785>
 Junghwan Lee <https://orcid.org/0000-0002-2910-479X>
 Youngsoo Park <https://orcid.org/0000-0001-5389-4245>

Author Contributions

Conceptualization: YP. Data curation: JL. Formal analysis: EC. Investigation: EC. Supervision: YP. Writing—original draft: EC. Writing—review & editing: YP, EC. Approval of final manuscript: all authors.

Conflicts of Interest

The authors declare that they have no potential conflicts of interest.

Funding Statement

No funding to declare.

References

1. Brosens LA, Jansen M. Peutz-Jeghers syndrome. In: WHO Classification of Tumours Editorial Board, ed. Digestive system tumours. WHO classification of tumours. 5th ed. Lyon: International Agency for Research on Cancer, 2019; 545-6.
2. Sone Y, Nakano S, Takeda I, Kumada T, Kiriyama S, Hisanaga Y. Solitary hamartomatous polyp of Peutz-Jeghers type in the jejunum resected endoscopically. *Gastrointest Endosc* 2000; 51: 620-2.
3. Endo K, Kawamura K, Murakami K, et al. A case of jejunal solitary Peutz-Jeghers polyp with intussusception identified by double-balloon enteroscopy. *Clin J Gastroenterol* 2020; 13: 1129-35.
4. Oncel M, Remzi FH, Church JM, Goldblum JR, Zutshi M, Fazio VW. Course and follow-up of solitary Peutz-Jeghers polyps: a case series. *Int J Colorectal Dis* 2003; 18: 33-5.
5. Itaba S, Namoto M, Somada S, et al. Two cases of solitary Peutz-Jeghers-type hamartoma of the duodenum. *Endoscopy* 2006; 38 Suppl 2: E32-3.
6. Liu BL, Zhou H, Risech M, Ky A, Houldsworth J, Ward SC. Solitary Peutz-Jeghers type polyp of jejunum with gastric fundic and antral gland lining mucosa: a case report and review of literature. *Int J Surg Pathol* 2022; 30: 539-42.
7. Ichiyoshi Y, Yao T, Nagasaki S, Sugimachi K. Solitary Peutz-Jeghers type polyp of the duodenum containing a focus of adenocarcinoma. *Ital J Gastroenterol* 1996; 28: 95-7.
8. Suzuki S, Hirasaki S, Ikeda F, Yumoto E, Yamane H, Matsubara M. Three cases of solitary Peutz-Jeghers-type hamartomatous polyp in the duodenum. *World J Gastroenterol* 2008; 14: 944-7.
9. Kato N, Sugawara M, Maeda K, Hosoya N, Motoyama T. Pyloric gland metaplasia/differentiation in multiple organ systems in a patient with Peutz-Jegher's syndrome. *Pathol Int* 2011; 61: 369-72.

Unusual biclonal IgA plasma cell myeloma with aberrant expression of high-risk immunophenotypes: first report of a new diagnostic and clinical challenge

Carlos A. Monroig-Rivera¹, Clara N. Finch Cruz^{2,3}

¹School of Medicine, Ponce Health Sciences University, Ponce;

²Department of Basic Sciences, School of Medicine - Ponce Health Sciences University, Ponce;

³Southern Pathology Services, Inc., Ponce, Puerto Rico, USA

IgA plasma cell myeloma (PCM) has been linked to molecular abnormalities that confer a higher risk for adverse patient outcomes. However, since IgA PCM only accounts for approximately 20% of all PCM, there are very few reports on high-risk IgA PCM. Moreover, no such reports are found on the more infrequent biclonal IgA PCM. Hence, we present a 65-year-old Puerto Rican female with acute abdominal pain, concomitant hypercalcemia, and acute renal failure. Protein electrophoresis with immunofixation found high IgA levels and detected a biclonal IgA gammopathy with kappa specificity. Histomorphologically, bone marrow showed numerous abnormal plasma cells (32%) replacing over 50% of the marrow stroma. Immunophenotyping analysis detected CD45-negative plasma cells aberrantly expressing CD33, CD43, OCT-2, and c-MYC. Chromosomal analysis revealed multiple abnormalities including the gain of chromosome 1q. Thus, we report on an unusual biclonal IgA PCM and the importance of timely diagnosing aggressive plasma cell neoplasms.

Key Words: Biclonal IgA; Plasma cell myeloma; Abdominal pain; High-risk phenotypes; Prognosis

Received: September 11, 2022 **Revised:** November 22, 2022 **Accepted:** February 7, 2023

Corresponding Author: Clara N. Finch Cruz, MD, Department of Basic Sciences, School of Medicine - Ponce Health Sciences University, 388 Zona Industrial Reparada 2 Ponce, Puerto Rico 00716-2347, USA

Tel: +1-787-840-2575, Fax: +1-787-844-3865, E-mail: cfinch@psm.edu

Biclonal IgA plasma cell myeloma (PCM) is a rarely reported entity (<2% of PCM) that arises when neoplastic plasma cells in the bone marrow secrete high levels of two distinct monoclonal immunoglobulins (biclonal M-protein), both of IgA specificity [1,2]. Recently, with the advent of new diagnostic criteria, the more common monoclonal IgA neoplasms (expressing a single IgA M-protein) have been associated with poorer long-term survival [1]. Moreover, the updated criteria now allow for the early diagnosis of high-risk PCM by including the detection of abnormal immunophenotypes and of genetic abnormalities that could predict PCM prognosis and guide treatment options [1,3,4]. To date, no published reports on molecular phenotypes are associated with high-risk disease in patients with biclonal IgA PCM. Herein, we report the first case of a patient with an unusual biclonal IgA PCM expressing high-risk phenotypes and discuss its diagnostic and clinical challenges.

CASE REPORT

A 65-year-old female, Hispanic (from Puerto Rico) presented to the Emergency Department with a history of abdominal pain of 6 hours' duration, a day after receiving the second dose of the coronavirus disease 2019 (COVID-19) vaccine. The patient denied fever, chills, dizziness, chest pain, trauma, and changes in urine or stool. Her past medical history included: obesity, hypertension, adult-onset diabetes, and status post cholecystectomy, but no history of smoking, alcohol intake, or of COVID-19 infection. She had a family history of diabetes and hypertension. Physical examination revealed mild tachycardia but was otherwise unremarkable. Subsequently, she was transferred and admitted to the hospital due to laboratory tests showing hypercalcemia with calcium level greater than 15.0 mg/dL (reference range, 8.3 to 10.6 mg/dL), increased blood urea nitrogen 36 mg/dL (refer-

ence range, 9 to 23 mg/dL) and creatinine levels 2.40 mg/dL (reference range, 0.6 to 1.1 mg/dL). Additionally, initial complete blood count results detected leukocytosis of 19.7×10^3 cells/ μ L (4.3 – 10.3×10^3 cells/ μ L) with an increase in the absolute counts of all leukocyte subtypes in the blood and morphologic findings suggestive of infection. Severe acute respiratory syndrome coronavirus 2 testing detected IgG antibody (positive), but not IgM or antigen.

During her hospitalization, peripheral blood evaluations showed resolving leukocytosis, but worsening normocytic anemia with hemoglobin levels dropping from an initial 10.8 to 7.8 g/dL (11.3–14.8 g/dL) that required blood transfusions. Also, rouleaux formation and slight leukoerythroblastosis were noted. Serum protein electrophoresis with immunofixation (PEP/IFx) found significantly high IgA levels at 3,410 mg/dL (87–352 mg/dL) and detected two M-protein bands in the beta region confirming the presence of a biclonal IgA gammopathy with kappa specificity (Table 1). Serum levels of IgG and IgM were decreased. Urine PEP/IFx detected increased Ig in the IgA region without a well-defined band. Additionally, serum beta-2 microglobulin was markedly increased at 8.4 mg/L (0.6–2.4 mg/L).

Imaging studies including computed tomography scans of the abdomen, pelvis, and brain were done and did not find abdominal or extraosseous mass lesions. However, a whole-body bone scan identified several nonspecific lesions suspicious of metastatic infiltration or post-trauma involving the left sacroiliac joint, ster-

num, and the right knee lateral femoral component.

Subsequently, a bone marrow sampling was obtained from her right iliac crest. Morphological and histological evaluations of bone marrow aspirate and biopsy samples showed the following: hypercellularity (85%–95% cellularity); increase proportion of abnormal plasma cells (32%), predominantly of intermediate-type morphology with features between immature and mature plasma cells; and replacement of over 50% of the marrow stroma by the neoplastic infiltrate (Fig. 1A, B). Additionally, using reticulin and collagen stains, the presence of myelofibrosis and osteosclerosis was identified within the focal areas replaced by sheets of plasma cells and graded as MF2 of 3 [5]. No myelofibrosis was observed in the uninvolved marrow areas. Semiquantitative morphometric analysis using immunohistochemical stains were performed and revealed that a significant proportion of the marrow plasma cells expressed CD138 (>90%) and MUM1 (>95%) with a high kappa/lambda ratio of ~49.5. Additionally, CD43 (>95%, a T-cell marker), OCT-2 (70%–80%), and c-MYC (15%–25%, low expression) were aberrantly expressed (Fig. 2A–D). These plasma cells did not appear to significantly express (<20% positivity) CD10, CD56, CD79a, CD117/c-KIT, IgG, IgM, PAX5, SOX-10, cyclin D1/BCL1, Epstein-Barr virus, or myeloid markers (CD11c, CD15, and myeloperoxidase). However, flow cytometry studies detected CD45-negative, CD19-positive plasma cells aberrantly expressing CD33, a myeloid marker (Fig. 3A, B). Cytogenetics studies showed an abnormal complex karyotype including odd-number trisomies, and gain of chromosome 1q (Fig. 4). Then, a final diagnosis was rendered of biclonal IgA PCM with aberrant expression of multiple high-risk markers such as CD33, CD43, OCT-2, c-MYC, and gain of chromosome 1q.

Ultimately, the revised International Staging System (R-ISS) was used to estimate the patient's prognosis [4]. Based on the Cytogenetics and other key laboratory results, the patient's predicted R-ISS score placed her in the stage III (of III) category. This information confirming the presence of an aggressive biclonal IgA myeloma was also reported and discussed with her treating physician to help guide treatment options. However, upon being discharged, the patient was lost to follow-up.

DISCUSSION

Studies of newly-diagnosed patients with biclonal IgA PCM are uncommon. A possible explanation for this apparent underreporting could be that IgA PCM is a rare entity and difficult to diagnose [6,7]. Until recently, no major differences in clinical

Table 1. Biclonal IgA-kappa plasma cell myeloma: key laboratory tests and results

Test	Result	Reference range	Comments
IgG	465 L	586–1,602 mg/d	Quantitative immunoglobulin (Ig) serum levels
IgM	7 L	26–217 mg/dL	
IgA	3410 H	87–352 mg/dL	
Albumin	3.4	2.9–4.4 g/dL	Serum protein electrophoresis
Alpha-1-globulin	0.2	0.0–0.4 g/dL	
Alpha-2-globulin	0.7	0.4–1.0 g/dL	
Beta globulin	4.5 H	0.7–1.3 g/dL	
Gamma globulin	0.4	0.4–1.8 g/dL	
M-spike	3.9 H	0.01 g/dL	
Beta 1	3.2 H	-	
Beta 2	0.7 H	-	
IgA, total	3.9 H	-	
Immunofixation, serum	Biclonal IgA with kappa specificity	-	
Beta-2 microglobulin	8.4 H	0.6–2.4 mg/L	High-risk factor, when ≥ 5.5 mg/L ^a

L, low; H, high.

^aAccording to the Revised International Staging System for Multiple Myeloma (R-ISS) [4], and The Multiple Myeloma Prognosis (R-ISS) calculator created by QxMD.

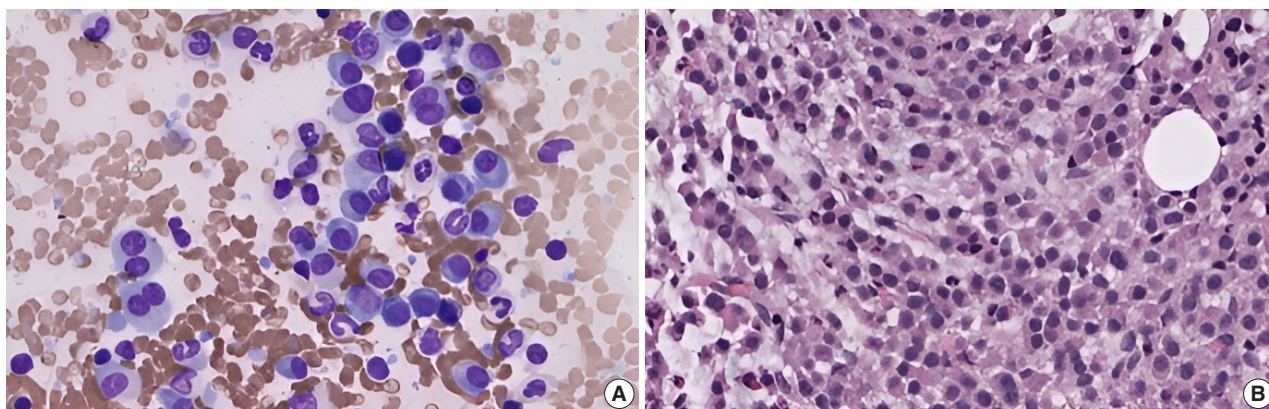


Fig. 1. Histomorphology of biclonal IgA plasma cell myeloma. (A) Bone marrow imprint shows increased (32%) atypical plasma cells with features between immature and mature forms (“intermediate-type” morphology); binucleation and rare plasmablasts are seen (Wright-Giemsa stain). (B) Bone marrow biopsy is hypercellular (85%–95%) with >50% replaced by sheets of plasma cells.

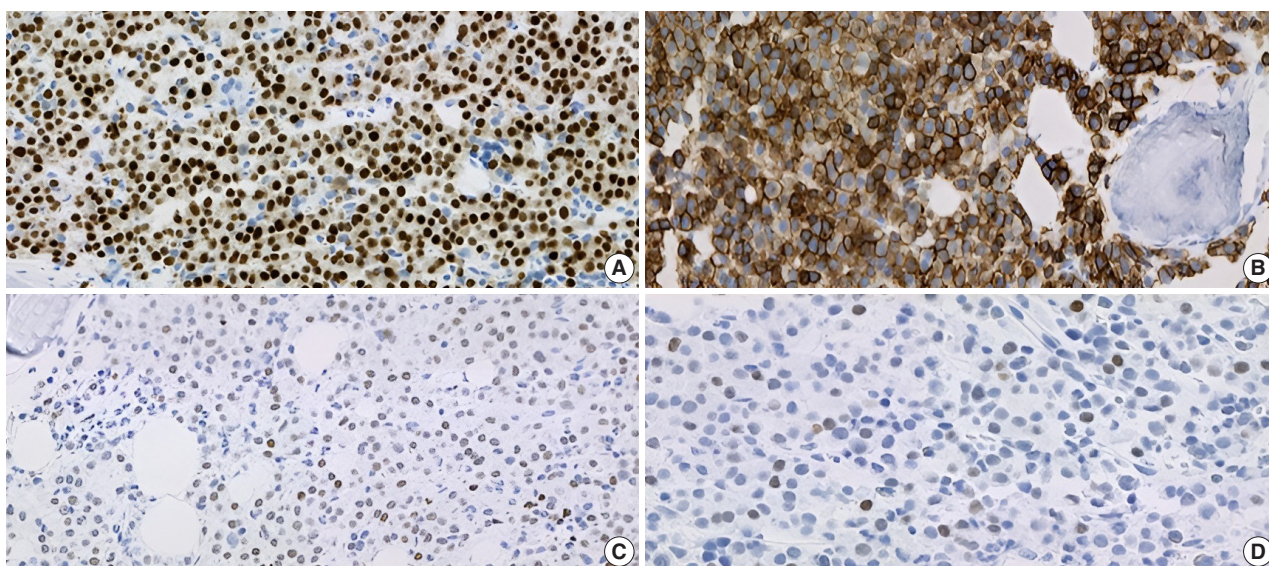


Fig. 2. Semiquantitative, morphometric analysis of biclonal plasma cells done using immunohistochemical stains on the decalcified, formalin-fixed bone marrow biopsy sample. Plasma cells express MUM1 (>90%) (A), but aberrantly express high-risk marker CD43 (>95%, a T-cell marker) (B), and overexpress high-risk markers OCT-2 (70%–80%) (C) and c-MYC (15%–25%) (D).

presentation, prognosis, and treatment of plasma cell neoplasms were identified among patients diagnosed with IgA or the most common IgG isotype, whether expressing monoclonal or biclonal M-protein(s) [8]. However, PCM is now recognized as a genetically heterogeneous neoplasm with a subset of patients targeted to develop high-risk disease [9]. Moreover, Habermehl et al. [1] reported on the poorer long-term survival of a cohort of patients with IgA gammopathy when compared to IgG patients. This recently recognized higher risk for adverse outcomes is potentially due to a decreased genomic stability in IgA neoplasms; and favors that IgA be considered in a separate diagnostic category from other PCMs. Further, their study demonstrates the impor-

tance of reporting unusual features, biomarkers, molecular abnormalities, and prognostic factors to further characterize high-risk, aggressive IgA PCM. To the best of our knowledge, this is the first report of a biclonal IgA PCM with an unusual clinical presentation in which a combination of multiple high-risk molecular phenotypes is detected.

Clinically, PCM presenting with abdominal pain as the initial symptom, like in our patient, is unusual and seldom reported. Upon review of the biomedical literature, we found only four reports of patients with IgA PCM presenting with abdominal pain (Table 2) [10–13]. In all four reports, a single monoclonal IgA paraprotein was identified. Interestingly, three of these four

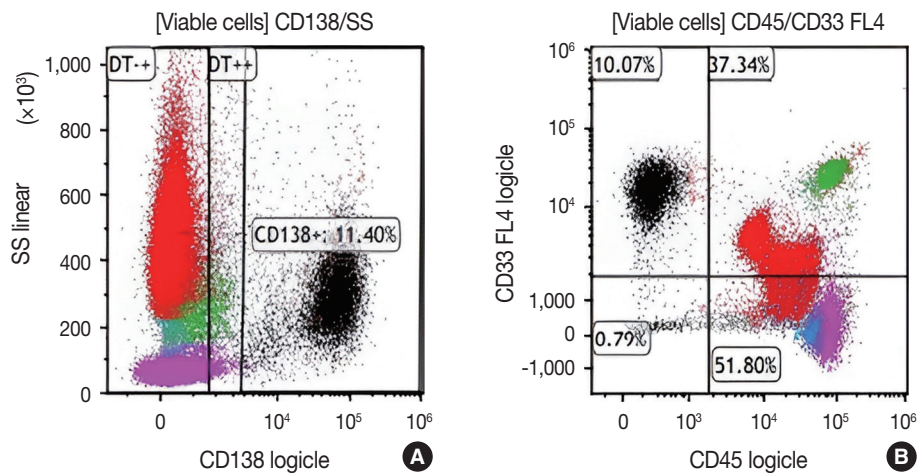


Fig. 3. Flow cytometry analysis of bone marrow cells detects increased clonal plasma cells (~11% of the viable cells; in black) that are positive for CD138 (A), lack CD45, and aberrantly express CD33 (a myeloid marker associated with high-risk myeloma) (B).

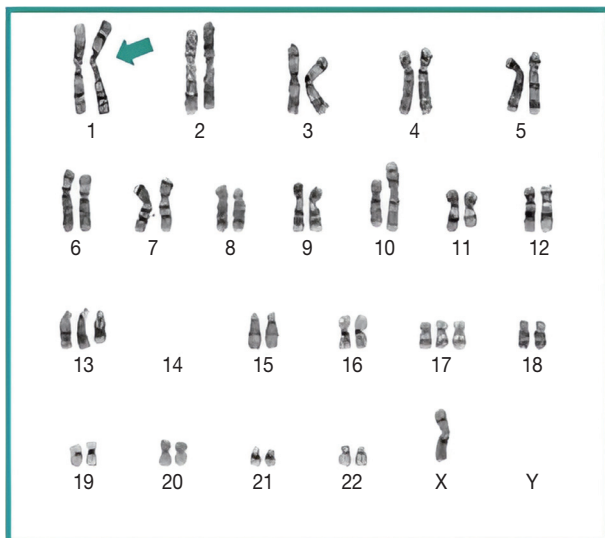


Fig. 4. Chromosome analysis revealed an abnormal complex karyotype including gain of 1q (arrow), a high-risk prognostic marker in plasma cell myeloma.

cases of IgA PCM presenting with abdominal pain occurred in adults of a younger age (39, 49, 57 years) [10-12] than the reported average age for IgA patients (66.5 years) [1]. Our 65-year-old patient would be the first report of an aggressive biclonal IgA PCM presenting as new-onset abdominal pain. Hence, findings such as non-localized abdominal pain in the adult population should alert clinicians to evaluate their patients for unsuspected malignancy and should prompt the ordering of imaging studies that could lead to an early diagnosis of PCM presenting with atypical symptoms.

Histologically, the bone marrow findings together with the

patient's clinical history and key laboratory results, including biclonal IgA gammopathy, were most consistent with bone marrow involvement by an IgA PCM, following the diagnostic guidelines of the International Myeloma Working Group [2,3]. In addition, a kappa/lambda ratio of ~50 supported the presence of PCM in the patient. Moreover, since over 50% of the marrow stroma was replaced by sheets of clonal plasma cells in the bone marrow biopsy, this finding met the criteria of histologic Stage III of III, as per the proposed Histopathology-based staging system [2]. According to McKenna et al. [2], there appears to be a good correlation between the histologic stage, clinical stage, and prognosis. Therefore, these histologic findings predicted an aggressive, high-risk IgA PCM in the patient.

Immunophenotypically, the patient's clonal plasma cells aberrantly expressed CD33 (a myeloid marker) and CD43 (a T-cell marker), and overexpressed transcription factors OCT-2 and MYC. The detection of any of these abnormal immunophenotypes in PCM is now associated with high-risk disease and poor survival [14-17]. Moreover, as published by Kodali et al. [17], MYC protein expression may serve as a potential predictor for prognosis and to assess residual disease in PCM. Based on their criteria, our patient fits in the low-MYC-expressing group (MYC < 30%) and could benefit from targeted treatment for high-risk myeloma.

Importantly, molecular cytogenetic studies in the patient identified several chromosomal abnormalities of known prognostic value in PCM. Based on the reported copy number abnormalities, her PCM could be categorized as non-hyperdiploid or hypodiploid (45 chromosomes) of complex karyotype including the loss of chromosomes 14, odd-number trisomies (chromosomes

Table 2. IgA plasma cell myelomas presenting with abdominal pain reported in the scientific literature

Case	Age (yr), sex	Clinical feature	Ig specificity	M-protein clonality	Location	Microscopic findings	Immunophenotyping/Cytogenetics/Molecular studies
Annibali et al. (2009) [10]	39, female Age at the time of initial diagnosis	Abdominal pain, and obstructive jaundice 7 yr after ASCT Extramedullary relapse	IgA-lambda	Monoclonal	Head of the pancreas, pleural effusion	US-guided FNA cytology of the pancreatic mass and cytology of pleural effusion revealed myeloma plasma cells	Unknown
Cerqueira et al. (2020) [11]	49, female	Presented with abdominal pain, biliary vomiting of 6 days duration Admitted to ICU for acute kidney failure	IgA-kappa	Monoclonal	Kidney, bone marrow	Kidney biopsy demonstrating myeloma kidney	Immunophenotyping: 60% of bone marrow monoclonal plasma cells with 100% CD138+, 100% CD38+, and 45% CD20+
Suo et al. (2020) [12]	57, male	History of liver cirrhosis presenting with abdominal pain and pancytopenia Extramedullary involvement	IgA-kappa	Monoclonal	Liver, MRI- left hepatic mass	Abundant plasmacytoid cells, kappa restricted neoplastic plasma cells	Plasmacytoid cells showed CD138+, kappa+, lambda- Cytogenetics and FISH suggestive of advanced disease progression
Yamane et al. (2021) [13]	73, male	Acute left lower abdominal pain	IgA-type	Monoclonal	Left vertebral arch of the 10th thoracic vertebra	Bone marrow biopsy: plasma cell neoplasm with 26.0% of plasma cells	Flow cytometry: CD38+, CD56+, CD138+, MPC-1+. Chromosomal analysis: 45,X,-Y,+5,+6,+7,-8,+9,+11,-13, and +21
Current case	65, female	Acute abdominal pain	IgA-kappa	Biclonal	Bone marrow	Hypercellularity (85%–95%), abnormal plasma cells (32%)	Immunophenotyping: CD138+, CD33+, MUM-1+, CD43+, OCT-2+, c-MYC+ Chromosomal analysis: gain of 1q,13,17, loss of 14

ASCT, autologous stem cell transplant; US, ultrasound; FNA, fine-needle aspiration; ICU; intensive care unit; FISH, fluorescence in situ hybridization.

13 and 17), and gain of 1q [9]. These results highlight the degree of genomic instability in her neoplastic plasma cells. According to Cardona-Benavides et al. [9], PCM patients with hypodiploid karyotypes and those with gain of 1q tend to have more aggressive clinical presentations and worse outcomes. Further, the R-ISS was used to estimate the patient's prognosis. Her predicted R-ISS score placed her in Stage III of III category with a median overall survival of 43 months and a median progression-free survival of 29 months [4]. Therapeutic options for these newly-diagnosed R-ISS/Stage III PCM patients with gain of 1q chromosomal abnormality are limited [9].

The translational relevance of identifying these high-risk IgA PCM could be significant for PCM patients, especially in Puerto Rico. Although PCM survival has improved due to new treatment modalities, the majority (~72%) of Puerto Ricans diagnosed with PCM are still likely to die from PCM [18]. Also, for unknown reasons, the decline in PCM-specific mortality in Puerto Rico is less than in other comparable US populations [18]. Future studies are needed to identify additional PCM patients with potential high-risk phenotypes such as biclonality, IgA subtype, MYC overexpression, gain of chromosome 1q. These studies should establish a definitive association between these high-risk markers and aggressive PCM. This could lead to improve medical care including the use of targeted therapies, which

could result in a further decline in PCM-specific mortality in Puerto Rico.

Ethics Statement

Formal written informed consent was not required with a waiver granted by the Institutional Review Board of Ponce Health Sciences University (IRB No. 2110075611).

Availability of Data and Material

The datasets generated or analyzed during the study are available from the corresponding author on reasonable request.

Code Availability

Not applicable.

ORCID

Carlos A. Monroig-Rivera
Clara N. Finch Cruz

<https://orcid.org/0000-0002-5147-2716>
<https://orcid.org/0000-0003-1612-2152>

Author Contributions

Conceptualization: CNFC. Formal analysis: CNFC. Funding acquisition: CNFC. Investigation: CAMR, CNFC. Methodology: CNFC. Project administration: CNFC. Resources: CNFC. Supervision: CNFC. Validation: CAMR, CNFC. Visualization: CAMR, CNFC. Writing—original draft: CAMR, CNFC. Writing—review & editing: CAMR, CNFC.

Conflicts of Interest

The authors declare that they have no potential conflicts of interest.

Funding Statement

No funding to declare.

Acknowledgments

The authors would like to acknowledge Adalberto Mendoza, MD, Jo-Ann Jusino, HT/QIHC, Rosa Velez, PhD, and Rose Reyes, MT at Southern Pathology Services for professional and technical support in the acquisition and analysis of data; and Richard Noel, Jr., PhD. at Ponce Health Sciences University-School of Medicine for review of the manuscript, editing support (Alina G. Cruz, MA), and costs of publication.

References

- Habermehl GK, Nakashima MO, Cotta CV. IgA plasma cell neoplasms are characterized by poorer long-term survival and increased genomic complexity compared to IgG neoplasms. *Ann Diagn Pathol* 2020; 44: 151449.
- McKenna RW, Kroft SH, Linden MA. Plasma cell neoplasms. In: Jaffe ES, Arber DA, Campo E, Harris NL, Quintanilla-Martinez L, eds. *Hematopathology*. 2nd ed. Philadelphia: Elsevier, 2017; 473-506.
- Rajkumar SV. Multiple myeloma: 2020 update on diagnosis, risk-stratification and management. *Am J Hematol* 2020; 95: 548-67.
- Palumbo A, Avet-Loiseau H, Oliva S, et al. Revised International Staging System for Multiple Myeloma: a report from International Myeloma Working Group. *J Clin Oncol* 2015; 33: 2863-9.
- Thiele J, Kvasnicka HM, Facchetti F, Franco V, van der Walt J, Orazi A. European consensus on grading bone marrow fibrosis and assessment of cellularity. *Haematologica* 2005; 90: 1128-32.
- Willrich MA, Katzmann JA. Laboratory testing requirements for diagnosis and follow-up of multiple myeloma and related plasma cell dyscrasias. *Clin Chem Lab Med* 2016; 54: 907-19.
- Keren DE, Schroeder L. Challenges of measuring monoclonal proteins in serum. *Clin Chem Lab Med* 2016; 54: 947-61.
- Rossi F, Petrucci MT, Guffanti A, et al. Proposal and validation of prognostic scoring systems for IgG and IgA monoclonal gammopathies of undetermined significance. *Clin Cancer Res* 2009; 15: 4439-45.
- Cardona-Benavides IJ, de Ramon C, Gutierrez NC. Genetic abnormalities in multiple myeloma: prognostic and therapeutic implications. *Cells* 2021; 10: 336.
- Annibaldi O, Marchesi F, Petrucci MT, Tirindelli MC, Avvisati G. Relapse of IgA lambda multiple myeloma presenting as obstructive jaundice and abdominal pain. *Onkologie* 2009; 32: 119-21.
- Cerqueira A, Seco T, Paiva D, Martins H, Cotter J. Acute kidney failure: when multiple myeloma doesn't give additional clues. *Cureus* 2020; 12: e7664.
- Suo L, Liu S, Vega I, Thrall M. Extramedullary multiple myeloma involving the liver and periportal lymph node, diagnosed by EUS-FNA in a patient with cirrhosis. *Diagn Cytopathol* 2020; 48: 657-61.
- Yamane F, Ohta R, Sano C. Left lower abdominal pain as an initial symptom of multiple myeloma. *Cureus* 2021; 13: e20652.
- Muchtar E, Gertz MA. The colorful landscape of multiple myeloma. *Leuk Lymphoma* 2019; 60: 2099-100.
- Ning X, Wei Y, Wei X, et al. CD43 expression is an adverse prognostic factor in newly diagnosed multiple myeloma. *Blood* 2021; 138 (Suppl 1): 4753.
- Toman I, Loree J, Klimowicz AC, et al. Expression and prognostic significance of Oct2 and Bob1 in multiple myeloma: implications for targeted therapeutics. *Leuk Lymphoma* 2011; 52: 659-67.
- Kodali S, Yu H, Cerny J. Assessing MYC expression in multiple myeloma. *J Hematol Thrombo Dis* 2015; 3: e119.
- Castaneda-Avila MA, Ortiz-Ortiz KJ, Torres-Cintron CR, Birmann BM, Epstein MM. Trends in cause of death among patients with multiple myeloma in Puerto Rico and the United States SEER population, 1987-2013. *Int J Cancer* 2020; 146: 35-43.

